STUDIES ON HEAT TRANSFER AND PRESSURE DROP CHARACTERISTICS OF NANOFLUIDS IN FLAT VERTICAL TUBES

A thesis submitted in partial fulfillment of the requirements
for the award of the degree of

DOCTOR OF PHILOSOPHY

By

GURPREET SINGH
Registration Number: 951201001

Under the supervision of

Dr. D. GANGACHARYULU
Professor
Department of Chemical Engineering
Thapar Institute of Engineering & Technology, Patiala

DEPARTMENT OF CHEMICAL ENGINEERING
THAPAR INSTITUTE OF ENGINEERING & TECHNOLOGY,
PATIALA 147004, INDIA
2019

THESIS CERTIFICATE

This is to certify that the thesis entitled "**Studies on Heat Transfer and Pressure Drop Characteristics of Nanofluids in Flat Vertical Tubes**" submitted by **Mr. Gurpreet Singh,** in the partial fulfillment of the requirements for the award of the Degree of **Doctor of Philosophy** in the Department of Chemical Engineering, **Thapar Institute of Engineering and Technology, Patiala (INDIA)** is a bonafide record of research work carried out by him under my supervision and guidance. The contents of this thesis, in full or in parts, have not been submitted to any other Institute or University for the award of any degree or diploma.

D. Gangacharyulu 23/10/2019

(D. GANGACHARYULU)
Professor
Department of Chemical Engineering
Thapar Institute of Engineering & Technology, Patiala

(Supervisor)

DECLARATION

I, Gurpreet Singh, hereby declare that the thesis entitled, "**Studies on Heat Transfer and Pressure Drop Characteristics of Nanofluids in Flat Vertical Tubes**" submitted to **Thapar Institute of Engineering and Technology, Patiala (INDIA)** in the partial fulfillment of the requirements for the award of the Degree of **Doctor of Philosophy** in the Department of Chemical Engineering is record of original and independent research work done by me during the period 2013-2019, under the supervision and guidance of Dr. D. Gangacharyulu, Professor, Department of Chemical Engineering, Thapar Institute of Engineering and Technology, Patiala

The research work of thesis has not been submitted to meet the requirements for any degree or diploma at this or any higher education institute.

23/10/2019

(Gurpreet Singh)
Regd. No. 951201001

ACKNOWLEDGEMENTS

The completion of this work was possible with support and guidance of several people. I would like to express the deepest appreciation to my supervisor Dr. D. Gangacharyulu, who has the substance of genius. He has the continually the conveyed the sprit in regard the research and motivation. Without his guidance and help, this research is not possible. The feedback and solution of problem at every stage of research is highly appreciable which help to learn and face the difficulties.

I would like to express my appreciation towards the Dr. Vijaya Kumar Bulasara, Associate Professor, CV Raman institute of engineering and technology, Bhubaneswar, Odisha. He has guided and helped in writing the research articles and offering the ways to reach to results.

I would like to thankful to the Head of the department, Dr. H. Bhunia for extending the opportunity to doctoral research. I am kind enough to doctoral committee, Dr. S. K. Mohapatra, Dr. Sanjiv Ahuja, Dr. Avinash Chandra, for their feedback of research at every stage. I would like thankful to Dr. Jai Parkash Khushwaha, Ph.D. coordinator and Dr. Raj Kumar Gupta for their suggestions to carry out research.

I would like to gratefully acknowledge the support provided by Centre of Excellence, TEQIP-II and management of Thapar Institute of Engineering and Technology, Patiala, Indian Institute of Technology, Roorkee and also M/s. Perfect Radiators, Haryana, India to carry out the present research work.

I would like to express my special appreciation to my younger brother, Mr. Kamaljit Singh for his support. He helped me every stage in each aspect and without his support this work not possible.

I would like to thank my fellow doctoral students, Dr. Harkirat Kaur Sarao, Mr. Manjit Singh Virk, Mr. Gurprinder Singh Dhindsa, for their feedback, cooperation and of course friendship.

The words cannot express how I grateful to my parents Mr. Ujaggar Singh and Mrs. Paramjit Kaur, my wife, Mrs. Mandeep Kaur for supporting me spiritually throughout writing this thesis and my life in general.

I am grateful to my family members, Mr. Gurpreet Singh, Mr. Gurmeet Singh, Mrs. Sandeep Kaur and Mrs. Gursharan Kaur for their cooperation during my work.

Last but not the least, I would like to thank God (Sri Guru Granth Sahib) for all good deeds. Nothing would be possible without the blessings of god.

23/10/2019

(Gurpreet Singh)

ABSTRACT

Cooling is one of the critical problems being faced by the modern industry due to the technological development such as microelectronic devices, high power engines, and ultrahigh heat-flux optical devices. Conventional heat transfer fluids such as water and ethylene glycol have been used for cooling purposes in automobile radiators; however, the heat transfer performance of these liquids is limited owing to their poor thermo-physical properties. An enhancement in the heat transfer performance of these fluids can result in improved performance of the automobile engines. Nanofluids can be used in heat exchangers and automobile cooling systems due to their better features than micrometer and millimeter sized particles i.e., high specific surface area, less erosion of components, low pumping power, etc.

In this work two types of nanoparticles such as aluminum oxide (Al_2O_3) and copper oxide (CuO) were used to prepare the nanofluids. The objective ^{of} the work is estimation of thermo physical properties of different concentrations of Al_2O_3 and CuO nanoparticles at different temperatures. The various thermophysical properties of prepared nanofluids such as thermal conductivity, density, specific heat and viscosity were measured experimentally using KD2 Pro, specific gravity bottle, differential scanning calorimeter and viscometer, respectively. The stability of nanofluids is checked by Zeta potential, measuring the absorbance using UV-vis spectrophotometer and thermal conductivity. The aluminum oxide nanofluids remain more stable than copper oxide nanofluids. The thermal conductivity enhanced significantly with increase in particle concentration and temperature. The thermal conductivity of nanofluids was more sensitive to temperature than that of the base fluid. The density and viscosity increased with increasing the particle concentration, while they both decreased with increase in temperature. The heat capacity of nanofluids increases with temperature but diminishes with increase in particle volume concentration.

The experimental study has been reported so far on the heat transfer performance of nanofluids in flat tubes of a radiator under turbulent flow conditions at which most of the automobile radiators are operated. Therefore, the main objective of the present work is to study the heat transfer and pressure drop performance of alumina-water and copper–water nanofluids in a flat vertical tubes under forced turbulent convection.

The nanoparticles plays a vital role in enhancing the Nusselt number and suspending the nanoparticles in base fluid leads to an increase in heat transfer coefficient for flat vertical tubes of radiator. The heat transfer rate increased with increase in fluid inlet temperature, particle concentration, Reynolds number as well as air inlet velocity. The pressure drop increased with increasing the Reynolds number and particle volume concentration, while it slightly decreased with increase in fluid inlet temperature because density and viscosity decrease with increase in temperature. The friction factor (*f*) of nanofluid in the flat tube increased with increase in Al_2O_3 and CuO nanoparticle concentration. However, it decreased with increase in Reynolds number and the lowest friction factor value was obtained for the base fluid. The pumping power needed by nanofluids was considerably higher than that needed for the base fluid.

The heat transfer performance of compact heat exchanger evaluated at various fluid inlet temperature such as 40 ^oC, 50 ^oC, 60 ^oC, 70 ^oC and 80 ^oC and at Reynolds number range from 5000 to 14000 and water based nanofluids in the range of 0.25% v/v to 1% v/v concentration of alumina oxide and copper oxide nanoparticles. The heat transfer rate increased with increase in fluid inlet temperature, particle concentration, Reynolds number as well as air inlet velocity. Heat transfer enhancement was more than the enhancement in the thermal conductivity of nanofluid at same temperature and concentration. This indicates that besides thermal conductivity, other factors such as fluid inlet temperature, Reynolds number and air velocity also affect heat transfer coefficient.

This study proves that the size of automotive cooling system can decreased with the use of nanofluids in place of conventional cooling fluids because the heat transfer is the primary concern for cooling systems.

TABLE OF CONTENTS

LIST OF FIGURES

LIST OF TABLES

NOMENCLATURE

Symbol	Description	Unit
A	Area of the tube	m^2
C_p	Heat capacity	kJ/(kg.K)
D_h	Hydraulic diameter	m
h	Heat transfer coefficient	$W/(m^2 \cdot K)$
k	Thermal conductivity	$W/(m \cdot K)$
m	Mass flow rate	kg/sec
Nu	Nusselt number	Dimensionless
Pe	Peclet number	Dimensionless
PP	Pumping power	W
Pr	Prandtl number	Dimensionless
Q	Heat transfer rate	W
Re	Reynolds number	Dimensionless
T	Temperature	°C
U	Uncertainties	Dimensionless
v	Velocity of fluid	m/s

Symbol	Description	Unit
β	Ratio of nano - layer thickness	Dimensionless
Ɛ	Effectiveness	Dimensionless
f	Friction factor	Dimensionless
ρ	Density	(kg/m^3)
μ	Dynamic viscosity	$kg/(m \cdot s)$
δ	Fin thickness	m

ΔP	Pressure drop	Pa
Ø	Particle volume fraction	Dimensionless

Subscript	**Description**
bf	Base fluid
fr	Frontal area
nf	Nanofluid
r	Radiator

Metal name	**Description**
Al_2O_3	Aluminum oxide
CNT	Carbon nanotubes
Cu	Copper
CuO	Copper oxide
MWCNT	Multiwalled carbon nanotubes
TiO_2	Titanium oxide
SiO_2	Silicon oxide
ZnO	Zinc oxide

Abbreviation	**Description**
DSC	Differential scanning calorimeter
EDS	Energy-dispersive spectroscopy
PID	Proportional integral derivative

CHAPTER 1

INTRODUCTION

1.1. Introduction

Cooling is one of the critical problems being faced by the modern industry due to the technological development such as microelectronic devices, high power engines, and ultrahigh heat-flux optical devices [1]. Efficient cooling system is not only necessary for the normal performance of the thermal devices but also for its long life and reliability. During normal operating conditions, temperature up to 2500°C is created within combustion chamber. If the engine is not properly cooled then this heat would lead to rapid expansion. A large amount of heat released during combustion is removed from the engine by exhaust gases. Some heat is absorbed by engine oil, however remaining heat has to be taken by engine's cooling system. Engine cooling systems can be based on either air or water. Air cooling is the most basic method for cooling of any system. It has limitation that it is not suitable for the system producing higher heat fluxes more than 100 W/cm^2 and such devices will require liquid cooling. But for sophisticated system or devices, heat transfer is realized through some heat transfer devices such as heat exchanger, heat sink, evaporators, condensers etc. The heat dissipation requirements from automobile engine has been increased significantly due to the rising demands of higher engine efficiency, smaller space and environment standards. The oil cooler and radiator have been used as the heat exchangers to dissipate heat from internal combustion engine. A lot of work has been done to increase the performance of these heat exchangers [2,3]. The space occupied by the device is more important with compactness requirements. In the transportation industry, high power engines or hybrid vehicles require larger radiators in the cooling system. Conventional coolants and oils have inherently poor heat transfer properties. So, there is need to develop advanced cooling system and high heat transfer performance fluids than those presently available. The rate of heat transfer can be increased by following methods:

a) Increase the heat transfer area (A) i.e. by introducing the fins on heat transfer surface.
b) Increase the flow rate (velocity).
c) Decrease the hydraulic mean diameter (d_h).
d) Increase the thermal conductivity of fluid (k_f).

Research activities are continuously carried out to enhance the heat transfer process. However, conventional heat transfer fluids such as water, oil and ethylene glycol have poor thermal conductivity. Heat removal can be enhanced significantly by designing fluids that are more conducting. To increase the thermal conductivity of fluids, one of the methods is incorporating the very small size particles such as metallic, non-metallic and polymeric into base fluids that is termed as nanofluids [4]. Nanofluids are dilute liquid suspensions of nanoparticles with at least one dimension smaller than 100 nm [5].

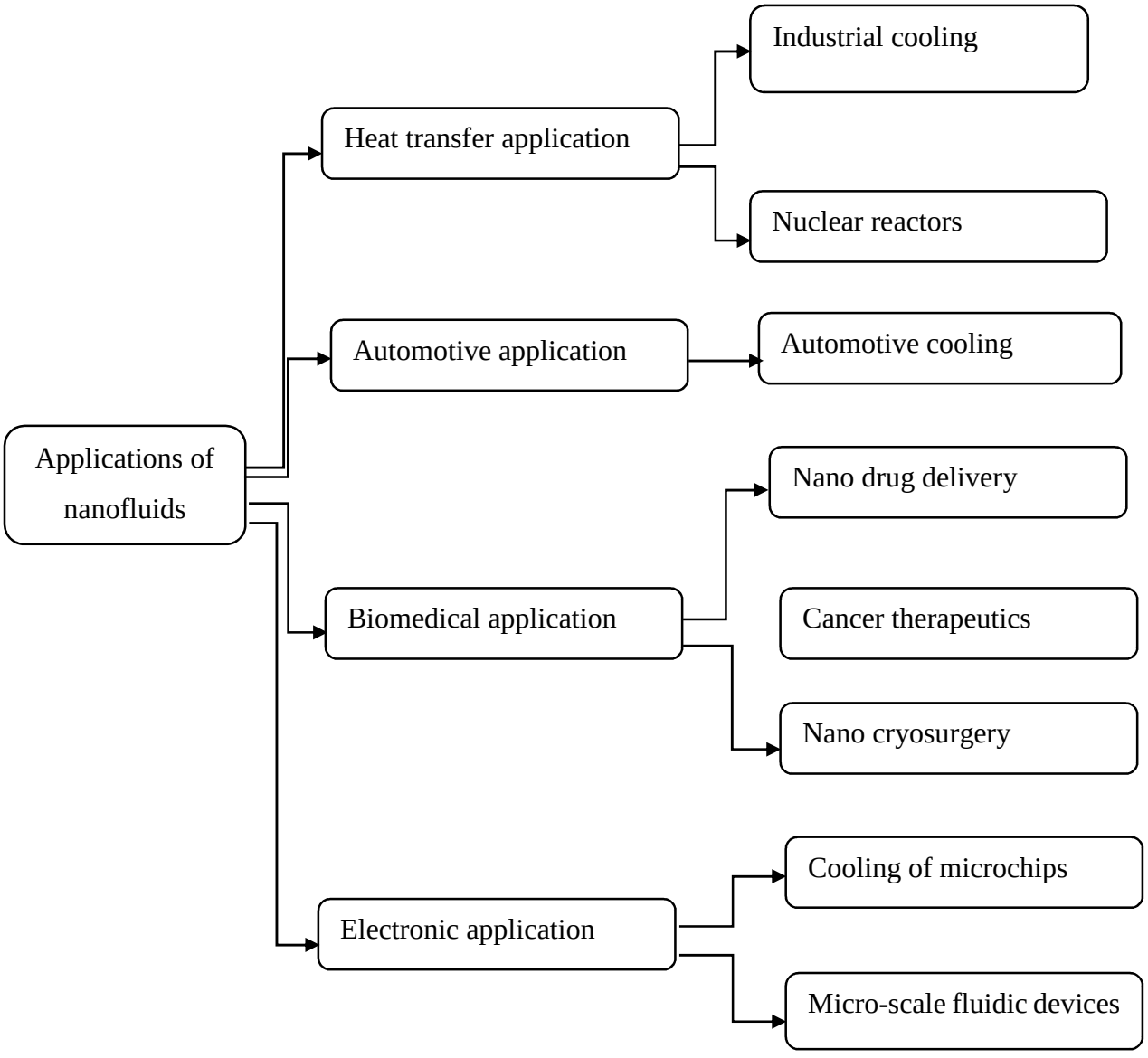

Figure 1.1: Applications of nanofluids

Nanoparticles stay suspended much longer than large particles. In addition, their surface area is 1000 times larger than micro particles. The suspended nanoparticles increase the surface area and heat capacity of the fluids [6]. The first theoretical work on the suspension was done by Maxwell more than 100 years back. Maxwell proposed theoretical enhancement of thermal conductivity of suspensions containing solid particles but it is difficult to suspend a solution with higher concentration which limits the use of micro and mini sized particles. As compared with suspended conventional particles of millimeter or micrometer dimensions, nanofluids show better stability, high thermal conductivity with very low or negligible viscosity [7–9]. Due to the higher stability of nanofluids, very less sedimentation occurs. The scale formation takes place inside the annuals of heat exchangers with use of nanofluids at elevated temperature which is called as fouling effect. The pressure drop increases if nanoparticles size increase and hence power required for pumping also increases. The properties of the base fluid like density and viscosity directly influence the pressure drop. If the viscosity and density of the fluid increases, then pressure drop and pumping power also increases. The modification of nanoparticles surfaces with surface modifying additives such as the surfactant has not any effect on the thermal conductivity enhancement while the with modification techniques enhances the stability of nanoparticles and surfactant act as thermal resistant between the nanoparticles and base which diminish the thermal conductivity enhancement. Surfactants are compounds that lower the surface tension between two liquids or between a liquid and solid. But, excess quantity of the surfactant has harmful (is a toxicant) effect on viscosity, thermal property and chemical stability. Due to superior stability and advantages of nanoparticles over micro sized particles, nanofluids have many applications in different fields as shown in figure 1.1.

1.2. Compact heat exchangers

Compact heat exchangers are the devices having a high heat transfer surface area with respect to their volume and is further associated with high heat transfer coefficients. These heat exchangers are further characterized by a large heat transfer surface area per unit volume of the exchanger. The compact heat exchangers having surface area density equal to or more than 700 m^2/m^3. The compact heat exchangers are having reduced space, less weight, energy requirements and cost as well as process design. The compact heat exchanger have smaller dimensions in flow direction and higher temperature gradients in the flow direction. The compact heat exchangers may be of

gas to gas, gas to liquid or liquid to liquid type. These compact heat exchangers are used or used as vehicular heat exchangers, aircraft coolers, air conditioning, automobile oil coolers, intercoolers of the compressor and space industry. The compact heat exchangers are also used in cryogenics processes, electronics, energy recovery, and other industries. A compact heat exchanger is generally not of small bulk and mass. Plate-fin, tube-fin, and rotary regenerators are examples of compact heat exchangers for gas flow on one or both fluid sides, and gasketed, welded, brazed plate heat exchangers and printed-circuit heat exchangers are examples of compact heat exchangers for liquid flows. Most common compact heat exchangers are plate-fin and tube-fin heat exchangers.

1.2.1. Tube-fin heat exchangers

Tube fin heat exchangers are classified as conventional and specialized tube-fin exchangers. In a conventional tube-fin exchanger the heat transfer takes place between the two fluids by conduction through the tube wall then from the tube surface to the other fluid which passes over the extended surface through an induced drat fan or by a forced fan by convection. The compact heat exchangers are described on the bases of area density and higher heat transfer coefficient. The area density of finned tube heat exchanger is about 210 ft^2/ft^3 (700 m^2/m^3). In a gas-to-liquid exchanger, the heat transfer coefficient on the liquid side is generally higher than that on the gas side, due to which the extended or the secondary surfaces are added on the gas side to enhance the heat transfer area on the gas side. These extended or the secondary surfaces are called fins. In a tube-fin exchanger, round and rectangular tubes are most common, although elliptical tubes are also used. Fins are generally used on the outside, but may be used on the inside of the tubes in some applications. Fins can be of various geometries like rectangular, square, cylindrical, annular and tapered, these fins bulge out rectangular base or a cylindrical base. Fins are attached to the tubes/bases by a tight mechanical fit, tension winding, adhesive bonding, soldering, brazing, welding, or extrusion. The high operating pressure on the tube side can be handled by the tube fin heat exchanger but it has certain restrictions at high temperature, the restrictions are material used, type of bonding, conductivity of material and material thickness. The tube fin heat exchangers are having lower compactness than the plate fin heat exchanger. The tube fin heat exchanger is having numerous configurations according to application area. The tube fin heat exchanger are mostly used for industrial purposes like condensers and evaporators in air conditioning and refrigeration. It can

further be used for water or oil cooling of combustion engine as radiators. Some other examples of compact heat exchangers are gas turbine heat exchanger, regenerator of stirling engine etc. The tube fin heat exchangers are also classified according to the type and arrangement of fins used.

a) Normal fins on individual tubes (individually finned tube); helical, plain circular, annular fins geometries like spine, studded, slotted and wire loop fins.
b) Longitudinal fins on individual tubes.
c) Flat or continuous external fins on an array of tubes; plain, wavy, interrupted/louvered.
d) Fins inside of tube; integrated fins, fins attached internally.

Radiator is one type of cross flow heat exchangers used to transfer the thermal energy for the purpose of cooling. The radiator of a vehicle plays a crucial role in cooling the engine [10]. A small and light weight radiator is the need for all types of automobile vehicles because the compactness of flow passage enhances the heat transfer performance. In heavy duty automobile engines, a large amount of heat is generated continuously, which should be dissipated efficiently by a radiator using a fluid flowing at high Reynolds number. Flat tubes are used in most automobile radiators to transfer heat because a flat tube has higher ratio of surface to cross sectional area than a circular tube, which leads to improved heat transfer performance and compactness of radiator [11]. Flat tubes have low pressure drop in air side as compared to circular tubes [12]. In radiator, primarily water based fluid circulates through the tubes and transfer the heat to tubes that transfer the heat to fins. Further, that heat is released to ambient air. To increase the contact surface of tubes to air, fins are attached with tubes, which increase the heat exchange efficiency. The core of radiator consists of number of tubes rows and fins. The cross section of tubes is rectangular with elliptical ends and fabricated from brass. The fins are plain and louvered fabricated with copper. For high performance vehicles, copper - brass radiator cores are preferred because of its superior cooling performance. In modern cars, radiators are made of brazing thin aluminum fins with flatten aluminum tubes. Due to low thermal conductivity, air has lower heat capacity than liquid coolant. To capture the heat from the coolant large volume flow rate of air flow through the radiator core is required. The heat transfer can be increased with use of nanofluids for heat transfer devices [13,14].

1.3. Closure

Conventional methods of heat removal have been found rather inadequate in case of ultra-high cooling, which is the very first need of the modern industries. Nanofluid is an effective way to increase heat transfer capabilities of existing heat transfer equipment. The heat transfer coefficient could increase with increasing the thermal conductivity of the coolant with use of nanofluids. With continuous technological development, it has increased the demand of high efficiency engine not only on its performance based but also for better fuel economy. Nanofluids have better heat transfer rate this could lead to reduce the size of tube-fin compact heat exchangers.

The thesis is organized as following:

Chapter 1 is introduction and covers the introduction of engine cooling system, background of compact heat exchanger and nanofluids and its applications in different field.

Chapter 2 is literature review of research work and covers the literature of various thermophysical properties of nanofluids, i.e. thermal conductivity, density, viscosity and specific heat and literature of experimental and theoretical studies of application of different nanofluids in various heat exchanging devices especially in flat tube and compact heat exchanger. In addition, it identifies the gaps which could be used for the further research and focused on the objectives for the present work.

Chapter 3 is the preparation, stability and thermophysical properties of nanofluids at various conditions.

Chapter 4 is the Experimental setup and performance evaluation method and this chapter discusses in detail about the fabrication of setup for the heat transfer and fluid flow studies.

Chapter 5 is results and discussion and covers the study of heat transfer and pressure drop characteristics of nanofluids inside a flat vertical tube and radiator of vehicle cooling systems.

Chapter 6 summarizes the conclusions and future scope of the present research work.

CHAPTER 2

LITERATURE REVIEW

2.1. Introduction

In last decade, a significant amount of experimental and theoretical research has been made to investigate the thermophysical behavior of nanofluids [5,15]. Nanometer particles have great potential to improve the thermal transport properties of heat transfer fluids than micrometer and millimeter sized particles. In this chapter, experimental and theoretical results on thermal conductivity, heat capacity, viscosity, heat transfer coefficient and performance of nanofluids in heat transfer devices based on experimental and theoretical results have been reviewed. The thermophysical properties of nanofluids have great significant on any heat transfer application. The literature has been presented the experimental and theoretical research as per the following categories:

a) Preparation and stability of nanofluids.
b) Thermophysical properties of nanofluids.
c) Performance of nanofluids in heat transfer devices.
d) Thermal and flow performance of flat tube and radiators.

2.2. Preparation and stability of nanofluids

Nanoparticles have been produced by physical and chemical synthesis [5,16,17]. Nanoparticles are in the powder form and in powder form can be dispersed in liquid to prepare the nanofluids [18]. Nanofluids have been produced by two techniques which are known as one step method and two step method [19]. The proper dispersion of nanoparticles in the base fluid is very important as the thermophysical properties depends on the preparation of nanofluids [20]. Further performance of heat transfer devices depends on thermophysical properties [21,22].

In one step technique, formation and dispersion of the nanoparticles in a single process only [18]. In this technique, direct evaporation has been used such as copper nanoparticles which uniformly dispersed and suspended in ethylene glycol as shown in figure 2.1(a). There were some difficulties in one step technique which were overcome by modification of one step method and this modified method was proposed by Wagener et al. [23]. Then some improvements also suggested by Eastman et al. [24] to prepare the copper based particles nanofluids. One step method is also used for the

coating of some nanoparticles. The chemical co-precipitation technique is also used for the synthesis of copper oxide particles which has also proved the good structural and surface morphology properties [25]. In second technique, two-step method, oxide nanoparticles are produced by evaporation and inert gas condensation processing. In two step method, there are high chances of agglomeration of nanoparticles which leads poor stability and thermophysical properties of prepared nanofluids [26].

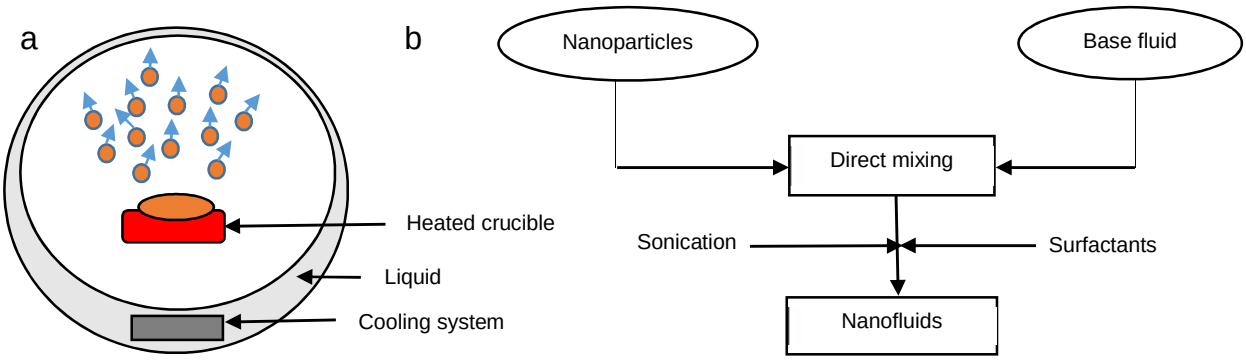

Figure 2.1: Nanofluid preparation method (a) one step method (b) two step method

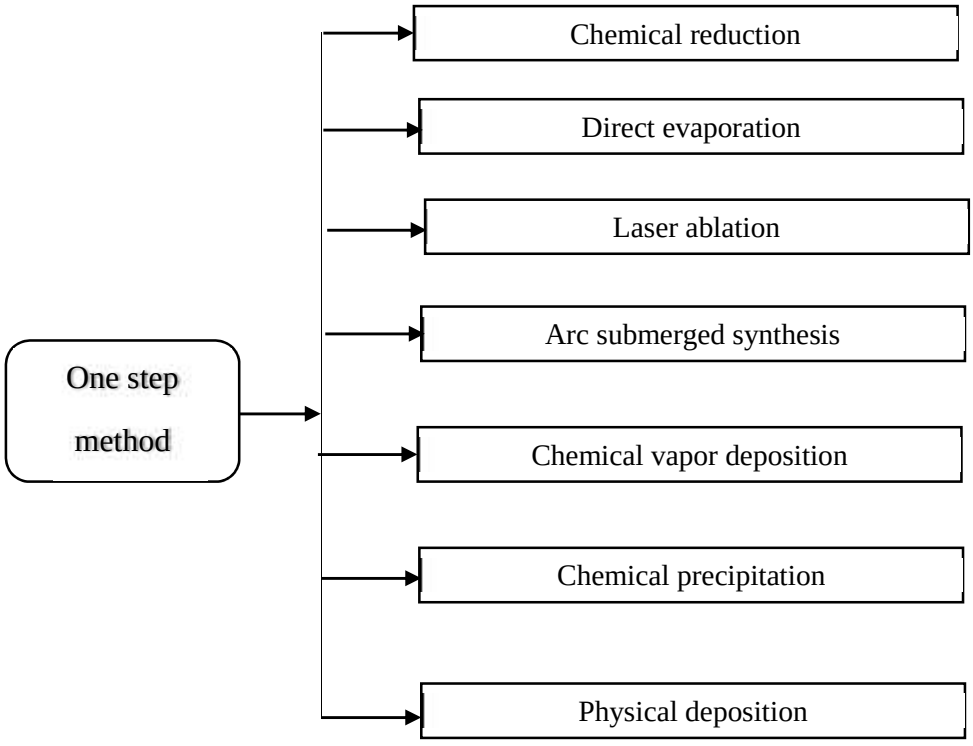

Figure 2.2: One step techniques for nanofluids preparation

In two step process, the nanoparticles in the powder form are dispersed in base fluid as shown in figure 2.1(b). The methods of single step technique is shown in figure 2.2 [27–30].

As the nanofluids is not simply mixture of base fluid and nanoparticles so there are chance to aggregate the nanoparticles due to high specific surface area. Some special requirements are essential for the suspension and negligible agglomeration of the nanoparticles [17]. There are different techniques used for the proper suspension of nanoparticles in the base fluid i.e. controlling pH value, use of surfactants and ultrasonic vibration [16,17,31]. Two types of interactions take place in nanofluids, one the interaction between the nanoparticles and another between the nanoparticle and surrounding base fluid which result in the agglomeration of nanoparticles [32]. The agglomeration can be reduced by electrostatic repulsion and steric mechanisms. The mechanism of electrostatic repulsion and steric repulsion is shown in figure 2.3.

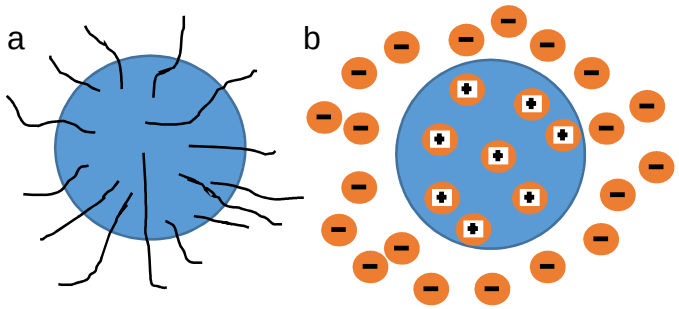

Figure 2.3: Steric repulsive (a) and electrostatic repulsion (b) mechanism

The nanofluids can be stabilized with physical methods i.e. ball milling, magnetic stirring, ultrasonic disruptor and ultra sonication. The ultra sonication method is good to reduce the agglomeration of nanoparticles. The ultra sonication can be done by either by probe type or bath type sonication and both methods improve the stability.

The addition of surfactants is simplest and economic method to enhance the stability of nanofluids. The surfactant can be either nonionic surfactant without charge or anionic surfactant with negative charged. For the cooling application good fluidity, low viscosity, minimum agglomeration are important requirements. The chemical modification is good method to enhance the stability of carbon nanotubes nanofluids [33] and plasma treatment is also used to increase the stability of nanofluids [34]. The nanofluids with low pH leads to good stability and high thermal conductivity but controlling the pH is not good for all nanofluids.

2.3. Thermophysical properties

For the enhancement of heat transfer of any heat exchanger with nanofluids, investigation of thermophysical properties i.e. thermal conductivity, viscosity, specific heat and density is important. Experimental and theoretical studies on thermophysical properties of nanofluids have been reported by several researchers but there is no consistency of observed value of thermal physical properties. There are several factors which affects the thermophysical properties of nanofluids which are given below:

a) Base fluid.
b) Concentration of nanoparticles.
c) Correlations used to estimate thermophysical properties.
d) Method of thermophysical properties measurement.
e) Mixing time.
f) Methods of nanofluids preparation.
g) pH of base fluid.
h) Size of nanoparticles.
i) Shape of nanoparticles.
j) Surfactants.
k) Sonication time.
l) Stability.
m) Temperature of fluid.
n) Types of nanoparticles.

2.3.1. Thermal conductivity

In heat exchange devices, heat transfer fluids play a vital role and affect the performance of heat exchangers [1]. Conventional heat transfer fluids such as water and ethylene glycol have been used for cooling purposes in automobile radiators; however, the heat transfer performance of these liquids is limited owing to their poor thermo-physical properties [35,36]. An enhancement in the heat transfer performance of these fluids can result in improved performance of the automobile engines. The thermal conductivity of most solids is higher than that of liquids [5]. A number of attempts have been made to improve the thermal conductivity of conventional fluids through the use of micro and millimeter sized particles; but, the major drawbacks of micro-sized and millimeter

sized particles include low specific surface area, high pumping power requirement and tendency to settle out of suspension. Thermal conductivity is most responsible parameter for the enhancement of heat transfer [9,37]. Transient hot wire and temperature oscillation techniques have been employed to measure the thermal conductivity of nanofluids. The suspended nanoparticles increase the effective thermal conductivity of the conventional fluid [38–40]. Thermal conductivity of nanofluids depends on particle volume fraction as well as on particle size also. The factors which influencing thermal conductivity of nanofluids are 1) influence of base fluid 2) influence of nanoparticles 3) influence of liquid solid interface [41]. Jana et al. [42] have experimentally measured thermal conductivity of single and hybrid nano additives of carbon nano tubes (CNT), copper nanoparticles and gold nanoparticles. The enhancement of thermal conductivity with copper nanoparticles is the 74% over base fluid. The stability of carbon nano tubes was higher as compared to Cu nanoparticles in nanofluids. The Brownian motion of nanoparticles is responsible phenomenon for thermal conductivity enhancement [43,44].

Sundar et al. [45] have been estimated the thermal conductivity of ethylene glycol and water mixture (50:50%) based Al_2O_3 and CuO nanofluids at different volume concentration (max. 0.8%) and temperatures (15^{o}C-50^{o}C). The thermal conductivity of nanofluids increased with increasing particle volume concentration. The enhancement of thermal conductivity varies from 9.8% to 17.89% with Al_2O_3 nanofluids and from 15.6% to 24.56% with CuO nanofluids. Eastman et al. [24] observed that thermal conductivity has been improved by 60% as compared to base fluid when Al_2O_3, CuO and Cu nanoparticles dispersed in water and HE-200 oil. Teng et al. [46] investigated that the thermal conductivity is higher in the case of small size particles at high temperature than large size particles at low temperature. Besides the thermal conductivity of nanofluids, other properties such as viscosity, specific heat and density also have a great influence on heat transfer.

Particle volume concentrations, particle size and shape, particle material, base fluid properties, and temperature greatly affect the heat transfer properties; however, the pH of base fluids has a negative effect on heat transfer [5,36,47]. Xuan and Li [48] reported that the thermal conductivity enhanced with Cu particles of size 36 nm compared to Cu particles 100 nm dispersed in water. The appropriate dispersants improved the stability of suspension. With increasing the temperature

thermal conductivity ratio also increased under same weight fraction. The thermal conductivity is higher in case of high temperature and small particle size as compared to low temperature and large particle size.

Murshed et al. [49] have measured the thermal conductivity of nanofluid with transient hot wire method. The thermal conductivity increased with increase in particle volume fraction of TiO_2 in water based nanofluids. The thermal conductivity enhanced by 33% over base fluid with 5% volume fraction of TiO_2 nanoparticles. Li and Peterson [50] have prepared nanofluid with Al_2O_3 and CuO of 36 nm and 29 nm size nanoparticles respectively in water. The thermal conductivity almost increased by three times with increase in temperature from 24 ^oC to 37.4 ^oC. The effects of pH value of the suspension and specific surface area of Al_2O_3 nanoparticles as reported by Xie et al. [51] and it has been found that enhancement of thermal conductivity highly depends on specific surface area of nanoparticles. As the difference increased between pH value and isoelectric point of Al_2O_3 thermal conductivity also enhanced.

Vajjha and Das [52] determined the thermal conductivity of nanofluid containing aluminum oxide (Al_2O_3), copper oxide (CuO) and zinc (ZnO) particles dispersed in ethylene glycol and water (60:40) base fluids. The thermal conductivity of nanofluid increased with increasing the particle concentration and temperature. The thermal conductivity increased by 21% with 10% volumetric concentration in Al_2O_3 particles, 21.4% with 6% volumetric concentration in CuO nanofluid and 18% with 7% volumetric concentration in ZnO nanofluids at different temperature ranges from 298K to 363K. Wang et al. [53] investigated that the enhancement of the thermal conductivity depends on volume fraction of graphite particles. The enhancement of thermal conductivity was 36% with adding 1.36 vol. % of graphite in oil. The thermal conductivity increased from 11% to 36% when amount of graphite increased from 0.68 to 1.36 vol. %. The shear thinning and significant viscosity increased for 1.36 vol. % graphite/ oil nanofluid. Patel et al. [54] revealed that thermal conductivity of nanofluids linear with particle volume fraction and nonlinear with temperature. The enhancement of thermal conductivity 5% to 21% reported for water with temperature range 30 ^oC to 60 ^oC at 0.00026 vol.% of Ag nanoparticles and improvement of thermal conductivity was around 7% to 14% at 0.011% v/v of Au particles. There was also

important effect of direct contact of the metal surface with solvent medium on thermal conductivity.

Reddy and Rao [55] have studied the thermal conductivity of ethylene glycol- water based TiO_2 nanofluids. The nanoparticles dispersed in base fluids water, ethylene glycol and water with ratio 40:60 and 50:50. The thermal conductivity of TiO_2 nanofluids increased with increase in the volume concentration of TiO_2 and temperature. It leads to enhancement of thermal conductivity by 10.64%. Khedkar et al. [56] reported that thermal conductivity of nanofluid increased with increasing volume fraction of nanoparticles. The enhancement of thermal conductivity with CuO - water nanofluids 1% to 7.5% reported. The enhancement in thermal conductivity for CuO - water nanofluids was found greater than that for CuO - monoethylene glycol nanofluids. Hwang et al. [57] have measured the thermal conductivity by a transient hot wire method for four kinds of nanofluids such as multiwalled carbon nanotubes, CuO, SiO_2 in water and CuO in ethylene glycol. The thermal conductivity water is enhanced upto 11.3% for multiwalled carbon nanotube in water with volume fraction of 0.01%.

Koo and Kelinstreuer [58] proposed a new model for estimation of thermal conductivity of different nanofluids and proposed model has good agreement with existing thermal conductivity of different nanofluids. The thermal conductivity of nanofluids can be also calculated with some available models, which are defined as follows:

Hamilton–Crosser [59] proposed a model to calculate the thermal conductivity two phase mixture fluid, which is defined as follows:

$$\frac{k_{nf}}{k_{bf}} = \frac{k_p + (n-1)k_{bf} - ¤(n-1)(k_{bf} - k_p)}{k_p + (n-1)k_{bf} - ¤(k_{bf} - k_p)} \qquad (2.1)$$

Yu and Choi [60] also introduced a model to calculate the thermal conductivity of nanofluids, which is expressed as follows:

$$\frac{k_{nf}}{k_{bf}} = \frac{k_p + 2k_{bf} - 2(k_{bf} - k_p)(1+ \quad)^3¤}{k_p + 2k_{bf} - (k_{bf} - k_p)(1+ \quad)^3¤} \qquad (2.2)$$

Where, β is the ratio of the nano-layer thickness to the original particle radius and for nanofluids. The summary of enhancement of thermal conductivity with different types of nanoparticles, base fluid and temperature variation is given in table 2.1.

Table 2.1: Summary of thermal conductivity enhancement with variation of different parameters

Author	Nanoparticles	Volume concentration	Particle size (nm)	Base fluid	Temperature range	Thermal conductivity enhancement ratio	Method used/ Remarks
Lee et al. [61]	Al_2O_3, CuO	1-4.30 1-5.0 1.0-3.41	38.4 38.4 23.6	Water Ethylene Glycol	--	1.03-1.10 1.03-1.18 1.03-1.12	Two step method used. Thermal conductivity increased with temperature
Hong & Kim [62]	Al_2O_3	1.0, 3.0 & 5.0	50	Water	25^0C	1.04-1.22	Thermal conductivity measured with 3ω method.
Wang et al. [63]	Al_2O_3, CuO	a) 3.0-5.50 5.0-8.0 b) 4.50-9.70	28 23	Water Ethylene Glycol	--	1.11-1.16 1.25-1.46 1.17-1.34	Two step method used
Eastman et al. [64]	Al_2O_3	1.0-5.0	35	Ethylene glycol	--	1.05-1.18	Two step method used
Das et al. [65]	Al_2O_3	1.0-4.0	38.4	Water	21-51^{0}C	1.02-1.08	Two Step method used Effect of temperature measured on thermal conductivity
Li & Peterson [50]	Al_2O_3	2.0-10.0	36	Water	27.5^{0}C	1.15-1.22	Two step method
Wen & Ding [66]	Al_2O_3	0.19-1.59	42	Water		1.01-1.10	Two step method used
Mahbubul et al. [67]	Al_2O_3	0.5-2.0	13	R141b Nano refrigerant	5-20^{0}C	1.626	Two step method Thermal conductivity increased with temperature and particle volume concentration
Teng et al.[46]	Al_2O_3	0.5-2.0	20 50 100	water	10-50^{0}C	1-1.04 1.02-1.035 1.03-1.08	Two step method used. Thermal conductivity increased with increase in temperature, particle concentration and reducing the size of nanoparticles
Priya et al. [68]	CuO	0.004-0.016	40-60	Water	28-55^{o}C	1.03-1.35	Two step method used.

							Thermal conductivity increased with increase in temperature and particle vol. fraction. Maximum enhancement 44% at 55^{O}C at 0.016 vol% has been reported.
Zhu et al.[69]	CuO	1-5	50-100	water	Room temperature	1.1-1.3	Nanofluids prepared by other than dispersing methods have higher thermal conductivity.
Wei et al. [70]	CuO	0.01-0.05	200.5	water	28-55ºC	0.83-1.24	Two step method used Maximum enhancement in thermal conductivity up to 24% achieved with $CuSO_4$ molar nanofluids
Kole & Dey [71]	CuO	0.005-0.025	40	Gear oil	5-80ºC	1.03-1.10	Two step method used At room temperature maximum enhancement approximately 10.4% and 11.9% at 80º C has been observed.
Zhu et al. [72]	CuO	0.2-1.2	10	water	25ºC	1.01-1.045	Wet chemical method has been used for synthesis of CuO Nanofluids. Thermal conductivity increased with increasing nanoparticle concentration in base fluid.
Saterile et al. [73]	Cu	0.55 & 1.0	60-100	water		1.2	The enhancement in thermal conductivity enhancement approximately 22% and 48% has been observed with 0.55 and 1.0 vol.% nanofluids.
Barbes et al. [74]	CuO	0.4-3.5	23-37	Water Ethylene glycol	25-65ºC	1.02-1.3 1.02-1.15	Two step method used It has observed that thermal conductivity increased with temperature and particle volume fraction

2.3.2. Viscosity of nanofluids

Viscosity of nanofluids is an important parameter in nanofluids because viscosity directly affects the pressure drop in forced convection. Research related to the viscosity is limited as compared to thermal conductivity of nanofluids. The extent of viscosity increase of nanofluids with respect to pure fluids should be investigated. Nguyen et al. [75,76] reported that viscosity of nanofluids depends on many parameters such as, particle volume fraction, particle size, temperature and extent of clustering. The viscosity increased with increasing the particle volume fraction but decreased with an increasing the temperature because increase of fluid temperature has weakening the effect on the inter-particle/ inter-molecular forces [77]. The increasing concentration of nanoparticles have directly influence on internal shear stress.

Jeong et al. [78] have experimentally investigated the viscosity and thermal conductivity of ZnO nanofluids with volume concentration 0.05 - 5.0% v/v of rectangular and sphere shape nanoparticles. The shape of the particles found to have significant effect on viscosity and thermal conductivity. The enhancement of viscosity with rectangular particles has 77% greater than spherical nanoparticles. The viscosity of the nanofluids increased up to 69% with increasing the volume concentration. Wang et al. [79] observed that viscosity increased up to 40% at room temperature with Al_2O_3 particles for volume fraction of 3.5% in ethylene glycol. Prasher et al. [80] reported that particle size has no effect on the nanofluid viscosity but on other hand Nguyen et al. [75] indicated that viscosity of nanofluid changes significantly with particle size and temperature whereas Pastoriza-Gallego et al. [81] reported that viscosity decreased with increasing particle size.

Kole and Dey [82] have studied the effect of aggregation on the viscosity of copper oxide nanoparticles in gear oil. Viscosity of the nanofluids has enhanced approximately by three times with copper oxide nanoparticles as compared to base fluid but viscosity decreased with increasing the temperature. With increasing copper oxide volume fraction Newtonian feature of the base fluid changes to non-Newtonian. Shear thinning behavior becomes prominent for nanofluid with higher copper oxide concentration. Duangthougsuk and Wongwises [83] measured the viscosity of TiO_2 nanofluids at different nanoparticles concentrations (0 – 2.0%) and fluid temperature (15 ^oC - 35 ^oC) and reported that the viscosity of nanofluids increased with addition of nanoparticles while decreased with rise in fluid temperature and results have good agreement with developed correlations. Sudar et al. [84] reported that the viscosity enhancement in the high viscosity base fluid is less as compared to high viscosity base fluids with addition of aluminum oxide

nanoparticles. The viscosity of ethylene glycol and water mixture with aluminum oxide nanoparticles was 2.75 times higher than base fluid.

Aladag et al. [85] investigated the effects of temperature on viscosity of alumina nanofluids and reported that depends on the shear rate nanofluids behaves as the Newtonian and non- Newtonian behavior. Zyla et al. [86] investigated the rheological properties of glycol based $MgAl_2O_4$ nanofluids under anisotropic pressure and electric field conditions. The electric filed has no effect on the viscosity which is valuable information for industry. The temperature has significant effect on viscosity of carbon nanotubes, aluminum oxide, copper oxide, copper, titanium oxide, silicon oxide nanofluids [87–89]. Some theoretical models are available to estimate the viscosity of nanofluids with different particle but these models have some variation with experimental observed viscosity [89,90].

For determining the dynamic viscosity nanofluids containing the spherical particles, Einstein [86] proposed an expression in which interaction between the particles are neglected:

$$«_{nf} = «_{bf}(1+2.5¤) \quad (2.3)$$

Later on, Brinkman [86] suggested an equation in which it is considered that viscosity should increase unboundedly as particle volume fraction:

$$«_{nf} = \frac{1}{(1-¤)^{2.5}} «_{bf} \quad (2.4)$$

Batchelor [91] improved the Einstein model, in which the interactions between particles were taken into account.

$$«_{nf} = (1+2.5¤+6.2¤^2)«_{bf} \quad (2.5)$$

Some other theoretical models for calculating the viscosity of nanofluids are:

Maiga et al. [92] for Al_2O_3/ ethylene glycol nanofluids:

$$«_{nf} = (1+0.19¤+3.6¤^2)«_{bf} \quad (2.6)$$

For for Al_2O_3/ water nanofluids:

$$«_{nf} = (1+7.3¤+123¤^2)«_{bf} \quad (2.7)$$

2.3.3. Density

Apart from the thermal conductivity and viscosity of nanofluids, density of nanofluids is also important property for estimate the thermal performance of any heat transfer equipment. Very limited experimental and theoretical investigations has been carried out for the density of nanofluids

with different types of nanoparticles loading. In most of research work, a general correlation has been used (given in the 2.8) for the estimation of density of nanofluids.

$$\rho_{nf} = (1-\phi)\rho_{bf} + \phi\rho_{np} \quad (2.8)$$

The density of nanofluids increases with increase in nanoparticle concentration while decease with increase the nanofluids temperature[19,93–95]. In an experimental study Shoghl et al. [96] measured the density of CuO, Al_2O_3, CNT, MgO, ZnO, TiO_2 and MWCNT and reported that density of all nanofluids increased with addition of different nanoparticles. The density of aluminum oxide particles based nanofluids (base fluid water and ethylene glycol mixture) increased with increase in nanoparticles concentration up to 10% and slightly diminishes with increase the temperature of the base fluids [97]. In an experimental study Vajjha et al. [98] measured the density of three different nanofluids (aluminum oxide, antinomy-tin oxide and zinc oxide) of ethylene glycol/water mixture and compared the density of nanofluids with equation 2.8. Density of aluminum oxide, antinomy-tin oxide nanofluids has good agreement with equation while zinc oxide nanofluids data has deviation from the equation. Vajjha et al. [98] also revealed that density of nanofluids increased with particle concentration and decreases with temperature of nanofluids.

Yousefi and Amoozandeh [99] proposed a new model by artificial intelligent technique to predict the density of different nanofluids by considering the various parameters such as volume fraction of nanoparticles, diameter of nanoparticles, fluid pressure, temperature of base fluid and Pak and Cho equation. Montazer et al. [100] also developed a correlation using response surface methodology for multiwalled carbon nanotubes for low volume fraction (up to 0.1%) and low temperature range (20 ^{o}C - 40 ^{o}C) and reported that there is small decrease in density of carbon based nanofluids with rise in temperature.

Zyla et al. [101] measured the density of ethylene glycol based nanofluids with addition of nitride nanoparticles with different sizes and specific surface area of nanoparticles. The density of nitride nanofluids decreased with rise in fluid temperature while increase with increase of nanoparticles loading. The addition of nanoparticles in refrigerant, also increase the density of refrigerant based nanofluids [102]. Mariano et al. [103] experimentally measured the density of different ethylene glycol mixture nanofluids by varying the temperature and pressure of nanofluids. They report that variation of pressure is also contributes for increase the density of nanofluids along with variation of temperature and volume fraction of nanofluids.

2.3.4. Specific heat

Specific heat of nanofluids is important property to analyze the exergy and energy[104,105]. In the most of studies, specific heat is measured with differential scanning calorimeter (DSC) [13,106–108] and well developed correlations [109] which are given in the equation 2.9 and 2.10

$$(c_p)_{nf} = ¤(c_p)_{np} + (1-¤)(c_p)_{bf} \quad (2.9)$$

$$(c_p°)_{nf} = ¤(°c_p)_{np} + (1-¤)(°c_p)_{bf} \quad (2.10)$$

The specific heat of water base alumina nanofluids decreased with addition of nanoparticles in the base fluid[107]. Kumaresan and Velraj [29] measured the specific heat of carbon nanotubes and water/ ethylene glycol mixture nanofluids with differential scanning calorimeter and results has been compared with developed equation. The specific heat measured for 0.15% - 0.45% of MWCNT and maximum heat capacity was observed at lowest concentration of nanoparticles. With the increase in nanoparticles concentration specific heat decreased.

Liu et al. [110] measured thermal conductivity of graphene nanofluids for medium to high temperature application of nanofluids and reported that decrease in specific heat 12% at 80 ^oC and 24% for 200 ^oC of the base fluid. Mohebbi [111] reported that the specific heat of silicon nitride nanofluids lower than the base fluid. Neih et al. [112] measured the specific heat of aluminum oxide and titanium oxide nanofluids for the heat transfer capacity enhancement of vehicle cooling system. The specific heat was measured in temperature range 80 ^oC – 90 ^oC. The heat capacity of aluminum oxide nanofluids higher than the titanium oxide nanofluids. The heat capacity of nanofluids increased with increase in fluid temperature while decrease with rise in nanoparticle concentration of in the base fluids (water and ethylene glycol). They also concluded that the specific heat of base fluid higher than the specific heat of dispersed nanoparticles and temperature have significant effect on rise of specific heat of nanofluids.

Pantzali et al. [113] reported that specific heat capacity of copper oxide nanofluids with 4% v/v was 20% lower than the base fluid. Shin and Banerjee [114] measured the specific heat of alkali salt with alumina nanoparticles dispersion and the specific heat enhanced by 32% with alumina nanoparticles. The specific heat of aluminum oxide nanoparticles with different particle concentration and fluid temperature decreased with addition of nanoparticles in the base fluids while slightly increase with increase in fluid temperature [19,94,95]. Ho and Pan [115] measured the specific heat of pure Hitec fluid and nano-Hitec fluid with differential scanning calorimeter and

observed that specific heat of nano-Hitec fluid is lower than pure Hitec fluid due to addition of alumina nanoparticles.

2.4. Performance of nanofluids in heat transfer devices

In the last decade, extensive work has been carried out to enhance the performance of heat transfer devices. The number of experiment and theoretical studies for the application of nanofluids in the heat transfer devices or energy field have been reported [116–121]. Heris et al. [122] reported that enhancement of the heat transfer by nanofluid greatly depends on particle type, particle size, base fluid, flow regime and boundary condition. The heat transfer coefficient of nanofluids increased with increasing nanoparticles concentration. Heat transfer coefficient enhanced up to 30% with 2.5% of volume fraction of Al_2O_3 nanoparticles. As reported by Wang and Mujumdar [123] there are many factors such as particle size, shape, distribution of nanoparticles, pH value and particle fluid interactions may have important effect on heat transfer performance of nanofluids.

Kakac et al. [47] have reported that with Al_2O_3 and CuO nanoparticles in water from laminar to turbulence flow, the heat transfer enhancement as high as 40% with Al_2O_3 nanoparticles. According to Yang et al. [124] heat transfer coefficient increased with increasing the temperature but temperature has no essential influence on the pressure drop for viscoelastic fluid flow containing copper nanoparticles. The pressure drop decreased with increasing the pressure. Suresh et al. [125] have investigated the effect of Al_2O_3-Cu/ water hybrid nanofluid on heat transfer. The maximum heat transfer enhancement was found with 0.1% volume concentration at Reynolds number of 1730 but friction factor is slightly higher when compared to water.

Zamzamian et al. [126] have evaluated the effects of Al_2O_3 and CuO nanofluids on heat transfer coefficient in turbulent flow by using double pipe and plate heat exchanger. It was found that the enhancement in heat transfer coefficient of nanofluids, ranging from 2% to 50% as compared to the base fluid. Heat transfer coefficient of nanofluids increased with increasing the nanoparticles concentrations and nanofluids temperature. Heyhat et al. [127] have investigated that heat transfer coefficient of nanofluid is higher than base fluid. Heat transfer coefficient increased with increasing the Reynolds number and particle concentration. The heat transfer coefficient increases by 32% in fully developed region at 2% v/v. Pressure loss for the nanofluid higher than pure water.

Arani and Amani [128] investigated the effects of TiO_2 nanoparticles with 0.002 – 0.02 volume fraction on the heat transfer and pressure drop in water. The heat transfer coefficient enhanced approximately 15% and 72% with nanoparticle concentration 0.002% and 0.02% respectively. The

difference of enhancement between laminar and turbulent flow presumably occurred. Pressure drop also increased with increasing the Reynolds number. It is observed that higher pressure drop in nanofluids as compared to base fluid water. As stated by Arani and Amani [1] there has some effects mean diameter of nanoparticles on the convective heat transfer and pressure drop. The TiO_2 nanoparticles with diameters of 10, 20, 50 nm dispersed in distilled water. The Nusselt number has not increased with decreasing the diameter of nanoparticles. The nanofluid with 20 nm particles size diameter showed higher thermal performance. Duangthongsuk and wongwises [129] have reported the experimental results of heat transfer coefficient of TiO_2/ water nanofluid in double tube counter flow heat exchanger. The heat transfer coefficient with TiO_2/ water nanofluid, 6-11% higher than base fluid. The heat transfer coefficient of nanofluid increased with increasing the mass flow rate and with decreasing in nanofluid temperature. Temperature of heating fluid has no significant effect on the heat transfer coefficient.

As revealed by the Das et al. [130] the boiling performance increased with increasing the particle concentration of Al_2O_3 and surface roughness. It was also found that the inclusion of nanoparticles degraded the boiling performance by increasing the wall superheat for a given heat flux. The pool boiling significantly enhanced with increase in the thermal conductivity. It also reported that pool boiling heat transfer not reduced with increasing particle volume fractions in the absence of acoustic field.

Maiga et al. [92] numerically investigated the thermal characteristics of nanofluids flowing through a uniformly heated circular tube. The ethylene glycol–γ Al_2O_3 has better heat transfer enhancement than the water–γ Al_2O_3 nanofluids. Nanoparticles have effects on the wall shear stress. Farajollahi et al. [131] have compared the heat transfer characteristics of γ-Al_2O_3/ water and TiO_2/ water nanofluid. The heat transfer coefficient increased with increasing peclet number and with increasing nanoparticles concentration. It observed that heat transfer coefficient higher with TiO_2/ water nanofluid at lower concentration and γ-Al_2O_3 nanofluid at higher concentration.

Roy et al. [132] studied numerically heat transfer for γ-Al_2O_3/ water nanofluids and reported that heat transfer rate increased with addition of nanoparticles in the base fluid. Heat transfer rates increased up to two fold with 10% nanoparticles as compared to base fluid. Khanafer et al. [133] numerically investigated the heat transfer behavior of nanofluids. The heat transfer rate increased with increasing the particle concentration at any Grashof number. Xuan and Yao [134] reported that with increasing the temperature of fluid, distribution of the nanoparticles increased which is important for enhancement of heat transfer coefficient in nanofluids. Xuan et al. [135] observed

that due to the irregular fluctuation of suspended nanoparticles, the Nusselt distribution fluctuated along the main flow direction The results indicated that the distribution and volume fraction of the nanoparticles are important factors for heat transfer enhancement with nanofluids.

In a study Ghozatloo et al. [136] studied the performance of graphene nanofluids in shell and tube heat exchanger under laminar flow conditions. The convective heat transfer coefficient increased up to 38% as compared to base fluid with the use of graphene nanofluids at low nanoparticle concentration and heat transfer coefficient increased due enhancement of thermophysical properties. Halefadl et al. [137] investigated the thermal performance of heat exchanger with four different types of carbon nanotube and constant wall temperature condition. The heat transfer coefficient increased with increase in Reynolds number and particles concentration.

Lee et al. [138] have investigated the effects of nanofluids on heat transfer in hot vertical tube to enhance the heat transfer with 0.1% Al_2O_3 and 0.1% carbon nano colloid dispersed in water, ethylene glycol and engine oil. The cooling performance enhanced more than 13s and 20s for Al_2O_3/ water nanofluid and carbon nano colloid respectively. The deposition of nanoparticles formed a thin layer on heating surface which attributed more cooling performance.

He et al. [139] investigated the effects of TiO_2 nanofluids flowing through a vertical pipe in both laminar and turbulent flow regimes. The heat transfer and thermal conduction increased with increasing the particle concentration and decreasing the particle size but viscosity increased with increasing particle concentration and size. Pressure drop in the turbulent regime was higher than that in laminar flow regime. Reynolds number increased with increasing particle concentration

2.5. Thermal and flow performance of nanofluids in flat tube and radiators.

Vajjha et al. [11] have numerically studied heat transfer performance of flat tubes radiator with flat fins using Al_2O_3 and CuO nanoparticles in water. Average heat transfer coefficient increased by 94% with 10% v/v of Al_2O_3 and 89% with 6% v/v of CuO nanofluid over the base fluid. Heat transfer coefficient also increased with increasing the Reynolds number as shown in figure 2.4.

Peyghambarzadeh et al. [140] experimentally studied effects on heat transfer enhancement with Al_2O_3 nanoparticles in flat tubes radiator. They reported that heat transfer of nanofluids dependent on the particle concentration, flow conditions and least dependent on temperature. Heat transfer coefficient increased by 40% when Al_2O_3 has been mixed in base fluid in range of 0.1 - 1% v/v. The heat transfer coefficient slightly improved with increase in the fluid inlet temperature. Heat

transfer coefficient is higher by using nanofluids as compared to the water. Heat transfer coefficient also increased when pure water has been used with higher Reynolds number.

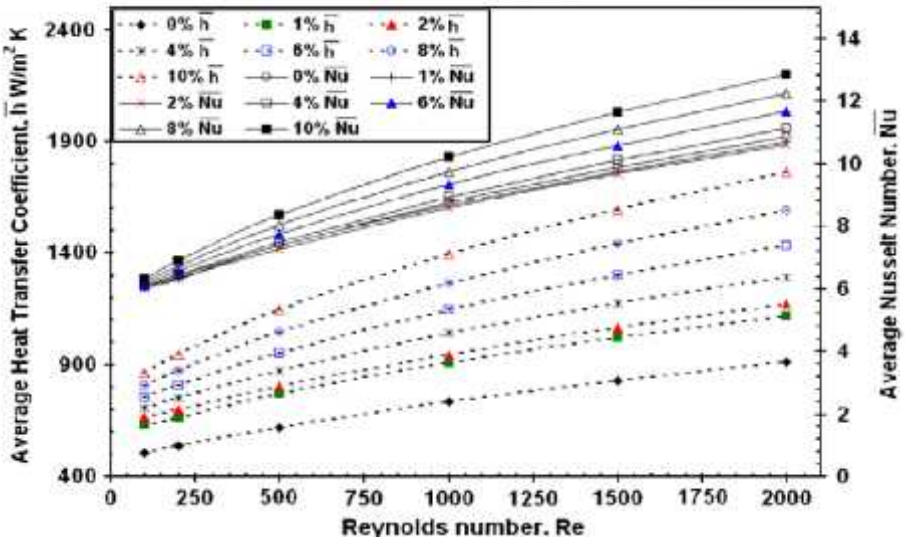

Figure 2.4: Effect of Reynolds number on heat transfer coefficient and Nusselt number [11]

In an another study, Peyghambarzadeh et al. [14] have added copper oxide (CuO) and iron oxide (Fe_2O_3) nanoparticles in water with different concentration (0.15, 0.4, 0.65% v/v) and reported that heat transfer coefficient increased with liquid flow rate, air flow rate. Heat transfer coefficient also increased with increasing the concentration of CuO and Fe_2O_3. Heat transfer coefficient increased with increasing the Reynolds numbers of air. Leong et al. [141] have been observed that heat transfer rate has been increased when the concentration volume increased from 0% to 2% of copper particles. Dynamic viscosity of nanofluids has been increased with increasing the volume fraction of copper nanoparticles. It has been observed that 45.2% heat transfer enhanced for ethylene glycol with 2% of copper particles when Reynolds numbers increased from 4000 to 6000. Naraki et al. [20] have investigated the overall heat transfer coefficient by using CuO/ water nanofluids as a coolant in car radiator. Heat transfer coefficient increased when concentration of CuO increased from 0 to 0.4% v/v as shown in figure 2.4. The overall heat transfer coefficient increased with increasing the particle concentration as compared to base fluid when flow rate of nanofluid was constant.

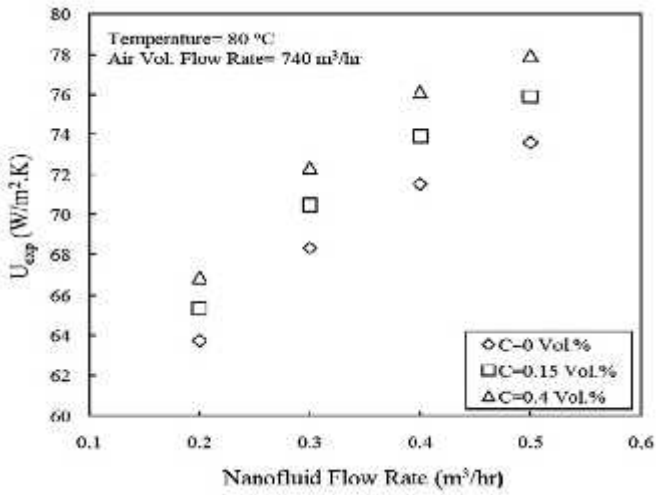

Figure 2.5: Effect of concentration and flow rate on heat transfer coefficient [20]

But, heat transfer coefficient was decreased with increasing the nanofluid temperature from 50°C to 80°C. Air flow rate, inlet temperature and concentration of nanofluids have 23%, 22% and 13% contribution in overall heat transfer coefficient. Peyghambarzadeh et al. [142] have been investigated that heat transfer rate of automobile radiator increased with presence of Al_2O_3 nanoparticles at concentration of 1% v/v. Heat transfer coefficient enhanced with increasing flow rate of pure water and nanofluid. Higher heat transfer coefficient obtained by using nanofluid instead of water. Heat transfer coefficient increased about 30-40% in comparison the pure water. Some correlation for heat transfer characteristics and pressure drop characteristic given in table 2.2 which are suggested by some authors.

Table 2.2: Compilation of heat transfer and pressure drop characteristics correlations

S. No	Equation	Nanoparticles	Concentration (%)	Reynolds number	Reference no.
1.	$Nu = 0.085\,\mathrm{Re}^{0.71}\,\mathrm{Pr}^{0.35}$	Aluminum oxide	10.0	10^4 -5×10^5	[143]
2.	$Nu = a\,\mathrm{Re}^{b}\,\mathrm{Pr}^{\frac{1}{3}}(\frac{D}{L})^{\frac{1}{3}}(\frac{\mu_w}{\mu_b})^{\frac{1}{3}}$	Graphite	2.5	5 – 120	[144]
3.	$Nu = 0.0059(1+7.6286^{\varphi\,0.6886}\,Pe_d^{0.001})\,\mathrm{Re}^{0.9238}\,\mathrm{Pr}^{0.4}$	Copper	2.0	10^4 – 2.5×10^4	[145]
4.	$Nu = 0.074\,\mathrm{Re}^{0.707}\,\mathrm{Pr}^{0.385\,\varphi\,0.074}$	Titanium oxide	2.0	3000 - 18000	[146]
5.	$Nu = 0.086\,\mathrm{Re}^{0.55}\,\mathrm{Pr}^{0.5}$	Aluminum oxide	10.0	3000	[147]
6.	$Nu = 0.28\,\mathrm{Re}^{0.35}\,\mathrm{Pr}^{0.36}$	Aluminum oxide	10.0	3000	[147]
7.	$Nu = 0.067\,\mathrm{Re}^{0.71}\,\mathrm{Pr}^{0.35} + 0.0005\mathrm{Re}$	Titanium oxide	0.25	50000 - 30000	[148]
8.	$Nu = 0.02172\,\mathrm{Re}^{0.8}\,\mathrm{Pr}^{0.5}(1+\varphi)^{0.5181}$	Iron oxide	0.2	3000 - 22000	[149]
9.	$Nu = 0.0023\,\mathrm{Re}^{0.8}\,\mathrm{Pr}^{0.3} + (0.617^{\varphi} - 0.135)\,\mathrm{Re}^{(0.445^{\varphi}-0.37)}\,\mathrm{Pr}^{(1.081^{\varphi}-1.305)}$	Silver	0.9	900 - 12000	[150]
10.	$Nu = 0.065(\mathrm{Re}^{0.65} - 60.22)(1+0.0169^{\varphi\,0.15})\,\mathrm{Pr}^{0.542}$	Copper oxide	0.06	3000 – 16000	[151]
11.	$Nu = 3.138\times10^{-3}\,\mathrm{Re}(\mathrm{Pr})^{0.6}(1+\varphi)^{1.22}(1+\frac{H}{D})^{0.03}$	Aluminum oxide	0.1	3500 – 8500	[152]
12.	$Nu = 0.5419(\mathrm{Re}\,\mathrm{Pr})^{0.53}(\frac{P}{d})^{-0.594}$	Aluminum oxide	0.1	2300	[153]
13.	$Nu = 0.065(\mathrm{Re}^{0.65} - 60.22)(1+0.0169^{\varphi\,0.15})\,\mathrm{Pr}^{0.542}$	Aluminum oxide	0.1	3000 – 16000	[151]
14.	$Nu = 0.5657(\mathrm{Re}\,\mathrm{Pr})^{0.5337}(\frac{P}{d})^{-0.6062}$	Copper oxide	0.1	2300	[153]
15.	$f = 26.4\,\mathrm{Re}^{-0.8737}(1+\varphi)^{156.23}$	Aluminum oxide	0.1	2300	[154]
16.	$f = 0.1648\,\mathrm{Re}^{0.97}(1+\varphi)^{107.89}(1+\frac{P}{D})^{-4.463}$	Copper oxide	0.3	2500 – 6000	[155]
17.	$f = 0.3491\mathrm{Re}^{-0.25}(1+\varphi)^{0.1517}$	Iron oxide	0.2	3000 - 22000	[149]
18.	$f = 0.3164\,\mathrm{Re}^{-0.25}(\frac{\rho_{nf}}{\rho_{bf}})^{0.707}(\frac{\mu_{nf}}{\mu_{bf}})^{0.108}$	Aluminum oxide	0.1	3000 – 16000	[151]

2.6. Novelty of present research work

The literature study indicates that thermophysical properties of nanofluids depends upon the many parameters i.e., fluid temperature, particles size and shape, particles concentration etc. The use of nanofluids leads to heat transfer performance enhancement. From the literature review it has been observed that extensive experimental and theoretical studies have been conducted to investigate thermal and transport properties of nanofluids in past decade. The effect of higher temperature on thermo physical properties of nanofluids has not been studied so far because in industrial application some process has been carried out at high temperature.

A critical review of existing literature on heat transfer enhancement of radiator tubes using nanofluids indicated that a majority of these studies were based on numerical simulations and a few were based on experimental studies under laminar flow conditions. However, no experimental study has been reported so far on the heat transfer performance of nanofluids in flat tubes of a radiator under turbulent flow conditions (Re > 10000), at which most of the automobile radiators are operated.

In the compact heat exchanger, limited research has been carried out with flat tube and louvered fin radiators. In the flat tube vehicle cooling systems, only numerical studies have been carried out only with oxide nanoparticles and no experimental study has not been reported. Most of research has been carried out only to calculate the heat transfer coefficient at low Reynolds number and low particle volume concentrations. The fluid flow performance of single flat tube and radiator with high Reynolds number and high volume concentration not reported. The effect of air velocity on heat transfer performance of flat tube not reported.

2.7 Scope of the present work

1. In the present work, aluminum oxide and copper oxide nanoparticles with an average size 20 – 30 nm are dispersed in base fluid (water) and nanoparticles are spherical in structure which posses the good stability.
2. Thermophysical properties i.e. thermal conductivity, density, specific heat and viscosity measured with temperature range from 30^{o}C to 90 ^{o}C and particle concentration up 1.0% v/v and mathematical equation developed.
3. The performance of water based aluminum oxide and copper oxide nanofluids studied in the flat vertical and compact heat exchanger (radaitor) with variation of different parameters i.e. particle concentration, Reynolds number, fluid inlet temperature, air inlet velocity.

4. Correlation for heat transfer coefficient and pressure drop of nanofluids in flat tube were developed in the terms of particle concentrations.

2.8 Objectives of work

The objective(s) of the work are as follows:

- Estimation of enhancement of cooling capacity of radiator by using nanofluids.

    a) Estimation of thermo physical properties of different nanofluids of Al_2O_3 and CuO nanoparticles at different temperatures (from ambient temperature to 85^oC).
    b) Study of heat transfer and pressure drop characteristics of nanofluids inside a flat vertical tube.
    c) To develop a correlation for heat transfer coefficient and pressure drop of nanofluids in flat tube.

CHAPTER 3

PREPARATION, STABILITY, THERMOPHYSICAL PROPERTIES OF NANOFLUIDS

3.1. Introduction

This chapter presents detailed description of preparation of nanofluids, their stability analysis and thermophysical properties of nanofluids. Stable nanofluids play an imperative role in heat transfer applications. Proper mixing and stabilization of nanoparticles in the base fluid is important for preparing the nanofluids. Three techniques have been used for suspension of nanoparticles – by controlling the pH value of suspension, use of surfactants and ultrasonic vibration [16,17,31].

3.2. Nanoparticle materials

In present thesis work two types of nanoparticles such as aluminum oxide (Al_2O_3) and copper oxide (CuO) were used to prepare the nanofluids. Nanoparticles were procured from the M/s. Nanoshell LLC, USA. Some physical properties of nanoparticles are given in table 3.1. The double distilled water was used as the base fluid for preparation of nanofluids.

Table 3.1: Characteristics of nanoparticles

S. No	Parameter	Unit	Al_2O_3	CuO
1.	Average particle size	Nm	20	20-30
2.	Appearance	-	Whitish	Black
3.	Purity	%	> 99	> 99
4.	Density	kg/m^3	3895	6310
5.	Thermal conductivity	$W/(m \cdot K)$	33	32
6.	Specific heat capacity	$J/(kg \cdot K)$	765	540

3.3. Characterization of nanoparticles

There are number of methods available to study the characterization of different nanoparticles. Some methods are given below:

a) Infrared spectroscopy
b) Optical spectroscopy
c) Raman Spectroscopy
d) X-ray diffraction (X-RD)
e) Scanning electron microscope (SEM)
f) Transmission electron microscopy (TEM)
g) Zeta potential

In the present work nanoparticles characterization was carried out with transmission electron microscopy and scanning electron microscope methods. The energy-dispersive spectroscopy (EDS) analysis of aluminum oxide and copper oxide nanoparticles was carried on scanning electron microscope (JEOL JSM 6510 LV) at SAI lab, Thapar Institute of Engineering and Technology, Patiala. Transmission electron microscopy and scanning electron microscope are the techniques to analyze the size, shape and distribution of nanoparticles. These techniques cannot be used for the nanofluids because dry samples are required during the testing. This problem might be resolved with cryogenic transmission electron microscopy and cryogenic scanning electron microscope as the structure of nanofluids is not changed during the cryogenic process.

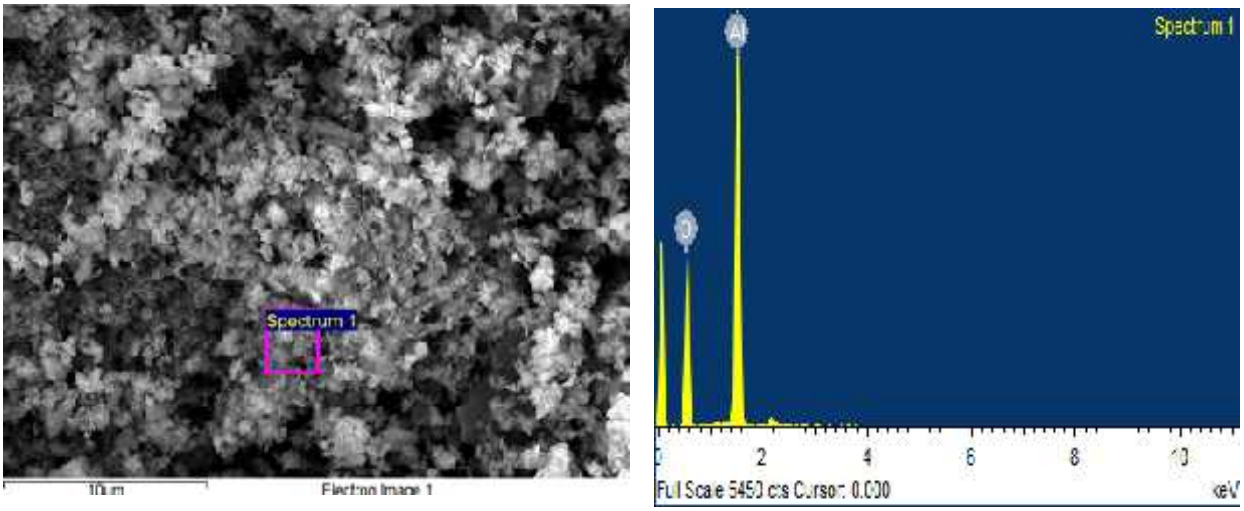

Figure 3.1: EDS analysis of aluminum nanoparticles

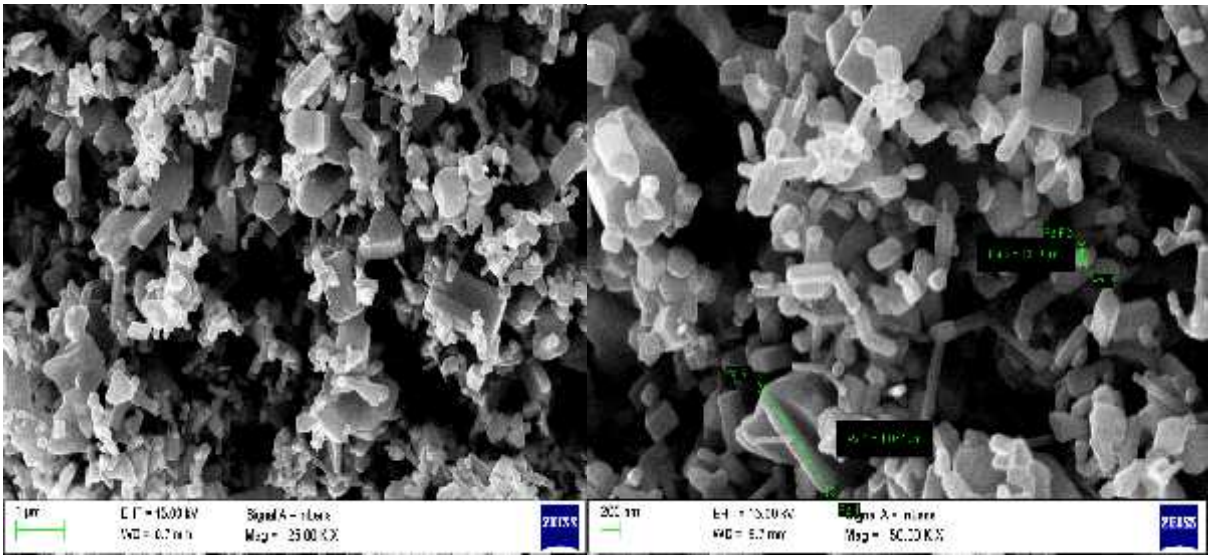

Figure 3.2: Scanning electron microscope image of aluminum oxide nanoparticles

The transmission electron microscopy gives the two types of information about nanoparticles; first is the size and shape of nanoparticles in terms of mean diameter and second is crystallinity from electron diffraction. The EDS analysis of aluminum oxide nanoparticles is shown in figure 3.1. The aluminum oxide nanoparticles contained 50.38% aliminum and 49.62% oxygen by weight percentage. The atomic percentage of alumina was 37.58. The surface morphology of alumiunm oxide is shown in figure 3.2 and it is clear from the figure that aluminum oxide nanoparticles are spherical in struture and average size of nanoparticles is 20 nm.

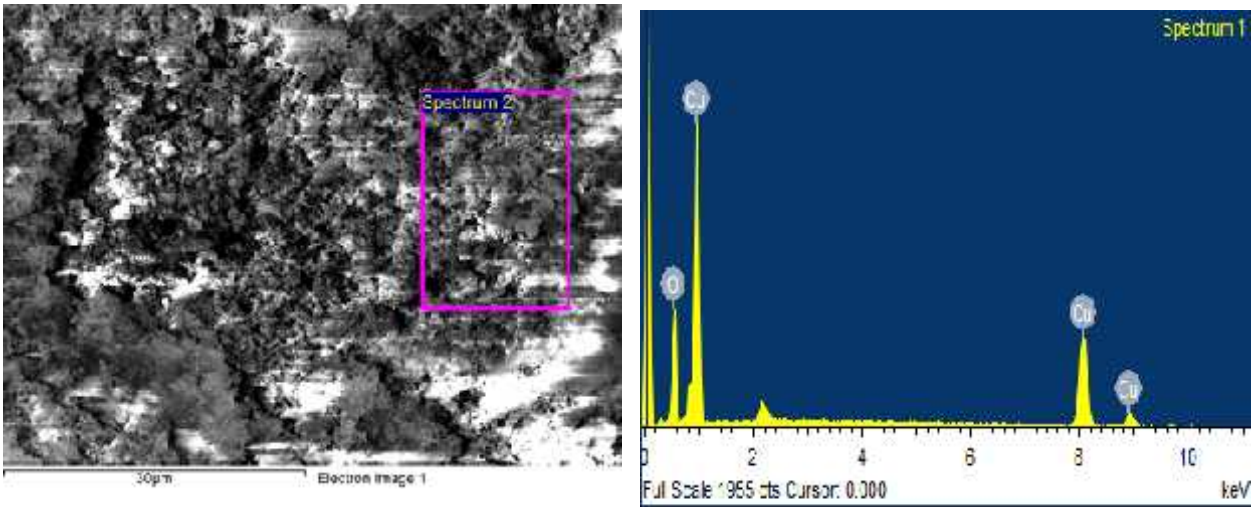

Figure 3.3: EDS analysis of copper nanoparticles

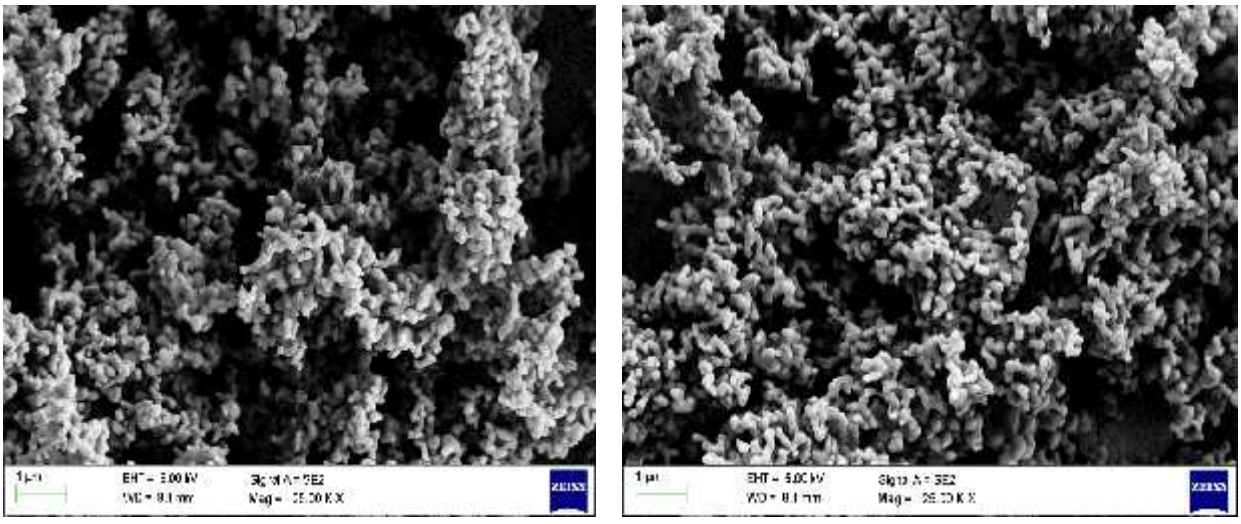

Figure 3.4: Scanning Electron microscope image of copper oxide nanoparticles

The EDS analysis of copper oxide nanoparticles is shown in figure 3.3 and it was analyzed that copper oxide nanoparticles contained 73.24% copper and 26.76% oxygen by weight percentage. The atomic percentage of copper was 40.80. The surface morphology of copper oxide is shown in

figure 3.4 and it is clear from the figure that copper oxide nanoparticles are spherical in struture with average size of nanoparticles is 20 nm.

3.4. Preparation of nanofluids

Two methods are widely used in the preparation of nanofluids, namely, one-step method and two-step method [156]. In present thesis work, nanofluids were prepared from 0–1.0% v/v concentration of nanoparticles. Two-step method was used to prepare the nanofluids and methodology to prepare nanofluids is shown in figure 3.5.

The nanofluids preparation methodology is as follows:

a) The amount of nanoparticles required for preparing a given sample of nanofluids, was calculated using eq. (3.1), which is based on volume concentration

$$\text{Volume concentration} = \frac{\frac{m_p}{\rho_p}}{\frac{m_p}{\rho_p} + \frac{m_{bf}}{\rho_{bf}}} \qquad (3.1)$$

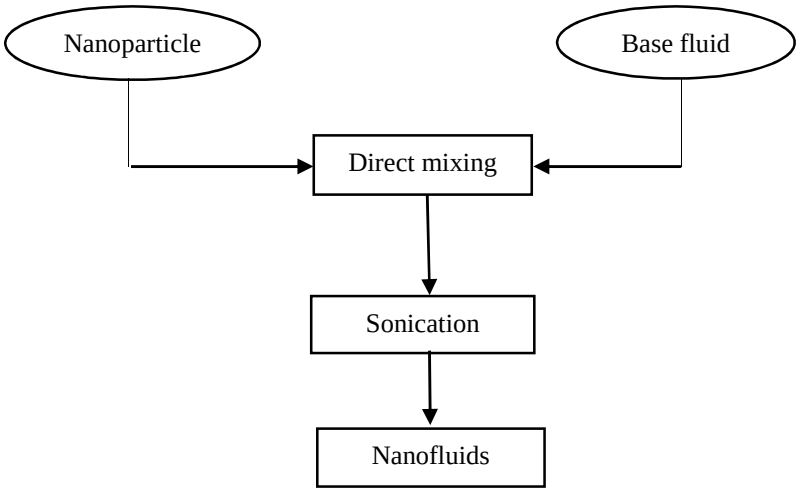

Figure 3.5: Preparation of nanofluids

b) Nanoparticles were added gradually to the base fluid in a glass flask while agitating with a magnetic stirrer for about one hour.

c) The surface activator (surfactants) has vital role in the stability of nanofluids. The aluminium oxide nanofluids were prepared without use of any surfactant while copper oxide nanofluids with use of surfactant. For the copper oxide nanoparticles, 0.2 wt% of SDS was added to prepare the stable copper oxide nanofluids.

d) The nanofluids were sonicated for 2–3 hours in an ultra sonicator in order to obtain a stable suspension of nanoparticles. The sonication of nanofluids was carried out Branson Ultrasonics, USA which is shown in figure 3.6.

Figure 3.6: Ultrasonicator

3.5. Stability of nanofluids

The stability of nanofluids is important for application of nanofluids as nanofluids are not simply liquid – solid mixture. Some special treatment i.e. addition of surfactant is required for the stable, durable suspension, minimum agglomeration of nanoparticles. The agglomeration of the nanoparticles is not leads only clogging of channels but also decrease the thermal conductivity of nanofluids. The stability of nanofluids was checked by Zeta potential, measuring the absorbance using UV-vis spectrophotometer and thermal conductivity. The Brookhaven 90 plus particle size analyzer was used for the Zeta potential measurement. The particle size analyzer was equipped with PALS Zeta potential software. The Zeta potential shows electric potential difference between the dispersed medium and layer of the fluid which is attached to suspended nanoparticle in base fluid. The stability of nanofluids measured with the significance of Zeta potential value. The high value of Zeta potential leads to good stability of nanoparticles in the base fluid. The suspension, with Zeta potential value more than 60 mV, have the excellent stability and the Zeta potential value in the range of 40 mV – 60 mV shows the good stability of nanoparticles in base fluid. The suspension is considered as physical stable if the value of Zeta potential is lies between the 30 mV – 40 mV and if the value of Zeta potential decreases upto 20 mV, the nanofluids are limited stability [156].

Further the value of Zeta potential less than 5 mV indicates the agglomeration of nanoparticles and nanofluids are not suitable for any application. The results of Zeta potential of present work are also compared with available literature.

The absorbance analysis is also a good method to check the stability of nanofluids. There is linear relationship between the nanoparticles and intensity of absorbance. The UV-vis analysis is reliable method if the particle suspended in base fluid have absorbance wavelength between 190 – 1100 nm. The stability of nanofluids measured over the days till absorbance value show >± 0.01 error relative to initial value of absorbance.

The thermal conductivity of nanofluids is an important transport property for heat transfer applications. Different techniques have been used to measure the thermal conductivity of nanofluids. In most of the studies, transient hot wire method has been used because it minimizes the effects of convection. In this work, thermal conductivity of nanofluids was measured with a battery operated KD2 thermal analyzer.

3.5.1. Stability of aluminum oxide nanofluids:

The stability of nanofluids measured with Zeta potential, UV-Vis absorbance and thermal conductivity of nanofluids. Nanofluids were prepared from 0–1.0% v/v concentration of nanoparticles.

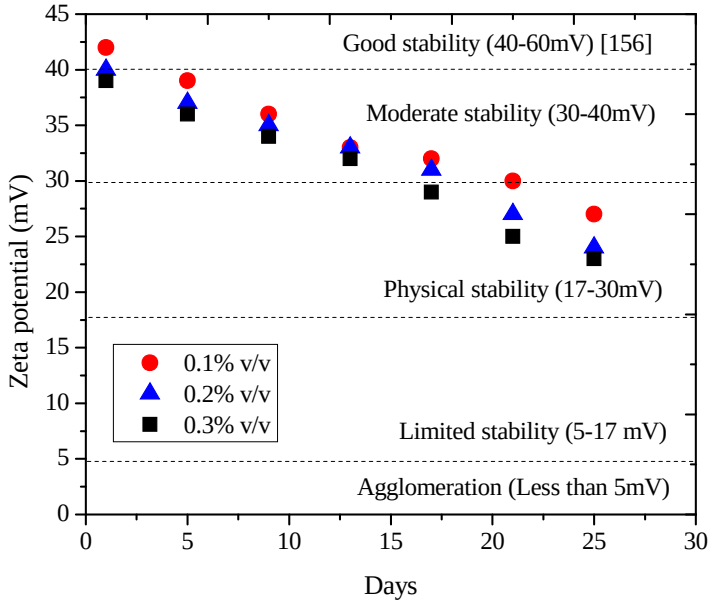

Figure 3.7: Zeta potential measurement of Al_2O_3 nanofluids

For the low concentration of nanoparticles, stability was measured with Zeta potential and UV-vis absorbance while for high concentration, thermal conductivity method was used.

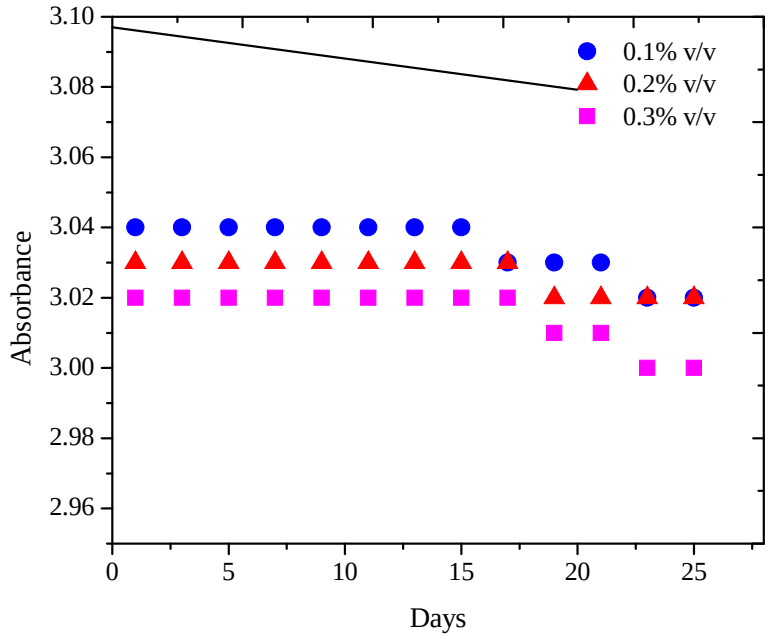

Figure 3.8: UV-vis absorbance measurement of Al_2O_3 nanofluids

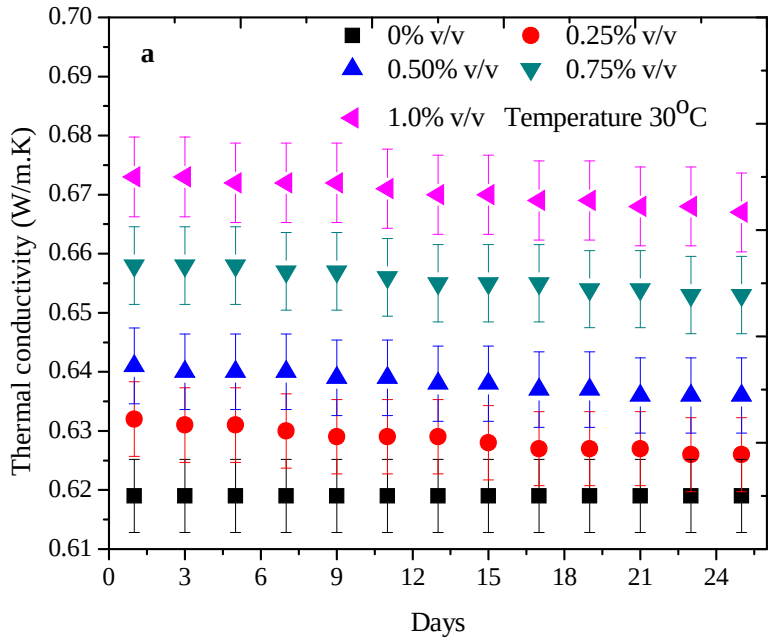

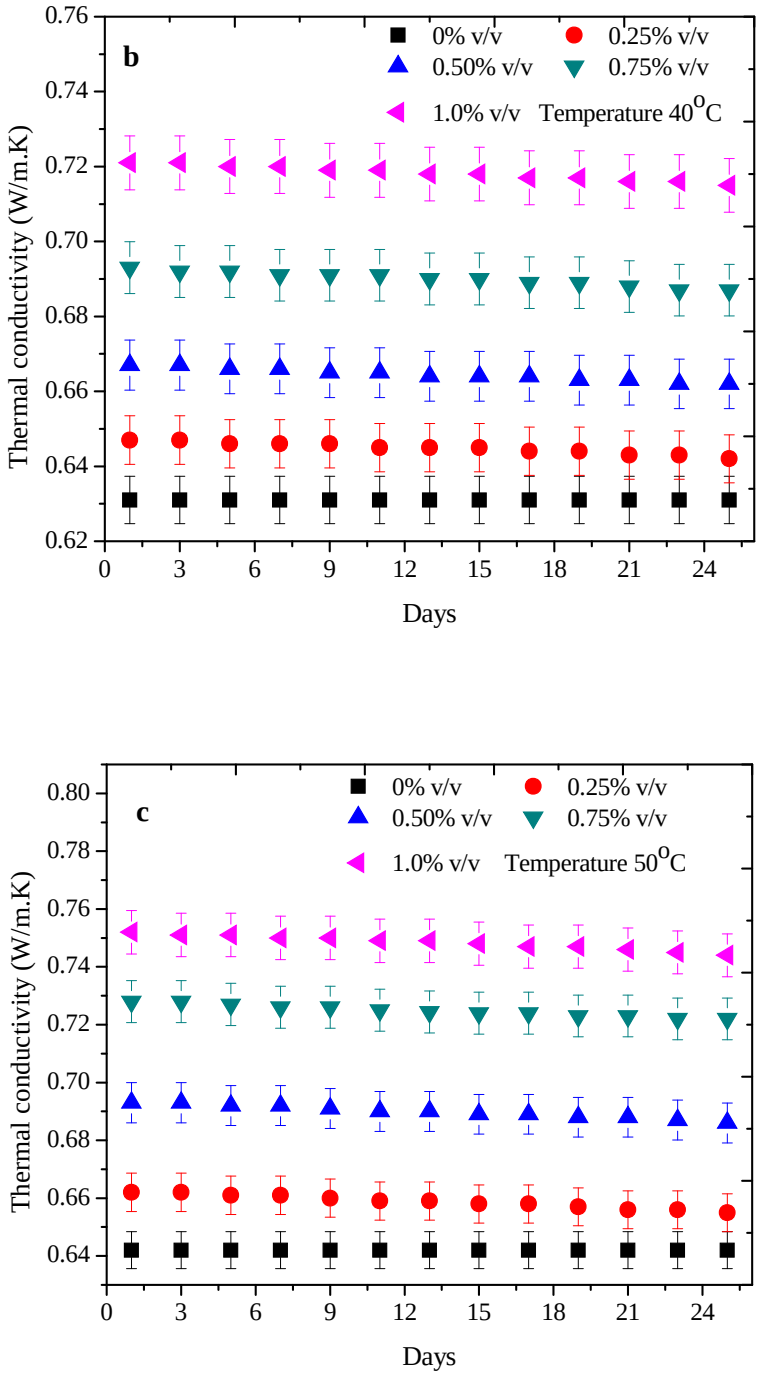

Figure 3.9: Thermal conductivity of Al_2O_3 nanofluids for different concentration and temperature (a) 30 ºC (b) 40 ºC (c) 50 ºC

The aluminum oxide nanofluids remained stable for more than 15 days as shown in figure 3.7. The value of Zeta potential was approximately 43 mV for 0.1% v/v concentration which indicates the good stability. While with increasing the particle concentration in base fluids, the value of Zeta

potential decreased as compared with 0.1% v/v concentration; but Zeta potential value near to 40 mV signifies the good stability.

On the 18th day, the value of Zeta potential was more than 30 mV so the nanofluids are in good stability. The minimum valve of Zeta potential was recorded 23 mV on 25th day which is more than limited stability value. The UV-vis absorbance measurement is shown in figure 3.8. According to the absorbance value, nanofluids remained stable up to 18th day after that absorbance starts decline. Furthermore value of absorbance also decreased with increasing the particle concentration as the linear relationship between the nanoparticles and intensity of absorbance. The thermal conductivity of aluminum oxide nanofluids is measured for 0.25% v/v - 1.0% v/v within the temperature range from 30 ^{o}C to 50 ^{o}C for 25 days. It was observed that thermal conductivity was decreased approximately 1% on when measured for 25 days which indicates the good stability of nanofluids with minimum agglomeration. The same results were observed at 40 ^{o}C and 50 ^{o}C fluid temperature.

3.5.2. Stability of copper oxide nanofluids

The copper oxide nanofluids are generally less stable than aluminum oxide nanofluids as the density of copper oxide is more as compared to aluminum oxide. The stability of copper oxide nanofluids with reference to Zeta potential values is shown in figure 3.10 and good stability was observed up to 10th day of nanofluids preparation.

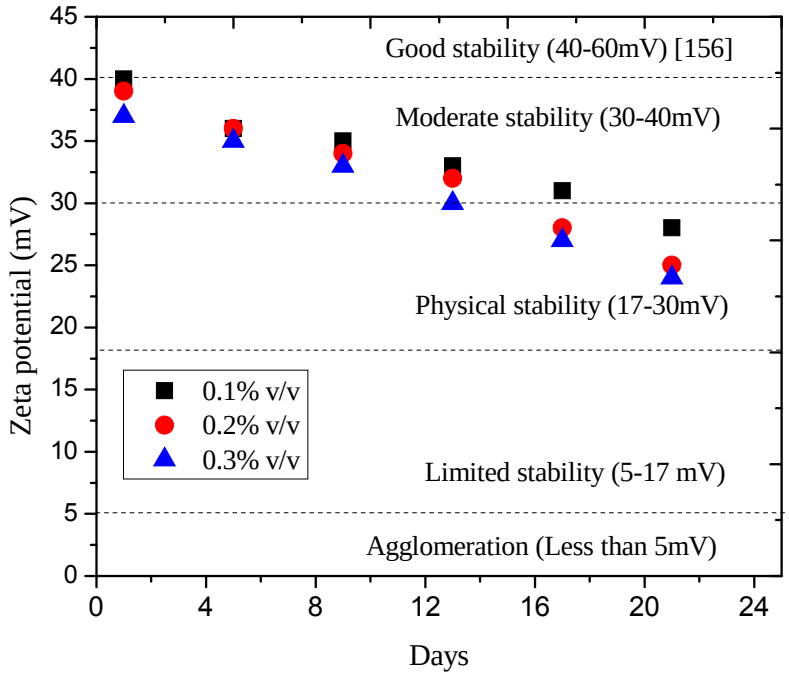

Figure 3.10: Zeta potential measurement of CuO nanofluids

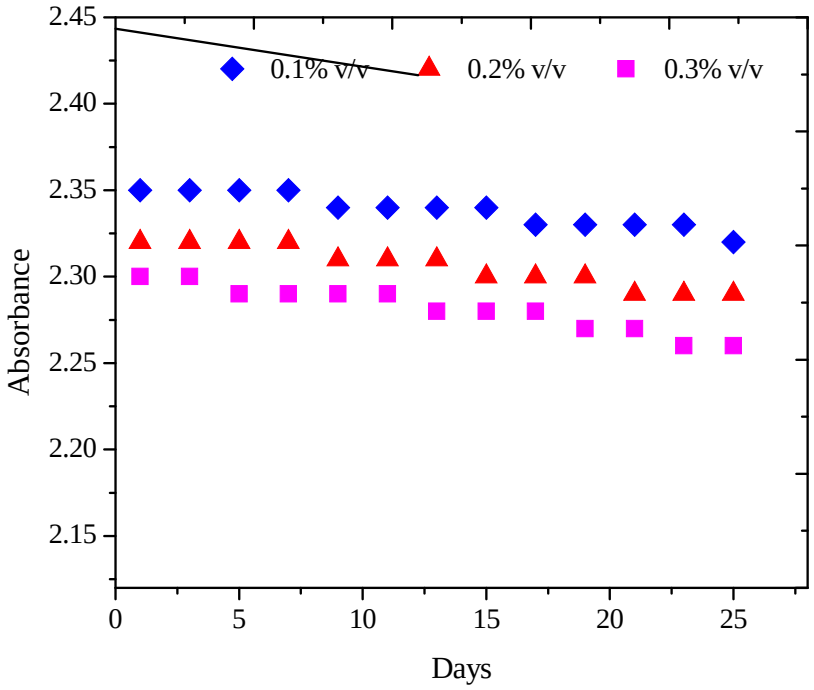

Figure 3.11: UV-vis absorbance measurement of CuO nanofluids

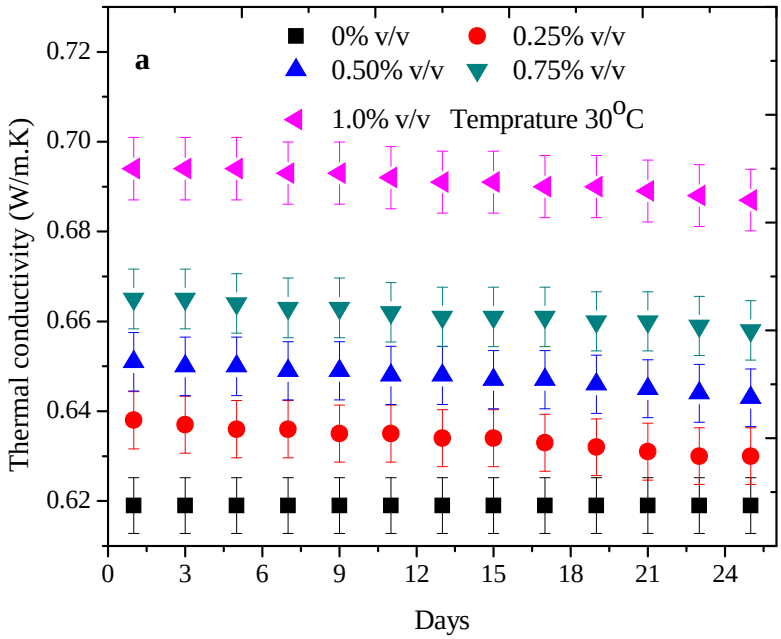

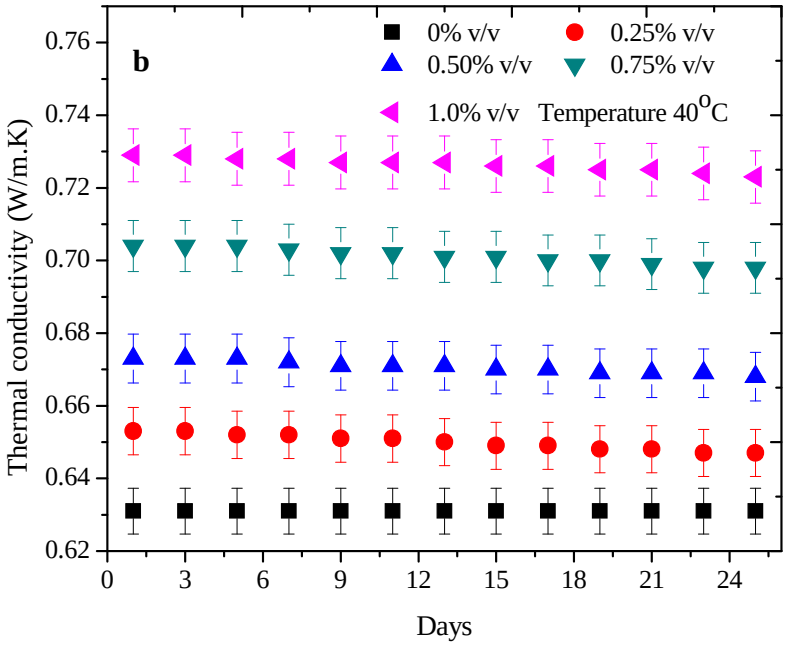

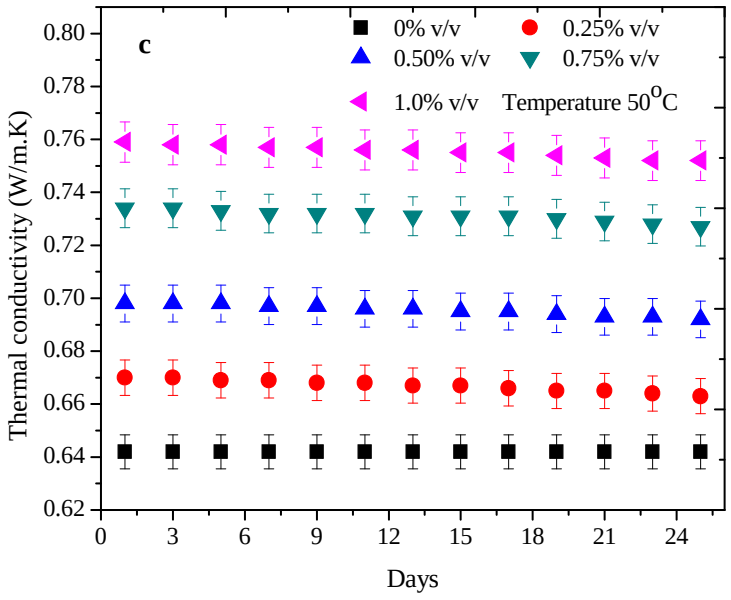

Figure 3.12: Thermal conductivity of CuO nanofluids for different concentration and temperature (a) 30 ºC, (b) 40 ºC & (c) 50 ºC

The value of Zeta potential was approximately 40 mV for 0.1% v/v concentration which indicates the good stability. While with increasing the particle concentration in base fluids, the value of Zeta potential is less as compared with 0.1% v/v concentration but Zeta potential value near to 40 mV signifies the good stability. On the 13^{th} day, the value of Zeta potential was more than 32 mV so the nanofluids are in good stability. The minimum valve of Zeta potential was recorded 22 mV for 0.3% v/v concentration on 25^{th} day which is more than limited stability value. The UV-vis absorbance measurement is shown in figure 3.11. According to the absorbance value, nanofluids remained stable up to 10^{th} day after that absorbance starts decline. Furthermore value of absorbance of copper oxide nanofluids decreased with increasing the particle concentration and absorbance intensity is less than aluminum oxide nanofluids. The thermal conductivity of copper oxide nanofluids is measured for 0.25% v/v – 1.0% v/v within the temperature range of 30 ^{o}C – 50 ^{o}C for 25 days as shown in the figure 3.12. It was observed that thermal conductivity was 0.638 W/m.K on first day and decreased up to 0.630 W/m.K on 25^{th} day which approximately decreased by only 1.25%, which indicates the good stability of nanofluids with minimum agglomeration. The same results were observed at 40 ^{o}C and 50 ^{o}C fluid temperature.

3.6. Thermophysical properties of nanofluids

This section presents detailed description of measurement of thermophysical properties i.e. thermal conductivity, density, specific heat and viscosity of water based aluminum oxide and copper oxide nanofluids for different concentration and fluid temperature. A correlation is also developed for thermal conductivity, viscosity and density.

3.6.1. Thermal conductivity

Some theoretical models are available to predict the effective thermal conductivity of nanofluids. More than 100 year ago Maxwell proposed a model for the enhancement of thermal conductivity of suspensions containing solid particles. Maxwell model suggested that thermal conductivity increases with volume fraction. To predict the Maxwell theory, a bench mark study on thermal conductivity of different nanofluids has been proposed. It was difficult to suspend solids in solution with higher concentration which limits the use of micro and mini sized particle for making a proper cooling liquid. In the most of studies transient hot wire method was used for measurement of the thermal conductivity of nanofluids. In this work, thermal conductivity of nanofluids was measured with KD2 PRO thermal analyzer, (Decagon Devices Inc. USA) which is also based on the transient hot wire method, apparatus measurement range 0.2 W/m.K to 2.0 W/m.k accuracy of ±5% of temperature ranges 30^{o}C – 90^{o}C. KD2 PRO thermal analyzer, as shown in figure 3.13, has a sensor needle (1.3 mm diameter and 60 mm long) consists thermistor and heating element, inserted in the

nanofluids sample to measure the thermal conductivity. The temperature of nanofluids maintained with temperature controller water bath which is shown in figure 3.14. Measurement of thermal conductivity takes one minute and reading is on the basis of temperature difference of sensor needle and nanofluids v/s time taken.

Figure 3.13: KD2 PRO thermal analyzer

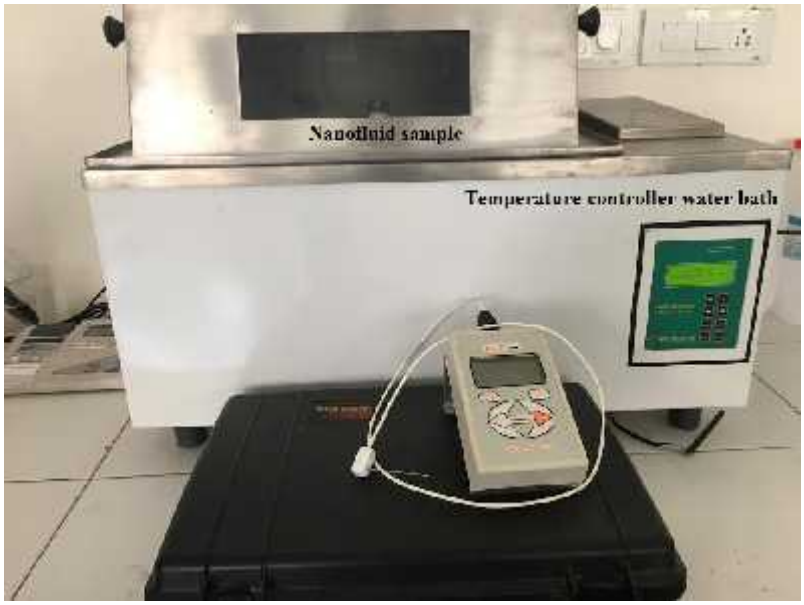

Figure 3.14: Thermal Property analyzer with temperature controller water bath

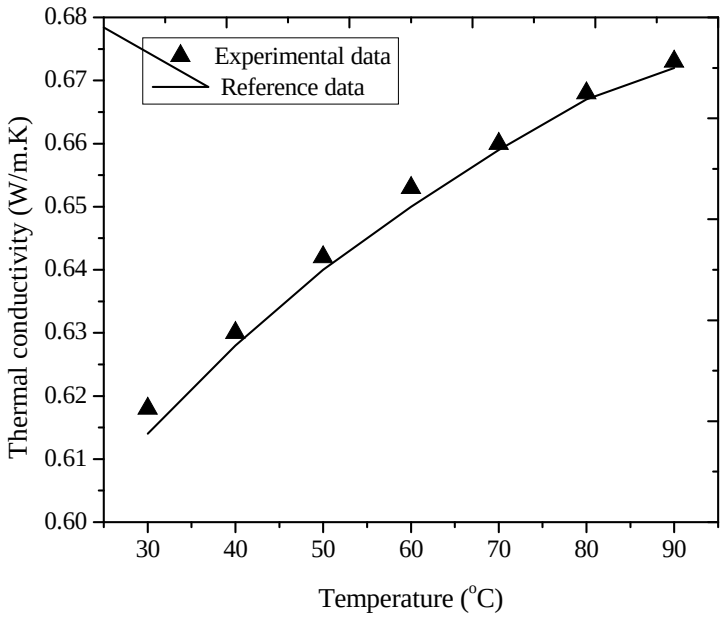

Figure 3.15: Comparison of experimental and references data of thermal conductivity

For each sample six reading have been taken and average value calculated. The thermal conductivity of distilled water was first measured prior to that of nanofluids to validate the accuracy of the instrument (KD2 Pro) as shown in the figure 3.15 in which results shows good relationship between the experimental and reference data and 0.64% error was observed.

3.6.1.1. Thermal conductivity of aluminum oxide

The thermal conductivity enhancement of nanofluids has great importance for heat transfer. It was observed that the thermal conductivity of water increases with increasing the temperature. The effect of nanoparticle concentration and temperature on the thermal conductivity of nanofluid is shown in figure 3.16. The thermal conductivity of nanofluids was more sensitive to temperature than that of the base fluid. Nanofluids have higher thermal conductivity than base fluid at elevated temperatures, because a rise in temperature accelerates particle movements.

For instance, the thermal conductivity of 0.1% v/v nanofluid at 30°C was 1% higher than that of the base fluid, whereas at 90°C it was approximately 2% higher than that of the base fluid while with increase the aluminum oxide particle concentration upto 1.0% v/v, the thermal conductivity of nanofluid at 30°C was 8% higher than that of the base fluid whereas at 80°C it was 21% higher than that of the base fluid. The experimental and fitted equation thermal conductivity of Al_2O_3 nanofluids is shown in figure 3.17.

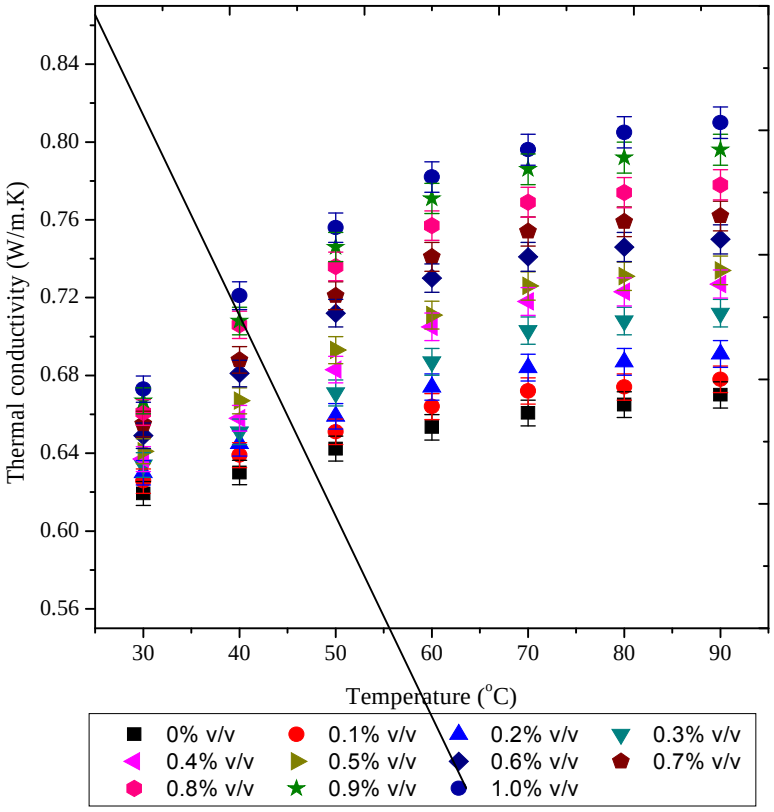

Figure 3.16: Experimental thermal conductivity of Al_2O_3 nanofluids with variation of nanoparticle concentration and fluid temperature

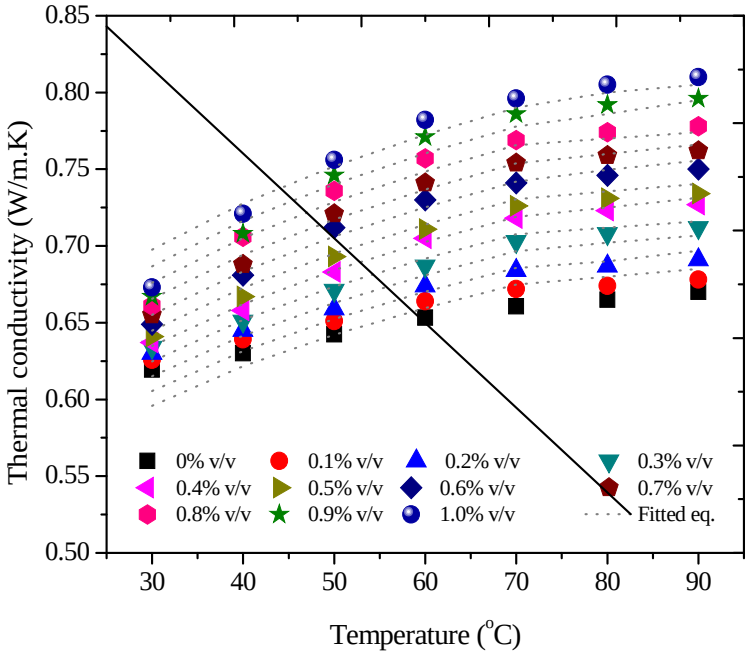

Figure 3.17: Experimental and fitted equation thermal conductivity of Al_2O_3 nanofluids

The percentage enhancement of thermal conductivity of alumina nanofluids with particle concentration and fluid temperature is given table 3.2. The enhancement of thermal conductivity declines as the temperature of fluid rise from 80°C to 90°C. A liquid nanolayer is the key for enhancing the thermal conductivity of nanofluids, because, it acts as a thermal bridge between the base fluid and nanoparticle. A similar result has been reported by Das et al. [157] for 1 - 4% v/v of Al_2O_3/water nanofluids in the temperature range 21–51°C.

They concluded that the considerable improvement in thermal conductivity of nanofluids at high temperatures is mainly due to the Brownian motion of nanoparticles. Jang and Choi [158], Koo and Kleintreuer [58], Prasher et al. [159] and Saxena et al. [19] also attributed the increase in thermal conductivity of nanofluids at high temperatures to the Brownian motion of nanoparticles.

Table 3.2: Percentage enhancement of thermal conductivity of Al_2O_3 nanofluids

	Aluminum oxide nanoparticles volume concentration (v/v %)									
Temperature (°C)	**0.1**	**0.2**	**0.3**	**0.4**	**0.5**	**0.6**	**0.7**	**0.8**	**0.9**	**1**
30	1.03	1.73	2.37	2.86	3.50	4.80	5.76	6.73	7.70	8.67
40	1.41	2.36	3.32	4.43	5.86	8.08	9.19	12.05	12.36	14.43
50	1.35	2.60	4.46	6.33	7.89	10.85	12.25	14.58	16.14	17.70
60	1.63	3.16	5.15	7.91	8.83	11.74	13.42	15.87	18.01	19.69
70	1.71	3.53	6.41	8.68	9.89	12.16	14.13	16.40	18.97	20.48
80	1.35	3.31	6.47	8.72	9.92	12.18	14.14	16.39	19.10	21.05
90	1.19	3.13	6.27	8.51	9.55	11.94	13.73	16.12	18.81	20.90

3.6.1.2. Thermal conductivity of copper oxide nanofluids

The thermal conductivity of nanofluids was also found to increase with an increase in the CuO particle volume concentration and temperature and these results are in good agreement with the literature data reported by Zhu et al. [72] and Khedkar et al. [56]. The enhancement of thermal conductivity was more than 2% for a low concentration (0.1% v/v) and this enhancement increased up to approximately 25% for the 1.0% volume concentration as shown in the figure 3.18. The increase in thermal conductivity with volume fraction might be because of higher thermal conductivity of solids (i.e. nanoparticles) than that of liquids (i.e. base fluids) ; and also because of the decrease in distance between nanoparticles with increase in particle volume concentration as revealed by Khedkar et al. [56]. With 0.1% of CuO nanoparticles at 30°C, the enhancement of thermal conductivity was only 2% and at 90°C this enhancement increased up to approximately 4%.

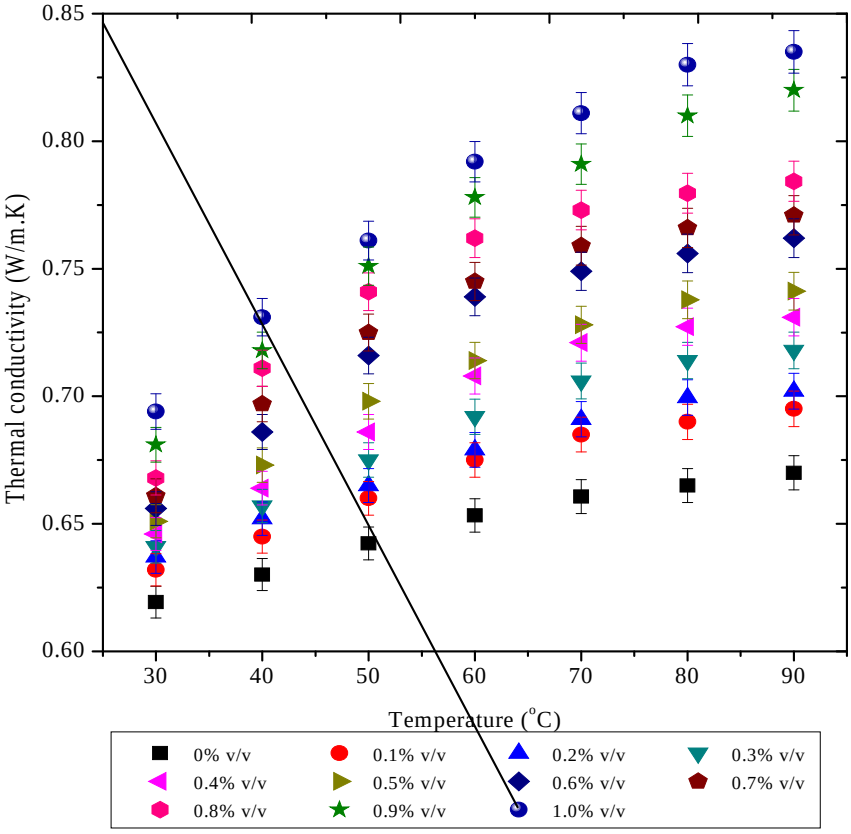

Figure 3.18: Experimental thermal conductivity of CuO nanofluids with variation of nanoparticle concentration and fluid temperature

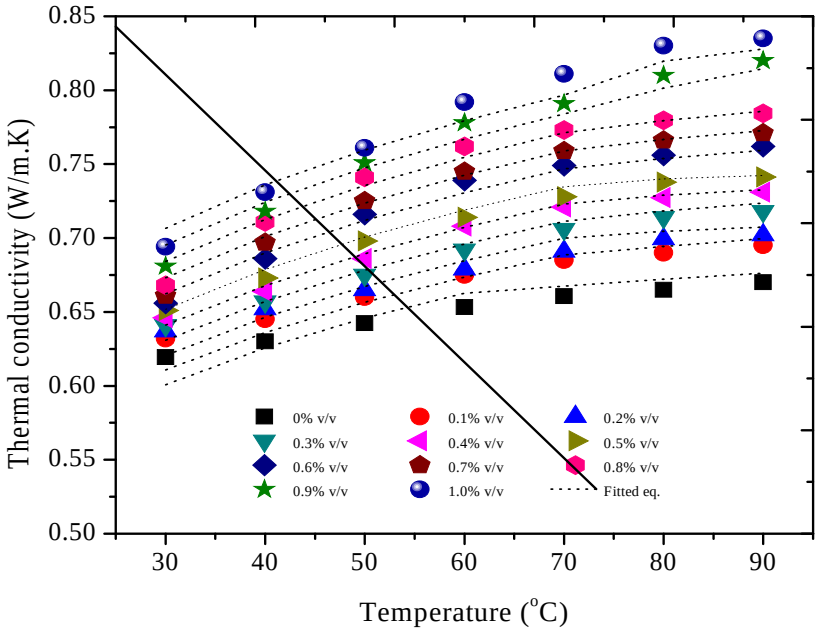

Figure 3.19: Experimental and fitted equation thermal conductivity of CuO nanofluids

Table 3.3: Percentage enhancement of thermal conductivity of CuO nanofluids

	Percentage enhancement of thermal conductivity									
	Copper oxide nanoparticles volume concentration (%)									
Temperature (ºC)	**0.1**	**0.2**	**0.3**	**0.4**	**0.5**	**0.6**	**0.7**	**0.8**	**0.9**	**1**
30	2.05	2.86	3.50	4.31	5.12	5.93	6.73	7.86	9.96	12.06
40	2.36	3.48	4.27	5.38	6.81	8.87	10.62	12.84	13.95	16.01
50	2.75	3.53	5.09	6.80	8.67	11.47	12.87	15.36	16.92	18.47
60	3.32	3.93	5.92	8.37	9.29	13.11	14.03	16.63	19.08	21.23
70	3.68	4.59	6.86	9.13	10.19	13.37	14.88	17.00	19.73	22.75
80	3.76	5.19	7.37	9.37	10.95	13.68	15.19	17.23	21.80	24.81
90	3.75	4.78	7.16	9.10	10.63	13.73	15.07	17.06	22.39	24.63

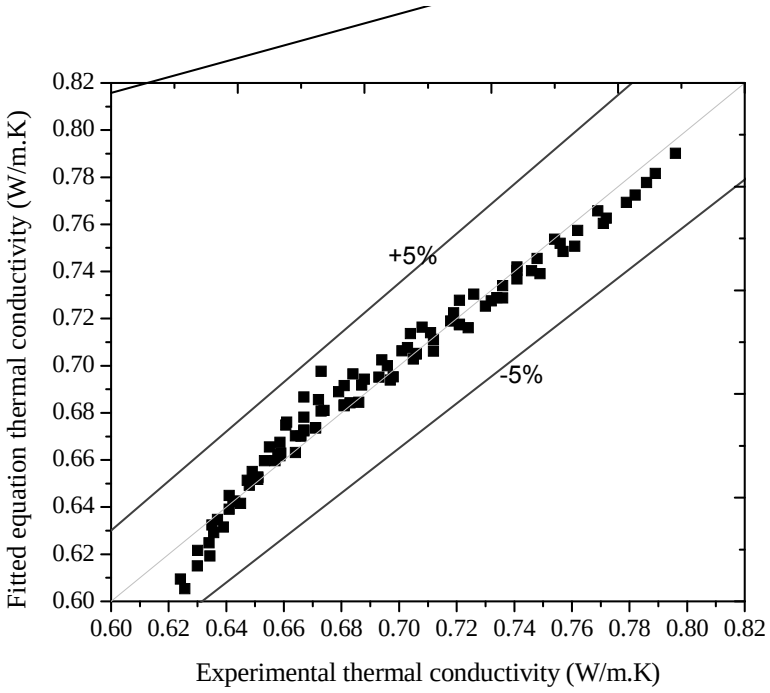

Figure 3.20: Comparison of experimental thermal conductivity and fitted equation thermal conductivity of Al_2O_3 nanofluids

For a higher particle concentration of 1.0%, the enhancement in thermal conductivity increased from 12% to 25% as the temperature was raised from 30ºC to 90ºC. The percentage enhancement of thermal conductivity of copper oxide nanofluids with particle concentration and fluid temperature is given table 3.3.

A similar observation on the increase of thermal conductivity of CuO nanofluids with temperature was reported by Das et al. [157] and Sitprasert et al. [7]. This may be due to the weakening of intermolecular forces between nanoparticles and base fluid.

A mathematically correlation was developed to predicted the thermal conductivity of water based aluminum oxide and copper oxide nanofluids which is given as the equation 3.2. There is good agreement between the experimental thermal conductivity and predicted model's thermal conductivity values for aluminum oxide and copper oxide nanofluids as shown the figures 3.20 and 3.21 respectively. The Chi-square value 0.00934 and 0.00764 was observed for aluminum oxide and copper oxide nanofluids, respectively. The R-square value observed for aluminum oxide nanofluids was 0.97 and copper oxide nanofluids was 0.98.

$$k_{nf} = k1(1+¤)^{m} T^{n} \tag{3.2}$$

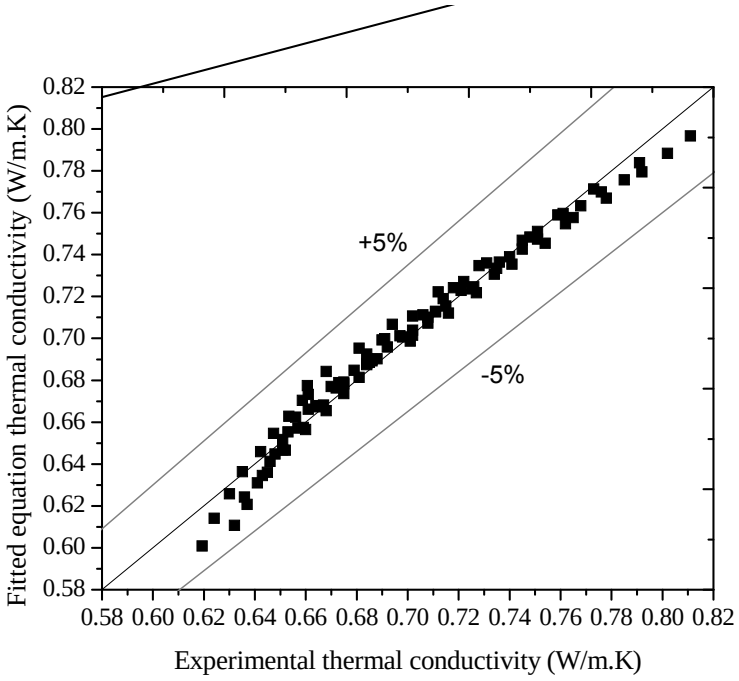

Figure 3.21: Comparison of experimental thermal conductivity and fitted equation thermal conductivity of CuO nanofluids

3.6.2. Viscosity

The viscosity of nanofluids influences the pressure drop, Reynolds number and pumping power. To measure the viscosity of prepared nanofluids Brookfield Viscometer DV-II plus pro of accuracy ±1.0% of full scale specific spindle running at specific speed was used. The instrument had temperature sensing range –10°C to 200°C with accuracy of ±1.0 °C. While measuring the viscosity

of sample, viscous drag force of fluid is measured with calibrated spring deflection which is operated by rotary transducer. Viscosity of nanofluids has measured at different concentration of nanoparticles at different temperature ranges which was controlled by in built water bath.

3.6.2.1 Viscosity of aluminum oxide

The variation of viscosity of aluminum oxide nanofluids (0–1 % v/v) with temperature (in the range 30–90°C) is shown in figure 3.22. The viscosity of nanofluids increased with increasing the particle volume concentration and decreased with increase in temperature. The experimental and predicted model viscosity of Al_2O_3 nanofluids is shown in figure 3.23. With an increase in particle concentration from 0.1 to 1.0 vol%, the viscosity of nanofluid at 30°C is 2.3% and 19.82% respectively higher than that of the base fluid. Prasher et al. [159] and Hojjat et al. [160] reported similar trends in viscosity change of Al_2O_3/water nanofluid with volume fraction of particles. In addition, Das et al. [130] and Putra et al. [21] also reported that the viscosity of nanofluids increases with increasing the alumina particle concentration from 1% v/v to 4% v/v and that the nanofluids behave as Newtonian fluids. With an increase in temperature from 30°C to 90°C, the value of viscosity decreased from 0.816 cP to 0.328 cP for 0.1% nanofluid and from 0.994 cP to 0.391 cP for 1.0% nanofluid. The viscosity of 1.0% v/v nanofluid at 90°C was only 16% higher than that of the base fluid.

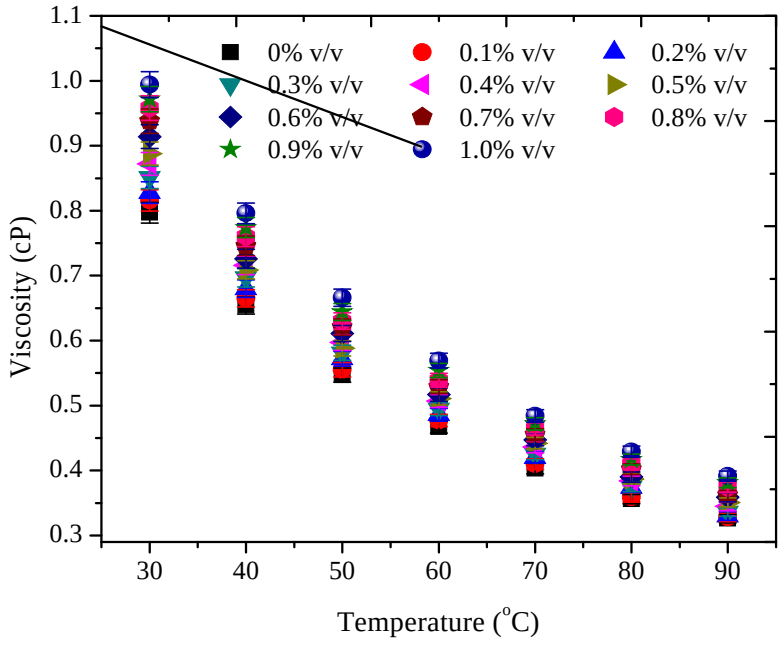

Figure 3.22: Variation of viscosity with aluminum oxide nanoparticle concentration and fluid temperature

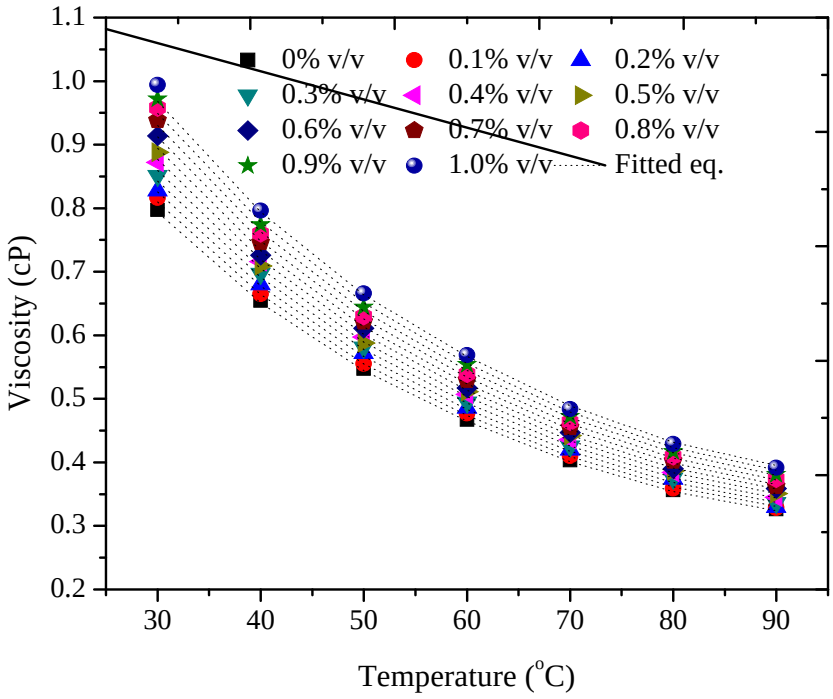

Figure 3.23: Experimental and fitted equation viscosity data with aluminum oxide nanoparticle concentration and fluid temperature

Therefore, it can be concluded that an increase in temperature not only decreases the viscosity of nanofluids, but also decreases the difference between the viscosities of nanofluids of different concentrations and the base fluid.

Table 3.4: Percentage increase in viscosity of aluminum oxide nanofluids

	Aluminum oxide nanoparticles volume concentration (% v/v)									
Temperature (°C)	**0.1**	**0.2**	**0.3**	**0.4**	**0.5**	**0.6**	**0.7**	**0.8**	**0.9**	**1**
30	2.33	3.74	6.37	8.60	10.25	12.80	15.03	16.81	18.00	19.82
40	1.65	3.82	6.13	8.66	7.76	9.92	12.33	13.95	15.50	17.84
50	1.44	4.37	5.86	8.38	6.97	10.47	11.92	13.17	15.06	17.87
60	2.10	3.91	5.59	7.89	8.61	9.67	11.72	13.36	15.70	17.93
70	1.71	4.05	5.28	7.57	8.82	9.84	11.43	13.15	14.62	16.74
80	0.84	4.81	4.99	7.29	8.01	8.72	11.44	13.04	14.63	17.02
90	0.61	1.21	2.98	5.51	7.12	9.19	9.94	12.83	14.44	16.71

The reason behind the decrease in viscosity with rise in temperature could be the decrease in intermolecular forces at high temperatures. The increasing temperature increases the average

distance between molecules, and hence decreases the average attractive forces. If the temperature is increased, the intermolecular forces become weak and kinetic energy increases. As the temperature increases the kinetic energy can overcome intermolecular forces, hence viscosity decreases and liquids can flow easily. Apart from the molecular forces, pH value of base fluid, nanoparticles shape and size also effects the viscosity of nanofluids. The results for different concentrations showed the similar trends in viscosity variation. Pastoriza-Gallego et al. [81] and Namburu et al. [161] also presented similar observation on the influence of temperature on viscosity of nanofluids. The percentage increase of viscosity of alumina nanofluids with particle concentration and fluid temperature is given table 3.4.

3.6.2.2 Viscosity of copper oxide

The effect of copper oxide nanoparticles concentration and fluid temperature on the viscosity of nanofluids is shown in figure 3.24. The experimental viscosity of copper oxide nanofluids were compared with the developed mathematical correlation as shown in figure 3.25. The viscosity of the nanofluids increased with increase in copper oxide nanoparticles concentration, while it decreased with increase in fluid temperature.

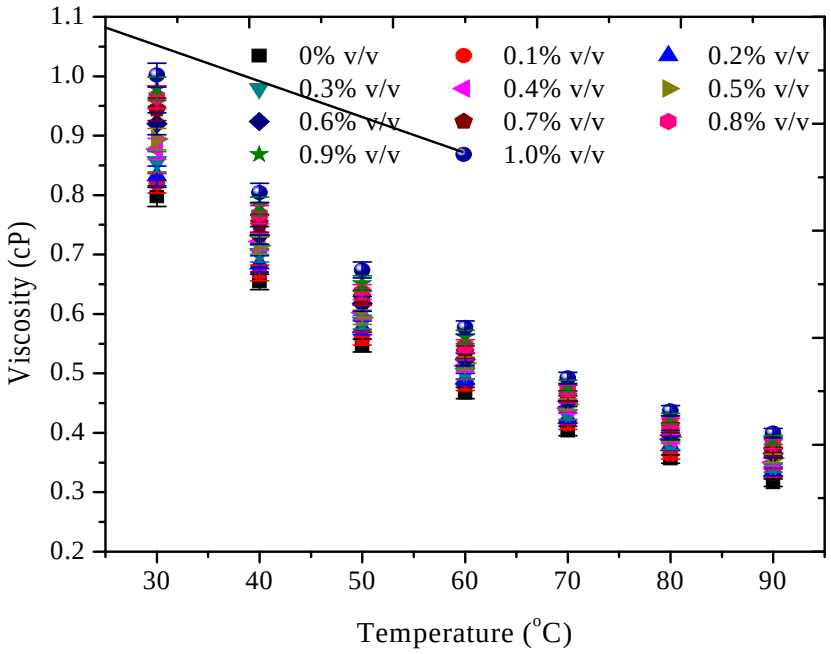

Figure 3.24: Effect of copper oxide nanoparticle concentration and fluid temperature on viscosity

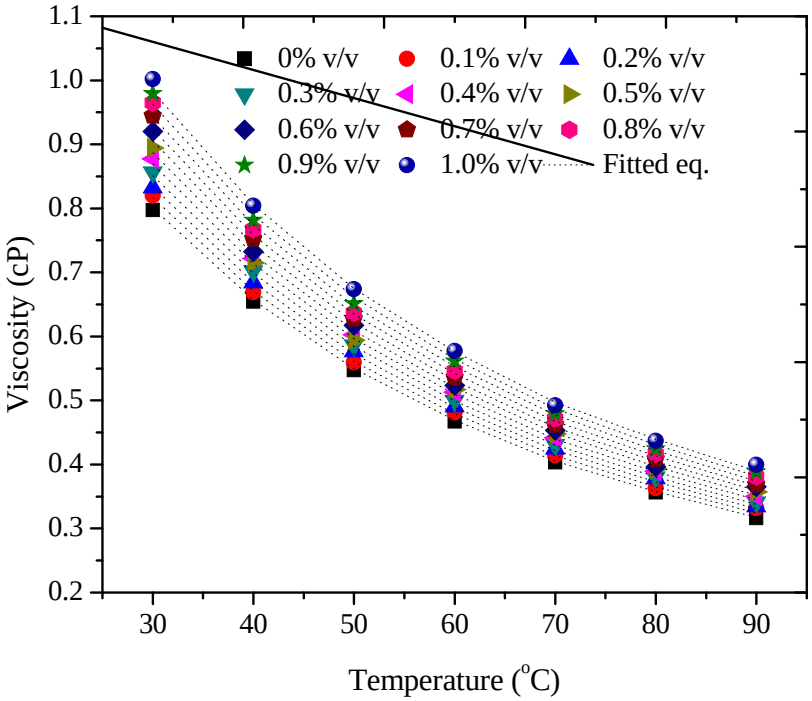

Figure 3.25: Experimental and fitted equation viscosity of copper oxide nanoparticle concentration and fluid temperature

The viscosity of nanofluids increased from 2.8% to 20.46% as the nanoparticles concentration was increased from 0.1% v/v to 1.0% v/v. For low concentration of nanoparticles, nanofluids showed the Newtonian behaviour, while with increase in particles concentration, nanofluids behaviour changed to non-Newtonian.

Increase in viscosity with increasing the nanoparticle loading also leads to clustering phenomenon. With increasing the concentration, the internal stresses become significant, which also contribute to rise in viscosity of nanofluids as compared to the base fluid. The fluid temperature had a great influence on viscosity of nanofluids. As the temperature was increased from 30ºC to 90ºC, viscosity decreased by 2% for 1.0% v/v concentration of nanoparticles. The reason behind the decrease in viscosity with rise in temperature could be the decrease in molecular forces with increasing the temperature. A similar finding on viscosity of nanofluids for different concentrations and fluid temperature has been reported by other authors [21,75,76,80,81,160].

Table 3.5: Percentage increase in viscosity of copper oxide nanofluids

	Copper oxide nanoparticles volume concentration (v/v %)									
Temperature (°C)	**0.1**	**0.2**	**0.3**	**0.4**	**0.5**	**0.6**	**0.7**	**0.8**	**0.9**	**1**
30	2.80	4.26	6.92	9.18	10.86	13.39	15.62	17.40	18.61	20.46
40	2.24	4.46	6.80	9.37	8.54	10.68	13.09	14.72	16.28	18.66
50	2.15	5.12	6.67	9.23	7.93	11.37	12.83	14.12	16.00	18.84
60	2.91	4.79	6.53	8.90	9.69	10.74	12.79	14.45	16.79	19.06
70	2.66	5.06	6.38	8.74	10.06	11.08	12.68	14.42	15.90	18.09
80	1.93	5.94	6.24	8.62	9.44	10.15	12.85	14.48	16.08	18.54
90	4.82	5.53	7.33	9.87	11.51	13.47	14.25	17.04	18.60	20.88

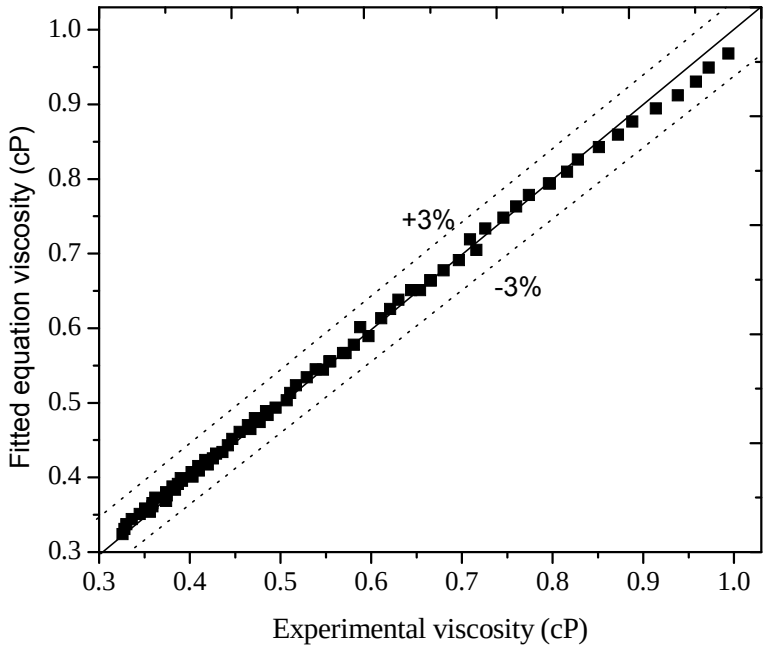

Figure 3.26: Comparison of experimental viscosity and fitted equation viscosity of Al_2O_3 nanofluids

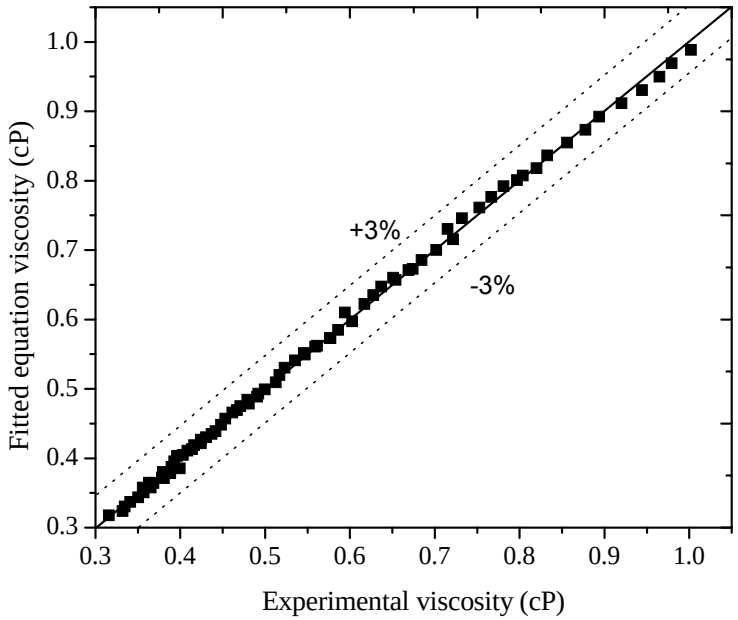

Figure 3.27: Comparison of experimental viscosity and fitted equation viscosity of CuO nanofluids.

The percentage increase in viscosity of copper oxide nanofluids with particle concentration and fluid temperature is given table 3.5. A fitted equation was developed to predict the viscosity of water based aluminum oxide and copper oxide nanofluids which is given as the equation 3.3. There is good agreement between the experimental viscosity and predicted model's viscosity values for aluminum oxide and copper oxide nanofluids as shown the figures 3.26 and 3.27, respectively. The Chi-square value 0.00734 and 0.00564 was observed for aluminum oxide and copper oxide nanofluids, respectively. The R-square value for aluminum oxide nanofluids 0.97 and copper oxide nanofluids 0.98 is observed.

$$«_{nf} = «_{bf}(1+¤)^{m}T^{n} \qquad (3.3)$$

3.6.3. Density

Density is an important properties in nanofluids which is directly affects the Reynolds number and pressure loss. In this study density of nanofluids has been measured with specific gravity bottle of capacity 5 ml. and it is closed the glass stopper which having a capillary hole in it. Accuracy of specific gravity bottle was ±0.2%. A digital pipette with accuracy of ±0.1% has been used to accurate measurement of the 5 ml nanofluids.

3.6.3.1. Density of aluminum oxide nanofluids

The variation of density of Al_2O_3/water nanofluids of different concentrations with temperature is shown in figure 3.28. The density of nanofluids increased with increase in particle concentration. In comparison with the base fluid, the density was 0.3% higher for 0.1% v/v nanofluid and 2.8% higher for 1.0% v/v nanofluids at 30°C. The density of base fluid as well as nanofluids declined with increasing the temperature. The deviation of density of nanofluids from the base fluid increased gradually with rise in temperature. At temperature 30°C, the deviation of density of 1.0% v/v nanofluid from the base fluid was 2.82%, while at 90°C this value increased to 2.92%. A similar observation on the effect of temperature on density of water-based alumina nanofluids was reported by Vajjha et al. [162] and Mahabul et al. [163]. The comparison of experimental data of density of aluminum oxide nanofluids with predicted model data of density is shown in figure 3.29. The percentage increase in density of aluminum oxide nanofluids with particle concentration and fluid temperature is given table 3.6.

3.6.3.2. Density of copper oxide

The increase in density of nanofluids as compared to the base fluid was 0.3% for 0.1% v/v particle concentration and 4.41% for particle concentration of 1.0% v/v. With a rise in temperature, density of base fluid and nanofluids declined. The deviation of density of nanofluids from base fluid increased gradually with rise in temperature.

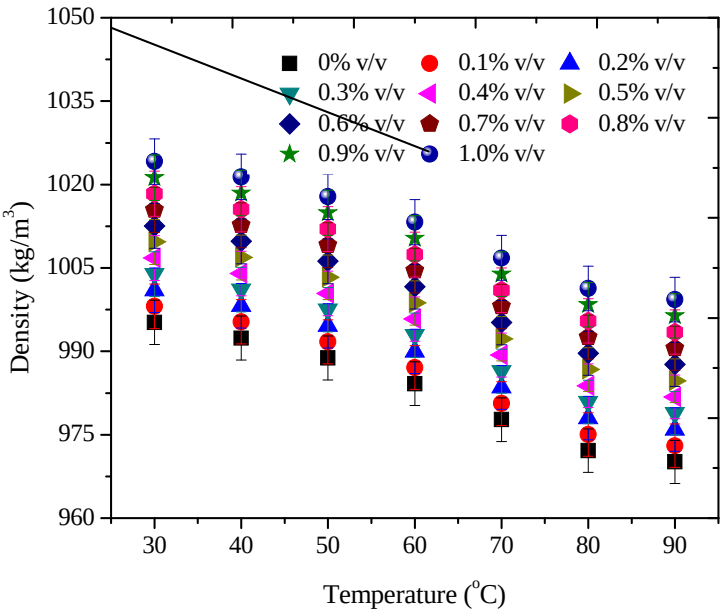

Figure 3.28: Effect of particle concentration and fluid temperature on variation of density of aluminum oxide based nanofluids

At temperature 30°C, deviation of nanofluids density from the base fluid was 4.41%, while at 70°C this value increased to 5.75% for 1.0% v/v concentration. The comparison of experimental data of density of copper oxide nanofluids with predicted model data of density is shown in figure 3.31. The percentage increase in density of copper oxide nanofluids with particle concentration and fluid temperature is given table 3.7.

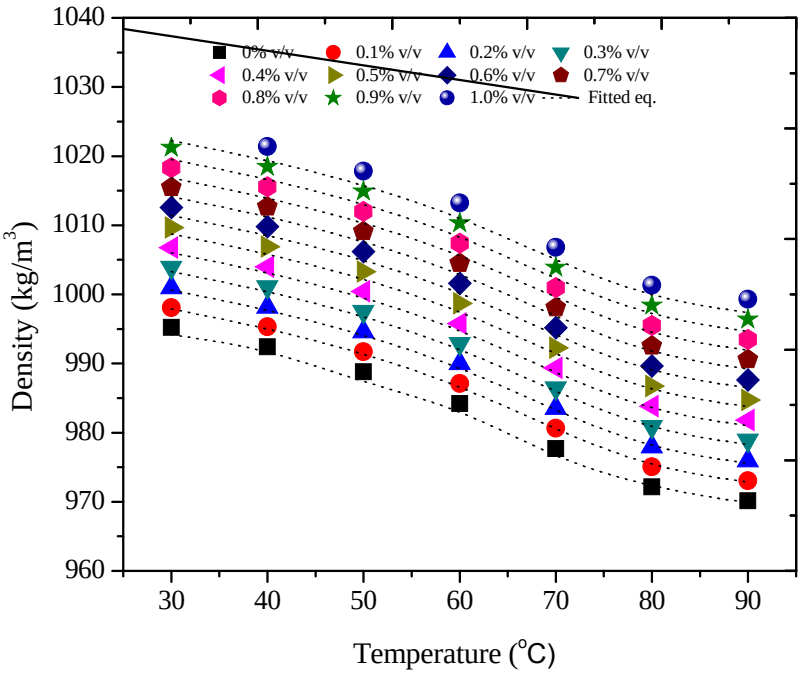

Figure 3.29: Comparison of experimental data with fitted equation data of density

Table 3.6: Percentage increase in density of aluminum oxide nanofluids with particle concentration and fluid temperature

	Aluminum oxide nanoparticles volume concentration (v/v %)									
Temperature (°C)	**0.1**	**0.2**	**0.3**	**0.4**	**0.5**	**0.6**	**0.7**	**0.8**	**0.9**	**1**
30	0.290	0.578	0.865	1.150	1.433	1.715	1.995	2.273	2.550	2.826
40	0.291	0.580	0.868	1.154	1.438	1.721	2.002	2.282	2.560	2.836
50	0.292	0.583	0.872	1.160	1.445	1.729	2.012	2.293	2.572	2.849
60	0.294	0.587	0.878	1.167	1.454	1.740	2.024	2.307	2.588	2.867
70	0.297	0.592	0.885	1.177	1.467	1.755	2.042	2.327	2.610	2.892
80	0.299	0.597	0.892	1.186	1.478	1.768	2.057	2.344	2.629	2.913
90	0.300	0.598	0.895	1.189	1.482	1.773	2.063	2.350	2.637	2.921

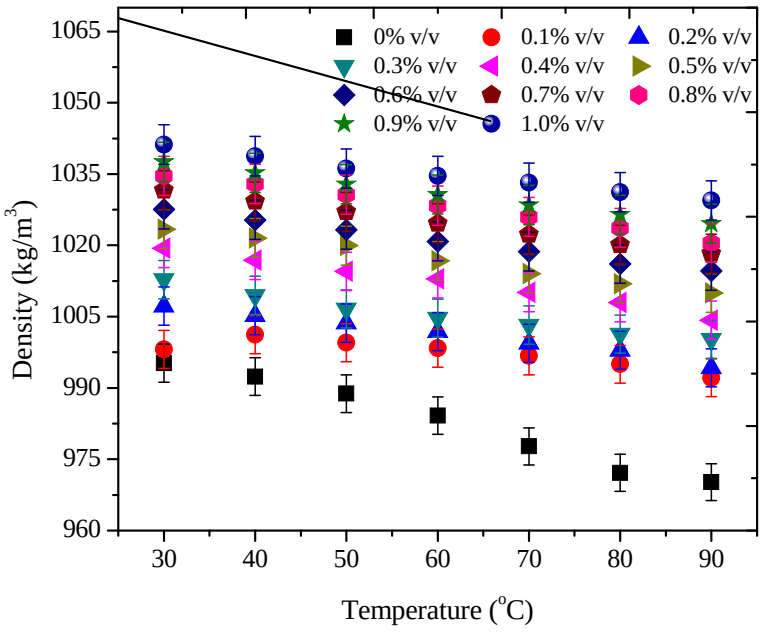

Figure 3.30: Effect of copper oxide particle concentration and fluid temperature on variation of density of copper oxide nanofluids

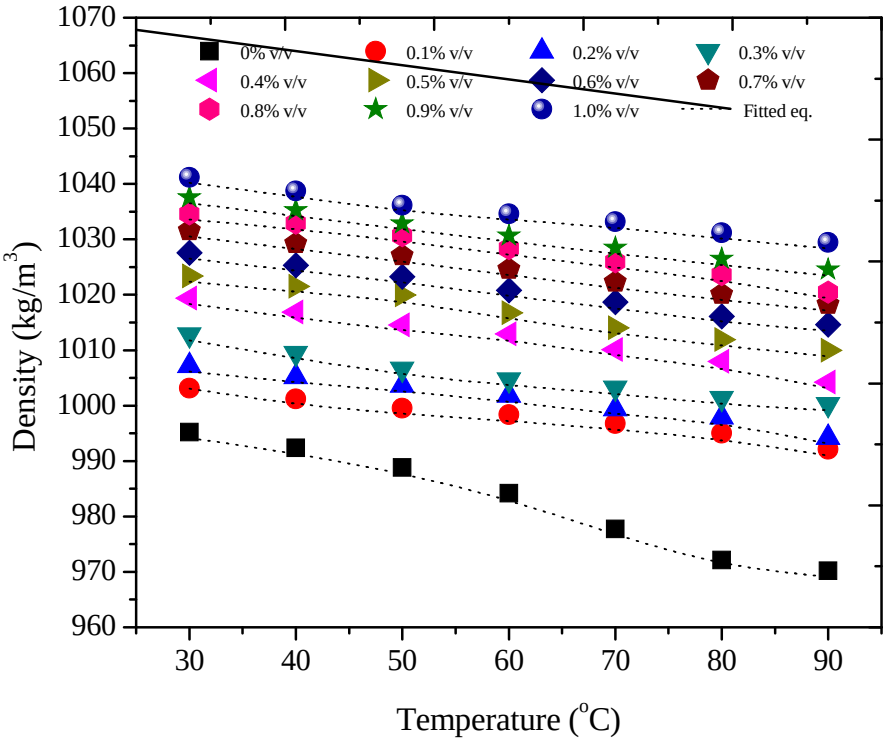

Figure 3.31: Comparison of experimental data with fitted equation data of density of copper oxide nanofluids

A mathematically correlation was developed to predicted the density of water based aluminum oxide and copper oxide nanofluids which is given as the equation 3.4. The experimental density and predicted model's density values for aluminum oxide and copper oxide nanofluids as shown the figures 3.32 and figure 3.33 respectively. The value coefficient "m" is 3697.77 used in developed correlation.

Table 3.7: Percentage increase in density of copper oxide nanofluids with particle concentration and fluid temperature

	Copper oxide nanoparticles volume concentration (v/v %)									
Temperature (ºC)	**0.1**	**0.2**	**0.3**	**0.4**	**0.5**	**0.6**	**0.7**	**0.8**	**0.9**	**1**
30	0.291	1.191	1.736	2.372	2.756	3.149	3.523	3.810	4.081	4.418
40	0.879	1.273	1.692	2.407	2.853	3.213	3.577	3.921	4.138	4.461
50	1.071	1.477	1.770	2.535	3.053	3.370	3.723	4.063	4.268	4.569
60	1.420	1.763	2.040	2.841	3.200	3.589	3.947	4.294	4.513	4.873
70	1.910	2.173	2.544	3.208	3.586	4.021	4.359	4.706	4.937	5.372
80	2.296	2.585	2.916	3.554	3.931	4.328	4.703	5.033	5.292	5.727
90	2.212	2.419	3.004	3.394	3.941	4.381	4.722	4.928	5.308	5.757

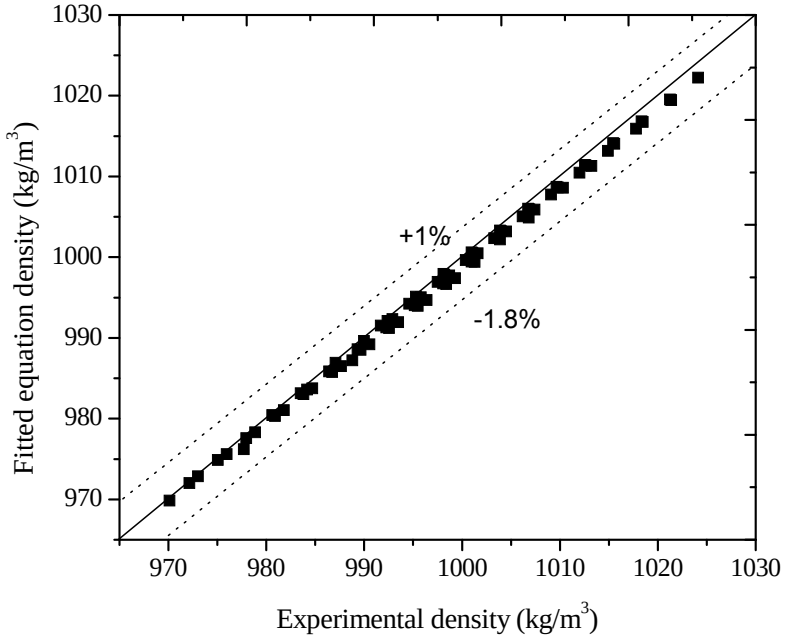

Figure 3.32: Comparison of experimental density data and fitted equation density data of aluminum oxide nanofluids

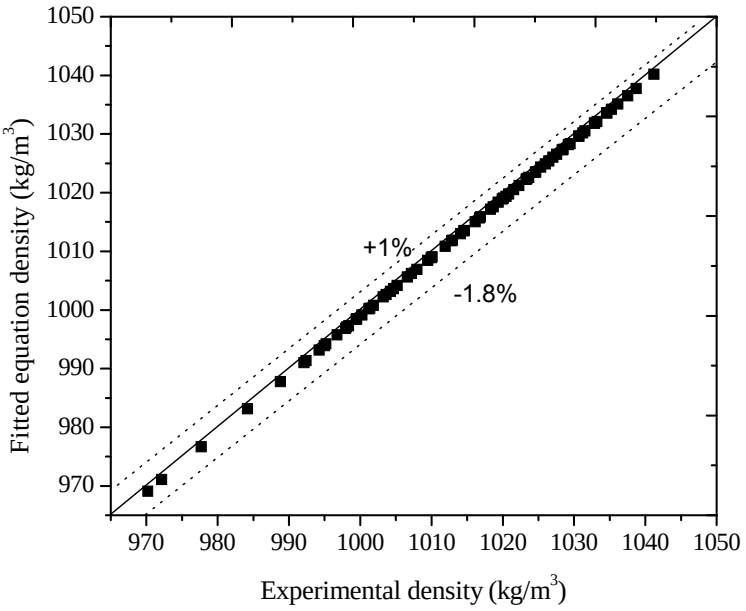

Figure 3.33: Comparison of experimental density data and fitted equation density data of copper oxide nanofluids

The Chi-square value 0.0105 and 0.0084 was observed for aluminum oxide and copper oxide nanofluids, respectively. The R-square value for aluminum oxide and copper oxide nanofluids 0.99 was observed.

$$\circ_{nf} = \circ_{bf}(1-¤) + ¤ \times m \qquad (3.4)$$

3.6.4. Specific heat capacity.

The specific heat capacity of nanofluids in the temperature range 30°C – 90°C was measured using a differential scanning calorimeter (DSC, Mettler Toledo) in three hierarchical steps: 1) measurement with two empty pans, 2) measurement with one pan containing a reference sample of known specific heat, keeping the other pan empty, and 3) measurement with one pan containing the reference sample and the other pan filled with nanofluid.

3.6.4.1. Variation of specific heat capacity of aluminum oxide nanofluids

The variation of specific heat of nanofluid with nanoparticles concentration and temperature is shown in figure 3.34. The specific heat of nanofluids was found to be more sensitive to alumina nanoparticle concentration than temperature. It was observed that the specific heat of base fluid increased by only 0.7% as the temperature was increased from 40°C to 90°C.

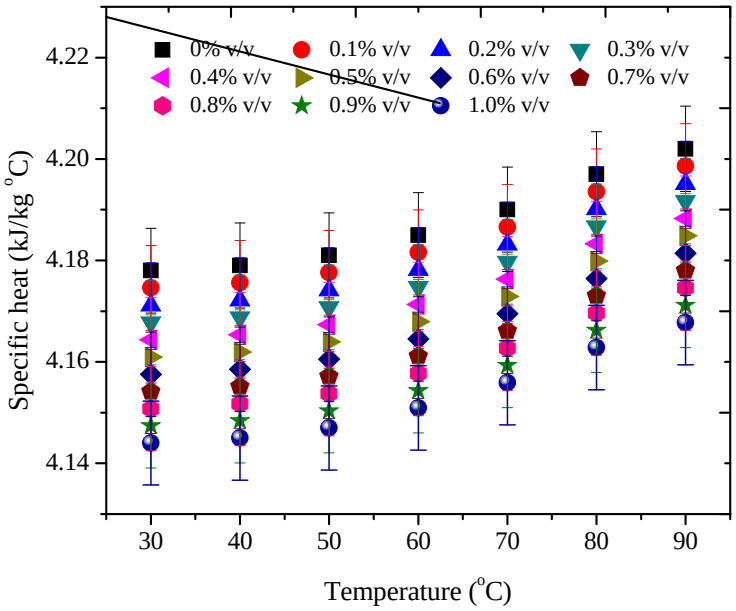

Figure 3.34: Effect of temperature and alumina nanoparticles on specific heat capacity of nanofluids

These results indicated that the heat capacity of nanofluids increases with temperature but diminishes with increase in particle volume concentration. This is because of the fact that the specific heat of alumina nanoparticles is lower than that of the base fluid (i.e. water). Similar outcomes on the variation of specific heat of different nanofluids with temperature and particle concentrations have been presented in many studies [161,164]. The percentage change in specific heat capacity with different aluminum oxide nanoparticle concentrations is given in table in 3.8.

Table 3.8: Percentage change in specific heat capacity with different aluminum oxide nanoparticle concentrations

	Aluminum oxide nanoparticles volume concentration (v/v %)									
Temperature (°C)	**0.1**	**0.2**	**0.3**	**0.4**	**0.5**	**0.6**	**0.7**	**0.8**	**0.9**	**1**
30	0.082	0.163	0.245	0.326	0.408	0.489	0.570	0.652	0.733	0.814
40	0.082	0.163	0.245	0.326	0.408	0.489	0.570	0.652	0.733	0.814
50	0.082	0.163	0.245	0.327	0.408	0.489	0.571	0.652	0.733	0.814
60	0.082	0.163	0.245	0.327	0.408	0.489	0.571	0.652	0.733	0.814
70	0.082	0.163	0.245	0.327	0.408	0.490	0.571	0.652	0.733	0.814
80	0.082	0.164	0.245	0.327	0.408	0.490	0.571	0.652	0.733	0.815
90	0.082	0.164	0.245	0.327	0.408	0.490	0.571	0.652	0.734	0.815

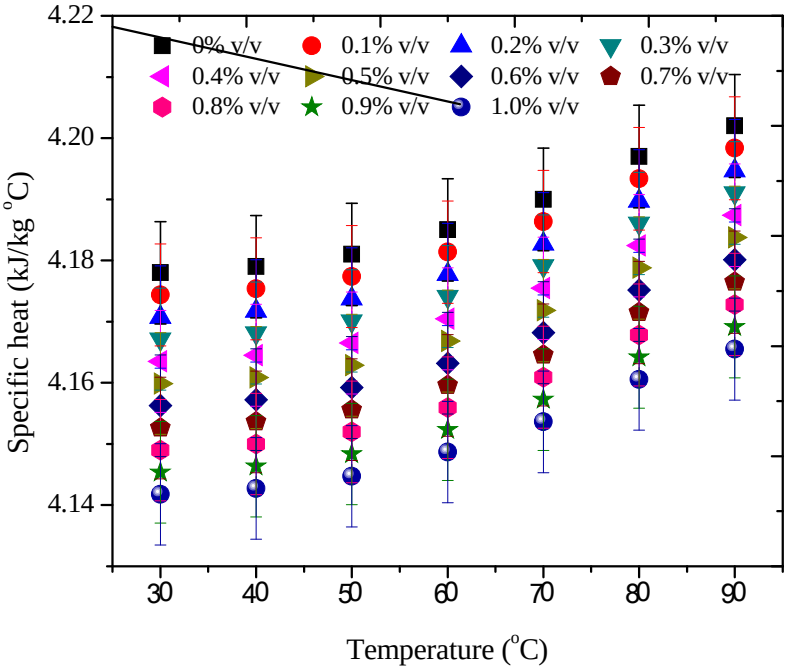

Figure 3.35: Variation of specific heat capacity with copper oxide nanoparticles concentration and fluid temperature

3.6.4.2 Specific heat capacity of copper oxide nanofluids.

The variation of specific heat capacity with copper oxide nanoparticles concentration and fluid temperature is shown in figure 3.35. The specific heat capacity of nanofluids decreased with increasing the nanoparticles concentration and increased with increase in fluid temperature. The heat capacity decreased by 1% for 0.1% v/v concentration of copper oxide nanoparticles and heat capacity decreased up to 0.8% as the nanoparticles concentration increases up to 1.0% v/v. On other hand, heat capacity of base fluid as well as nanofluids for different concentration increased with the fluid temperature.

Table 3.9: Percentage change in specific heat capacity with different copper oxide nanoparticle concentrations

	Aluminum oxide nanoparticles volume concentration (v/v %)									
Temperature (°C)	**0.1**	**0.2**	**0.3**	**0.4**	**0.5**	**0.6**	**0.7**	**0.8**	**0.9**	**1**
30	0.0868	0.1735	0.2603	0.3471	0.4338	0.5206	0.6073	0.6941	0.7809	0.8676
40	0.0868	0.1735	0.2603	0.3471	0.4338	0.5206	0.6074	0.6941	0.7809	0.8677
50	0.0868	0.1735	0.2603	0.3471	0.4339	0.5206	0.6074	0.6942	0.7810	0.8677
60	0.0868	0.1736	0.2604	0.3471	0.4339	0.5207	0.6075	0.6943	0.7811	0.8679
70	0.0868	0.1736	0.2604	0.3472	0.4340	0.5208	0.6076	0.6944	0.7812	0.8680
80	0.0868	0.1736	0.2605	0.3473	0.4341	0.5209	0.6078	0.6946	0.7814	0.8682
90	0.0868	0.1737	0.2605	0.3474	0.4342	0.5210	0.6079	0.6947	0.7816	0.8684

3.7. Comparison of thermo physical properties:

The percentage enhancement in thermophysical properties i.e. specific heat capacity, density, viscosity and thermal conductivity with aluminum oxide and copper oxide nanoparticles concentration is shown in figure 3.36. There is great enhancement in thermal conductivity as compared to the viscosity, density and specific heat capacity of aluminum oxide and copper oxide nanofluids. The enhancement in thermal conductivity has great importance for heat transfer performance of any heat transfer equipment. There is also rise in viscosity of nanofluids but the percentage of rise in viscosity of nanofluids is less than enhancement of thermal conductivity. Density is also increased with nanoparticles concentrations while specific heat capacity has no significant change with addition of nanoparticles in base fluid.

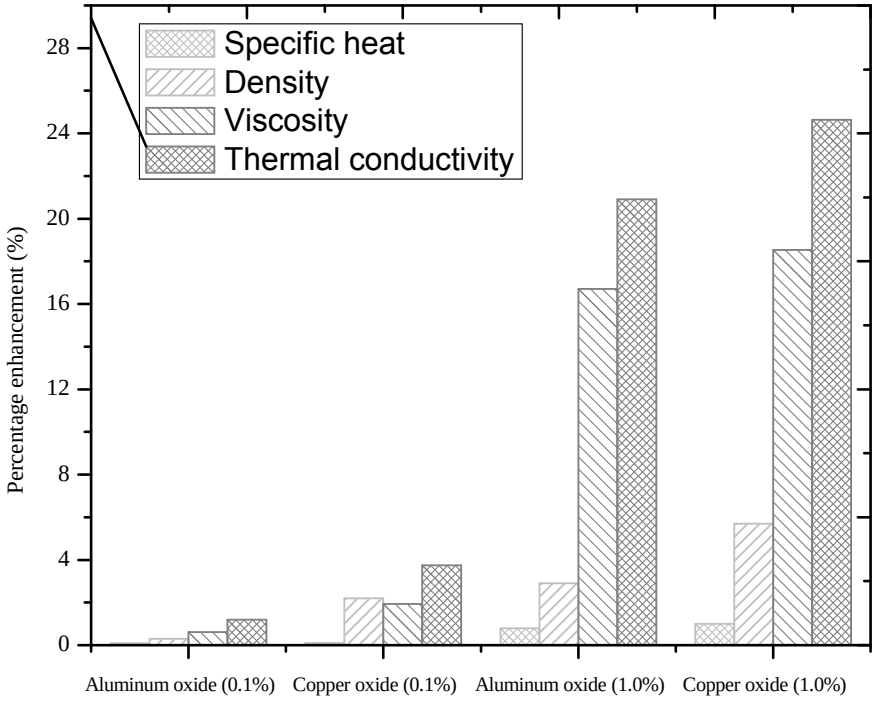

Figure 3.36: Percentage enhancement in thermophysical properties of different nanofluids

3.8 Closure

In the present work, detailed study of characterization of nanoparticles, preparation of nanofluids and stability of nanofluids is carried out. The aluminum oxide nanofluids were prepared without use of any surfactant while copper oxide nanofluids with use of SDS surfactant. As the stability is more important for application of nanofluids so the stability of nanofluids measured with Zeta

potential, UV-Vis absorbance and thermal conductivity of nanofluids. The alumina nanofluids were observed to be more stable compared to copper oxide nanofluids. After carrying out, preparation of nanofluids and stability of nanofluids, the next step is measurement of the thermophysical properties i.e. thermal conductivity, viscosity, density and specific heat for different nanoparticle concentration and fluid temperatures.

CHAPTER 4

DESIGN CONSIDERATION AND FABRICATION OF EXPERIMENTAL SETUP

In the previous chapter preparation of nanofluids, stability of nanofluids and estimation of thermophysical properties i.e. specific heat, viscosity, thermal conductivity and density has been discussed. This chapter deals with the development of experimental setup for single flat vertical tube and radiator, methodology, calculation procedure and analytical model. The uncertainties analysis of different measurements also discussed in this section. In the present work cross flow compact heat exchanger is taken for analysis. The compact heat exchanger consists finned surface having louvered fins and flat tubes.

4.1. Analytical consideration.

4.1.1. Fluid physical properties

For the analysis of any type of heat exchanger, fluid properties such as thermal conductivity, viscosity, density and specific heat are required. In the present work thermophysical properties of base fluid (water) and nanofluids at different particle concentration and temperature are measured at mean temperature of fluid to calculate heat transfer coefficient. For the small change of temperature, thermophysical properties at mean temperature are satisfactory but when the change in the temperature is large, it leads to error. This error can be minimized by evaluate the heat transfer coefficient at inlet temperature.

4.1.2. Fluid velocity

The higher velocity of fluids leads to higher heat transfer coefficient as well high pressure drop. The velocity of fluid should be such enough to prevent any settling of suspended solid particles in fluid but not as much high which can cause the erosion. The typical design value of velocity for for tube side fluid is 1.5 to 2.5 m/s.

4.1.3. Pressure drop

An economic analysis could be made to determine the exchanger design which give lowest operating costs, taking in consideration of capital cost and pumping cost. With the application of nanofluids in compact heat exchangers pressure drop increase should be less than enhancement of heat transfer performance.

4.1.4. Fluid temperatures

The closer approach temperature (the difference between the outlet temperature of one fluid and inlet temperature of other fluid) used, the larger the heat transfer area required for a given duty. The greater temperature difference should be at least 20^{o}C and the least temperature difference 5 ^{o}C to 7 ^{o}C for coolers using water.

4.1.5. Fluid allocation

The more corrosive fluids are allocated to tube side thereby reducing the cost of clad components. The fluid which have greater tendency to foul on heat transfer surface is placed to in tubes because the cleaning of tubes is easy.

4.1.6. Assumptions

The following assumption were considered while analyzing the performance of radiator.

a. There is no loss of heat to surroundings.
b. Air flow rate was uniform across the heat exchanger.
c. Temperature drop distribution over the tube rows is equal.
d. No phase change of fluid was considered.
e. The temperature of fluid was considered constant over each cross section of heat exchanger.
f. The bond efficiency between the tube and fins assumed 100 percent.
g. Thermophysical properties were evaluated at mean temperature.
h. The tube wall resistance neglected.
i. The entrance and exit loss coefficient were not considered.

4.2. Calculation procedure

4.2.1. For single vertical flat tube

1. For the analysis of performance of single vertical flat tube , firstly it is required to evaluate the fluid properties of water and water based nanofluids i.e. thermal conductivity, density, viscosity and specific heat at average temperature.
2. The equivalent diameter of flat tube is calculated by using appropriate correlation.
3. Based upon the equivalent diameter, Reynolds number for water and nanofluids evaluated.
4. The coolant side heat transfer coefficient and Nusselt number calculated.
5. The individual pressure drop and friction factor calculated.
6. Based upon the pressure drop, the required pumping power for water and nanofluids calculated by using appropriate correlation.

4.2.2. For compact heat exchanger

4.2.2.1. Fluid properties

For the analysis of performance of compact heat exchanger, firstly it is required to evaluate the fluid properties of water, water based nanofluids and air i.e. thermal conductivity, density, viscosity and specific heat at average temperature. The evolution of the heat capacity of flow streams is required.

4.2.2.2 Air side calculations

The following steps required for air side calculations:

1. Evaluate the surface geometry, core geometry and equivalent diameter of air side.
2. Mass velocity and Reynolds number evaluated based upon the equivalent diameter.
3. The Colburn factor and friction factor are evaluated using the appropriate correlations.
4. The heat transfer coefficient and pressure drop are estimated.
5. The fin efficiency and surface temperature effectiveness are calculated.

4.2.2.3. Coolant side calculations

The following steps required for tube side calculations:

1. The equivalent diameter of coolant side calculated.
2. The mass velocity of water and nanofluids for tube side evaluated.
3. Based upon the equivalent diameter and mass velocity, the Reynolds number are calculated for tube side fluids.
4. The heat transfer coefficient and Nusselt number calculated for water and nanofluids.
5. The individual pressure drop and friction factor calculated.
6. Based upon the pressure drop, the required pumping power for water and nanofluids calculated by using appropriate correlation.
7. Then overall heat transfer coefficient is evaluated.
8. The rate of heat transfer is calculated.

4.3. Data processing

The hydraulic diameter of flat tube is calculated using the following equation [26]:

$$D_h = \frac{4\times[(®/4)d^2 + (D-d)\times d]}{®\times d + 2\times(D-d)} \tag{4.1}$$

Where, ‘D’ and ‘d’ are the major diameter and minor diameter, respectively.

Reynolds number for the nanofluid is calculated as

$$\mathrm{Re} = \frac{\rho_{nf} \times v \times D_h}{\mu_{nf}} \tag{4.2}$$

The convective heat transfer coefficient (h) in the flat tube is calculated as

$$h_{\exp} = \frac{m_{nf} \times c_{p(nf)} \times (T_{in} - T_{out})}{A_s \times (T_b - T_w)} \tag{4.3}$$

The bulk mean temperature (T_b) of nanofluids is given by

$$T_b = \frac{T_{in} + T_{out}}{2} \tag{4.4}$$

The Nusselt number is calculated by using the following equation:

$$Nu = \frac{h_{\exp} \times D_h}{k} \tag{4.5}$$

The friction factor (f) is calculated as

$$f = \frac{2 \times D_h \times \Delta P}{\rho \times V^2 \times L} \tag{4.6}$$

Where, ΔP is pressure drop across the flat tube.

The pumping power (PP) were calculated as follows:

$$PP = \Delta P \times v \times A \tag{4.7}$$

4.4. Surface geometry of compact heat exchanger

The surface geometry of compact heat exchanger is given in table 4.1.

Table 4.1. Surface geometry of compact heat exchanger.

Specifications	Symbol	Units	Value
Core Geometry	L_r, H_r, D_r	m	0.497, 0.398,0.016
Number of Tubes	N		38
Tube wall Thickness	A	m	0.0003
Inside tube geometry	L_{it}, H_{it}	m	0.015, 0.0024
Outside tube geometry	L_{out},H_{out}	m	0.016, 0.0025
Tube-Plate spacing	b_c	m	0.00177
Fin Pitch	P	in/cm	10.63
Fin Plate spacing	b_a	m	0.00635
Fin thickness		m	0.00015
Fin and Tube thermal conductivity	k_f	W/(m.K)	181
Fin Length	l_f	m	0.003175
Total transfer area/volume between plates	B	m^2/m^3	2465
Fin area/total area	A_{ft}		0.883
Air side hydraulic Diameter	$D_{ha}= 4r_{ha}$	m	0.001423

The surface geometry presented below is mentioned in Kays and London **[11, 20, 140, 142]**
Frontal Area

Air side

$$A_{fr,a} = L_r H_r \tag{4.8}$$

Coolant side

$$A_{fr,h} = D_r H_r \tag{4.9}$$

1) Total Transfer Area

Coolant side

$$A_{t,h} = NL_r\left[2\left(L_{it} - H_{it}\right) + \text{®}\left(H_{it}\right)\right] \tag{4.10}$$

Volume of radiator

$$V_r = L_r D_r H_r \tag{4.11}$$

2) Total transfer area/Total exchanger area

Air side

$$\sim_a = \frac{\times b_c}{\left(b_c + b_a + \left(2 \times a\right)\right)} \tag{4.12}$$

Coolant side

$$\sim_h = \frac{A_{t,c}}{V_r} \tag{4.13}$$

3) Total flow area/Frontal area

$$\pm_a = \sim_a r_{h,a} \tag{4.14}$$

4) Free flow area

Air side

$$A_{c,a} = A_{fr,a}\pm_a \tag{4.15}$$

Coolant side

$$A_{c,h} = N\left[\left(L_{it} - H_{it}\right)H_{it} + \frac{\text{®}}{4}H_{it}^2\right] \tag{4.16}$$

5) Hydraulic diameter

Coolant side

$$D_{h.h} = \frac{4\left[\left(L_{it} - H_{it}\right)H_{it} + \frac{\text{®}}{4}H_{it}\right]}{2\left(L_{it} - H_{it}\right) + \text{®}H_{it}} \tag{4.17}$$

6) Air side calculations

Air side calculations and its thermophysical properties are given below

V_a = 5.5 m/sec. ρ_a = 1.154 Kg/m^3 k_a=0.02364 W/(m.K)

$C_{p,a}$ = 1006 J/(Kg.K) μ_a = 0.0000173 Kg/(m.s) D_{ha} = 0.001423 m

7) Mass flow rate

$$m_a = \rho_a \times A_{c,a} \times V_a \quad (4.18)$$

8) Heat capacity rate

$$C_a = m_a \times C_{p,a} \quad (4.19)$$

9) Reynolds number

$$\mathrm{Re}_a = \frac{\rho_a \times V_a \times D_{h,a}}{\mu_a} \quad (4.20)$$

10) Colburn factor

$$j_a = \frac{0.1459}{\mathrm{Re}^{0.3588}} \quad (4.21)$$

11) Prandtl number

$$\mathrm{Pr}_a = \frac{\mu \times C_p}{k_a} \quad (4.22)$$

12) Convective heat transfer coefficient

$$h_a = \frac{j_a \times \rho_a \times V_a \times C_{p,a}}{\mathrm{Pr}_a^{2/3}} \quad (4.23)$$

13) Fin parameter

$$m = \sqrt{\frac{2 \times h_a}{k_f \times \delta}} \quad (4.24)$$

14) Fin efficiency

$$\eta = \frac{\tanh(m.L_f)}{m.L_f} = 0.9710 \quad (4.25)$$

15) Surface effectiveness

$$\eta_0 = 1 - (1 - \eta) \times A_{ft} \quad (4.26)$$

16) Hot Fluid side calculations

fluid side calculations and its thermophysical properties are given below

ρ_h = 992.3 Kg/m^3 k_h = 0.6305 W/(m.K)

$C_{p,h}$ = 4179 J/(Kg.K) μ_h = 0.000653 Kg/(m.s) $D_{h,h}$ = 0.004392 m

$T_{h,\,inlet}$ = 41.42°C $T_{h,\,outlet}$ = 31°C

$T_{a,\,inlet}$ = 22.63°C $T_{a,\,outlet}$ = 24.6°C $T_{surface}$ = 23.95

$$T_{bulk.mean} = \frac{T_{h,inlet} + T_{h,outlet}}{2}$$

17) Fluid mass flow rate

$$W = \frac{Flow.Rate}{60} \tag{4.27}$$

18) Heat capacity rate

$$C_h = W \times C_{p,h} \tag{4.28}$$

19) Volume Flow Rate

$$G_w = W/A_{c,h} \tag{4.29}$$

20) Reynolds Number

$$\mathrm{Re}_h = \frac{G_h \times D_{h,h}}{\mu_h} \tag{4.30}$$

21) Prandtl Number

$$\mathrm{Pr}_h = \frac{\mu_h \times C_{p,h}}{k_h} \tag{4.31}$$

22) Nusselt number

$$Nu_h = 0.3164\mathrm{Re}_h^{-0.25}\left(\frac{\phi_h}{\phi_c}\right)^{0.797}\left(\frac{\mu_h}{\mu_c}\right)^{0.108} \qquad \mathbf{3000 \le Re \le 30000} \tag{4.32}$$

23) Convective heat transfer coefficient

$$h_h = \frac{Nu_h \times k_h}{D_{h,h}} \tag{4.33}$$

24) Overall heat transfer coefficient

$$\frac{1}{U_a} = \frac{1}{\eta_0 \cdot h_a} + \frac{1}{\left(\frac{\sigma_h}{\sigma_a}\right) \cdot h_h} \tag{4.34}$$

25) Number of transfer units

$$NTU = \frac{U_a \cdot \sigma_a \cdot V_r}{C_{\min}} \tag{4.35}$$

26) Capacity ratio

$$C^* = \frac{C_{\min}}{C_{\max}} \tag{4.36}$$

27) Effectiveness

$$£ = 1 - \exp\left\{ - \frac{1}{C^*}\left[1 - \exp\left(- C^* \cdot NTU\right)\right]\right\} \tag{4.37}$$

28) Heat absorbed

$$Q = W \times C_{p,h}\left(T_{h,inlet} - T_{h,outlet}\right) \tag{4.38}$$

29) Friction factor

$$f = 0.316\,\mathrm{Re}_{nf}^{-0.25}\left(\frac{°_{nf}}{°_{bf}}\right)^{0.797}\left(\frac{«_{nf}}{«_{bf}}\right)^{0.108} \tag{4.39}$$

30) Pressure Drop

$$\Delta P = \frac{fL_r \,°G_h^{\,2}}{2 \cdot D_{h,h}} \tag{4.40}$$

4.5. Development of experimental setup

As the objective of the present study is enhance the heat transfer performance of compact heat exchanger, firstly experimental setup for single flat vertical was developed. The test rig used to study the heat transfer and pressure drop performance of alumina/water and copper oxide/water nanofluids in a vertical flat tube is shown in figure 4.1 and pictorial diagram is shown in figure 4.2. The test rig is to be divided in to two parts namely, water side loop and air side loop. The experimental set up comprised of a reservoir tank of capacity 6 L insulated with glass wool, an electrical heater placed in reservoir tank to raise the temperature of the fluid, a proportional integral derivative (PID) controller (accuracy ±0.1°C in the temperature range 10°C to 200°C) to control the temperature of the nanofluid. The flow rate of fluid was measured by using a flow meter (0–5 LPM) and a by-pass valve was used to control the flow rate. A U-tube manometer with two plastic connector tubes (0.25 in) was used to measure the pressure drop between the two ends (entrance and exit) of the tube. The water side loop was designed to prevent mixing of air and water vapors. The hot water tank is connected to inlet of test section. The temperature was recorded at steady state condition with in permissible variation in the water inlet temperature. The water side measuring instruments were calibrated before the start of test.

A test rig consisting of a vertical flat tube of hydraulic diameter 5.39 mm and length 610 mm was placed centrally inside a low speed wind tunnel. An axial fan with a regulator to control its rpm was used to force air over to the test section. The velocity of air was measured at grid positions around duct of the tube with propeller fan type digital anemometer for calculating the average air velocity.

A honeycomb mesh (2.5 cm × 2.5 cm) was used at one end of the wind tunnel to ensure proper distribution/direction of air over the flat vertical tube. Two T-type thermocouples (accuracy ±0.1°C) were kept in direct contact with the fluid for measuring the inlet and outlet temperatures (T_{in} and T_{out}). Six K-type thermocouples (accuracy ±0.1°C) were soldered on the surface of the flat vertical tube at equal distances along its length as shown in figure 4.4 to measure the wall temperatures, T_1 – T_6. The air side surfaces of these thermocouples were insulated so that these will not indicate air temperature. Six thermocouples (accuracy ±0.1°C) were used to measure the air inlet (T_7 – T_9) and outlet (T_{10} – T_{12}) temperatures at different positions. The fluid was pumped into the tube with a magnetic water pump.

A pictorial representation of heat transfer mechanism of nanofluid in flat vertical tube is shown in figure 4.6**.** In all experiments, constant wall temperature condition was employed. The different operating conditions for experimentations are given in table 4.2.

Table 4.2: **Various parametric conditions of experimentation**

Parameter	**Test Condition**
Base fluid	Distilled water
Nanoparticles	Al_2O_3, CuO
Volume fraction (% v/v)	0.25, 0.50, 0.75, 1.0
Nanofluid inlet temperature (°C)	40, 50, 60, 70, 80, 90
Air inlet velocity (m/s)	1 – 5
Nanofluid flow rate (L/min)	1.0, 1.25, 1.5, 1.75, 2.0, 2.25, 2.5
Air inlet temperature	At ambient conditions (25°C)

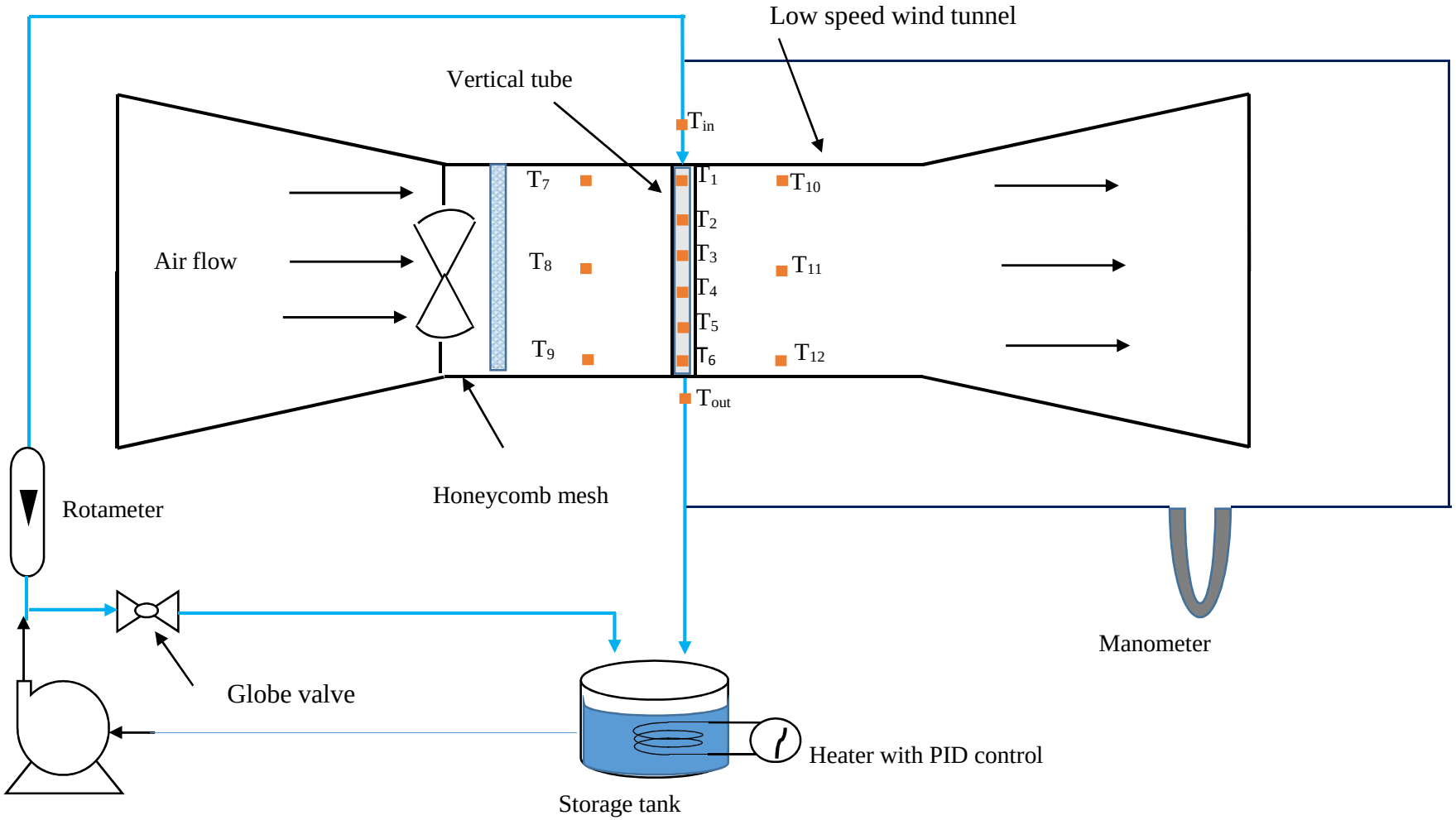

Figure 4.1: Schematic diagram of experimental set up

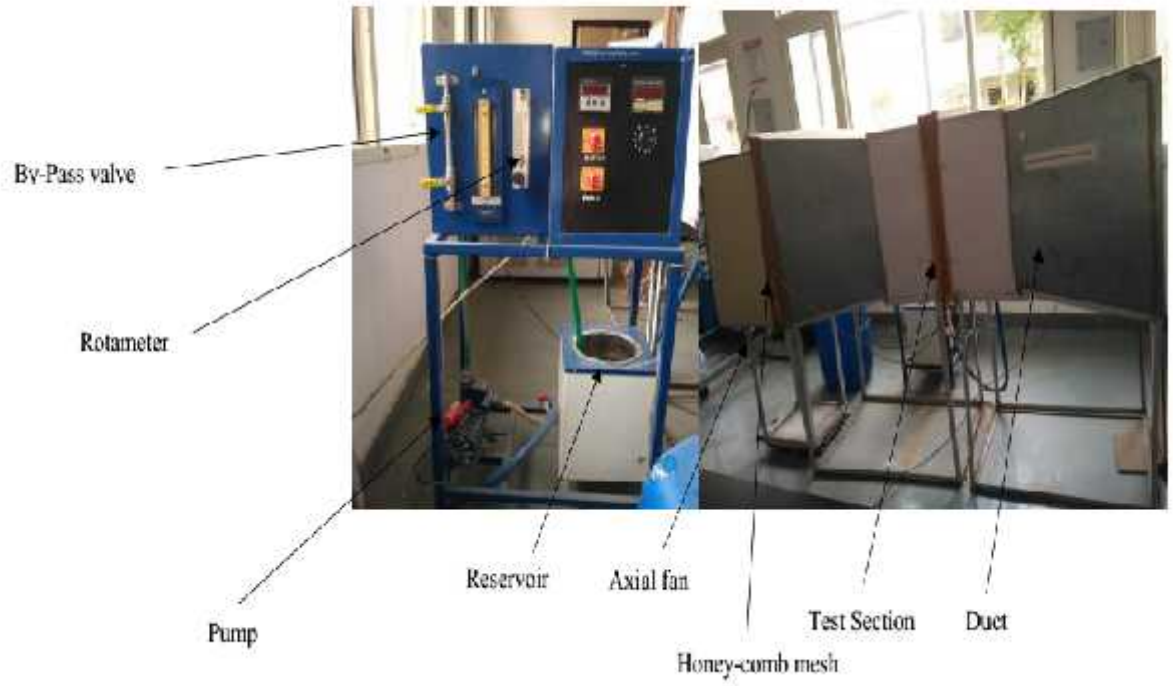

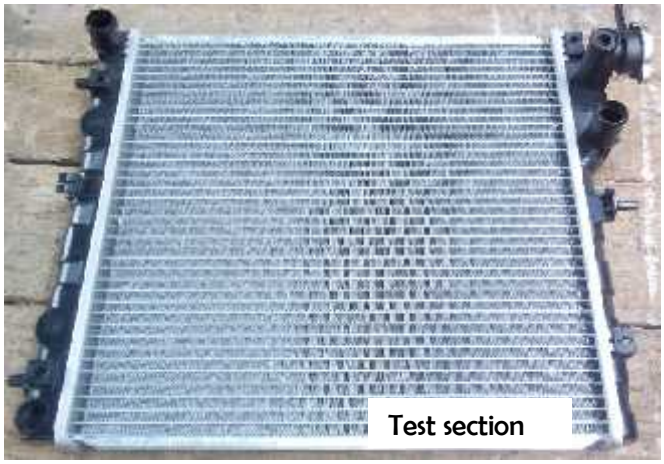

Figure 4.2: Pictorial diagram of experimental setup

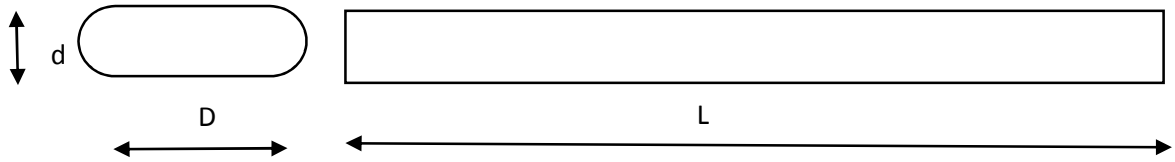

Figure 4.3: Flat tube geometry

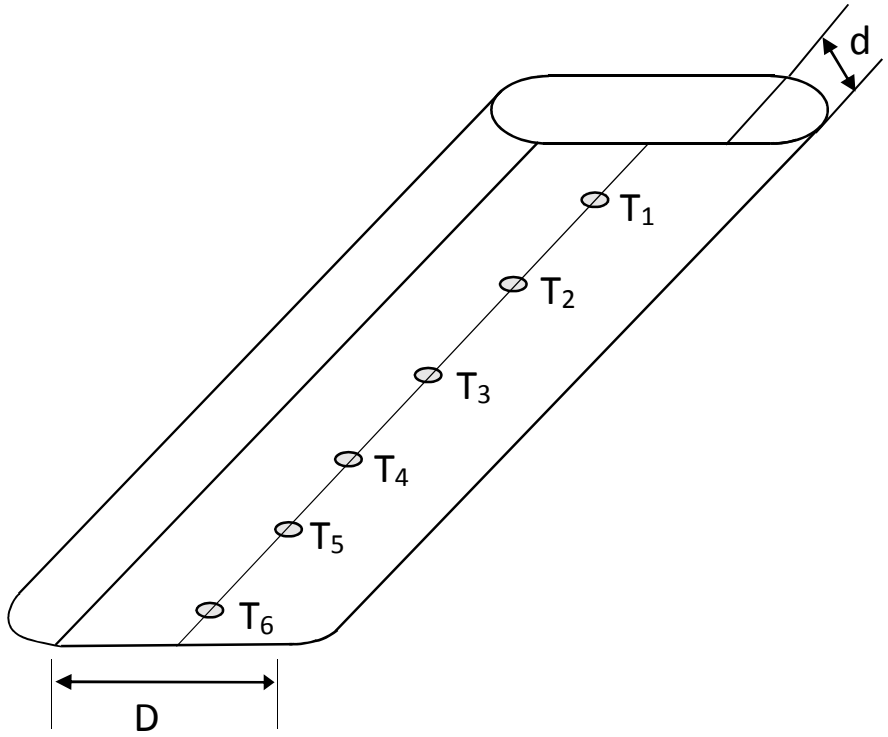

Figure 4.4: Position of thermocouples of flat tube surface

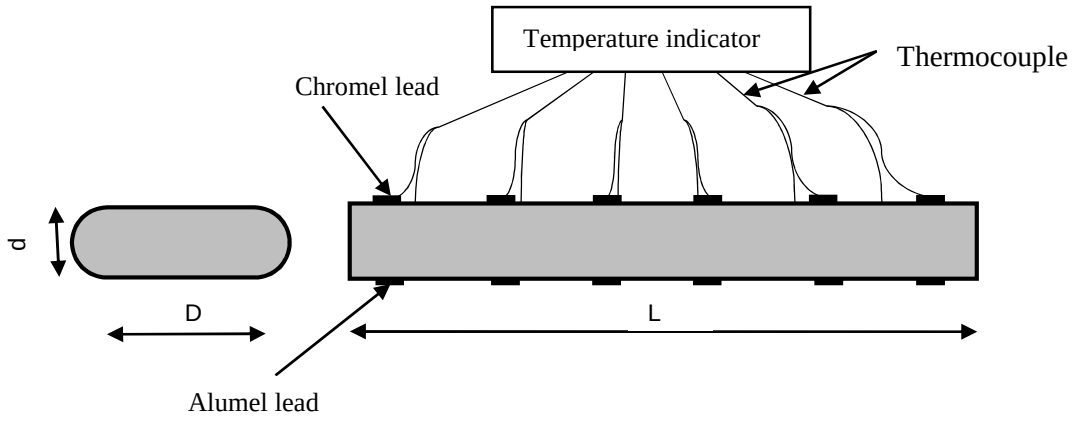

Figure 4.5: Geometry of flat tube with temperature measurement set up

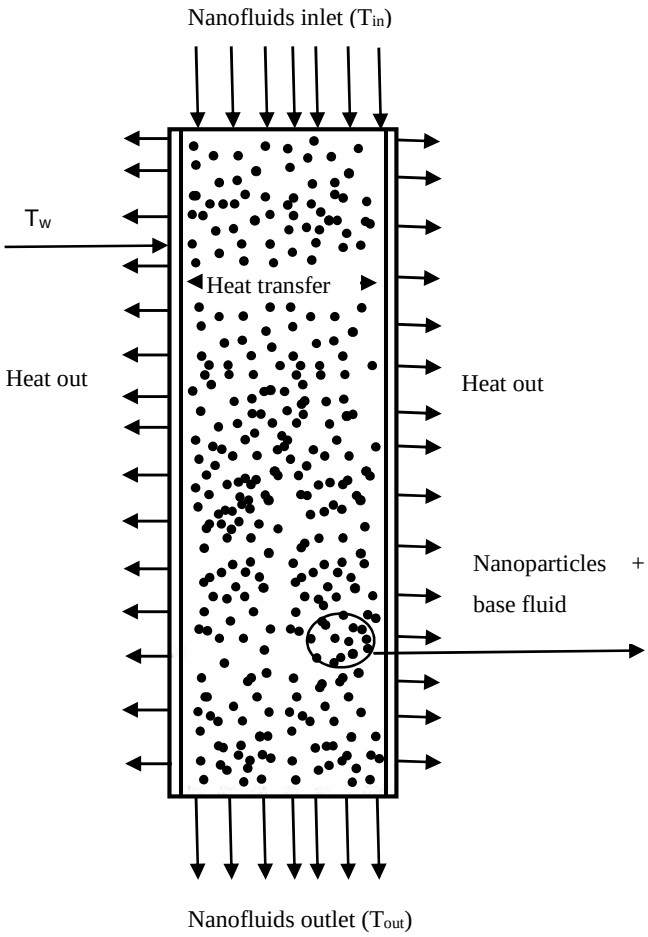

Figure 4.6: Heat transfer mechanism in tube

The radiator was tested up to the maximum capacity of test rig facility. The maximum water temperature was maintained at around 85 ^{o}C at maximum flow rate. The air velocity was varied by using electric speed controller regulator. The operating parameters monitored during the testing of single flat tube were as following:

a. The inlet temperature of water and nanofluids entering the single flat tube.
b. The outlet temperature of water and nanofluids entering the single flat tube.
c. Volumetric flow rate of water and nanofluids passing through single flat tube.
d. Inlet temperature of air entering the wind tunnel.

The operating parameters monitored during the testing of radiator were as following:

a. The inlet temperature of water and nanofluids entering the radiator.
b. The outlet temperature of water and nanofluids entering the radiator.
c. The volumetric flow rate of water and nanofluids passing through radiator.
d. The inlet temperature of air entering the radiator.

e. The outlet temperature of air leaving the radiator.

f. The volumetric air flow rate of air passing through radiator.

4.6. Uncertainties analysis

Before the conduct of experiments, uncertainties analysis of measuring instruments and results have been calculated. The uncertainties of measuring instruments, such as flow meter, thermocouples, pressure measuring systems, is obtained from the manufacturing and uncertainties of results such as Reynolds number, Nusselt number, heat transfer coefficient and friction factor calculated by using equation.

$$U_{\mathrm{Re}} = \left[(\frac{d}{\nu} U_{\nu})^2 + (\frac{V}{\nu} U_d)^2 + (\frac{Vd}{\nu^2} U_{\nu})^2 \right]^{1/2} \tag{4.41}$$

$$U_{Nu} = \left[(\frac{d}{k} U_h)^2 + (\frac{h}{k} U_d)^2 + (\frac{hd}{k^2} U_k)^2 \right]^{1/2} \tag{4.42}$$

$$U_f = \left[(\frac{2d}{\circ L\nu^2} U\Delta P)^2 + (\frac{2\Delta P}{\circ L\nu^2} U_d)^2 + (\frac{2\Delta Pd}{\circ^2 L\nu^2} U_\circ)^2 + (\frac{2\Delta Pd}{\circ L^2\nu^2} U_L)^2 + (\frac{4\Delta Pd}{\circ L\nu^3} U_L)^2 \right]^{1/2} \tag{4.43}$$

$$U_h = \left[\begin{array}{l} (\frac{\nu dc_p}{L} U^\circ LN\frac{\Delta T_i}{\Delta T_o})^2 + (\frac{^\circ dc_p}{U_\nu} LN\frac{\Delta T_i}{\Delta T_o})^2 + (\frac{\nu^\circ c_p}{L} UdLN\frac{\Delta T_i}{\Delta T_o})^2 + (\frac{\nu^\circ dc_p}{L} U_L LN\frac{\Delta T_i}{\Delta T_o})^2 \\ +(\frac{\nu^\circ dc_p}{L} U_{\Delta T_s}\frac{1}{\Delta T_s})^2 + (\frac{\nu^\circ dc_p}{L} U_{\Delta T_o}\frac{1}{\Delta T_o})^2 \end{array} \right]^{1/2} \tag{4.44}$$

CHAPTER 5

PERFORMANCE OF SINGLE TUBE AND COMPACT HEAT EXCHANGER

5.1 Introduction

This chapter presents the detailed study of heat transfer and fluid flow performance of nanofluids in vertical tubes. The correlations used to evaluate the performance has been given in the previous chapter. The performance evaluation of vertical tubes has been carried out in two stages. In first set of experiments, heat transfer and fluid flow performance of single flat vertical tube has been carried out and in second set of experiments performance of compact heat exchanger, which consists multiple flat vertical tube, has been carried out. A correlation has been developed of heat transfer and pressure drop characteristics for single flat vertical tube to evaluate the performance of nanofluids.

5.2. Heat transfer performance of nanofluids in single flat tube

The base fluid and prepared nanofluids employed as the working fluid to evaluate the performance of nanofluids in flat vertical tube. The heat transfer performance evaluated at various fluid inlet temperature such as 40 ^{o}C, 50 ^{o}C, 60 ^{o}C, 70 ^{o}C and 80 ^{o}C and at Reynolds number range from 5000 to 20000 and water based nanofluids in the range of 0.25% v/v to 1% v/v concentration of alumina oxide and copper oxide nanoparticles.

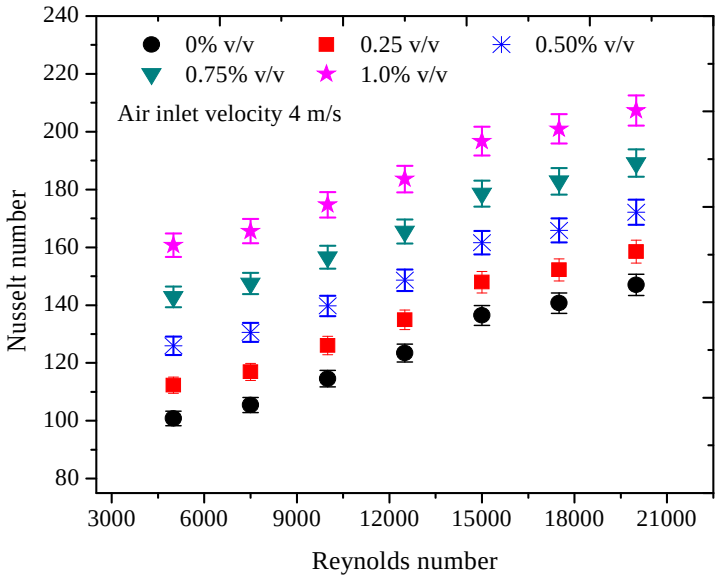

Figure 5.1: Variation of Nusselt number with Reynolds number and particle concentration.

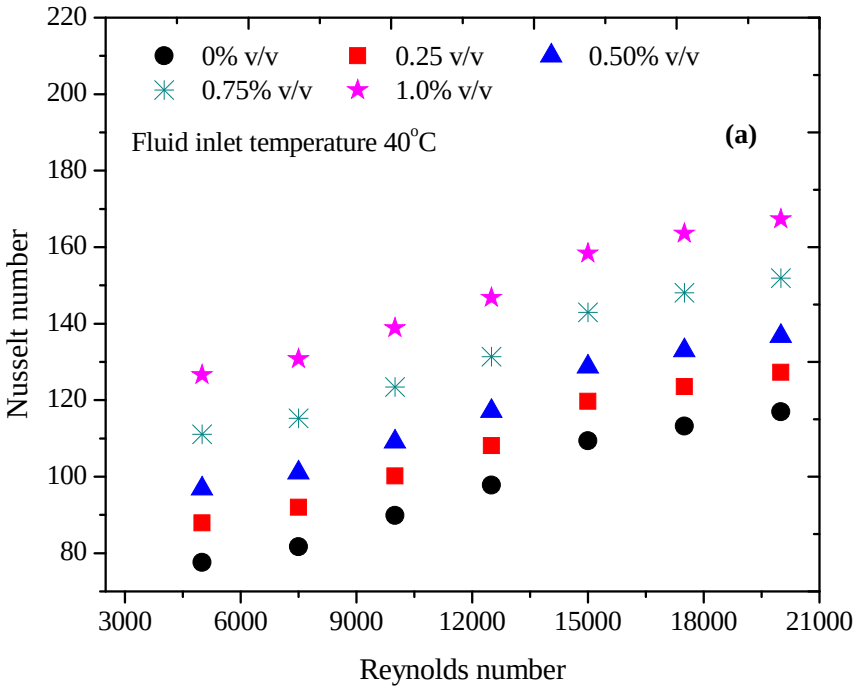
0% v/v
0.25 v/v
0.50% v/v
0.75% v/v
1.0% v/v
Fluid inlet temperature 40°C
(a)
Nusselt number
Reynolds number
220
200
180
160
140
120
100
80
3000
6000
9000
12000
15000
18000
21000

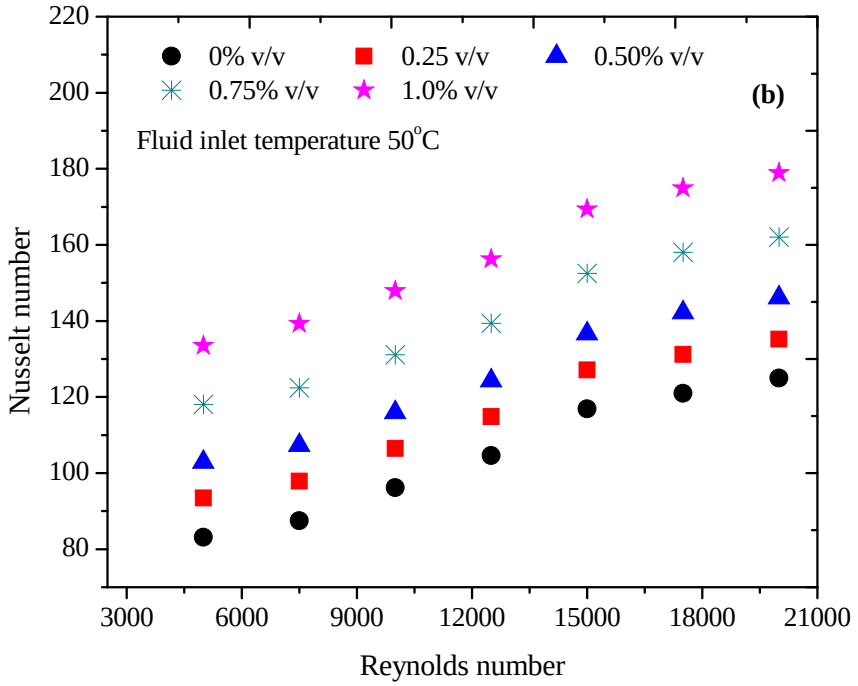
0% v/v
0.25 v/v
0.50% v/v
0.75% v/v
1.0% v/v
Fluid inlet temperature 50°C
(b)
Nusselt number
Reynolds number
220
200
180
160
140
120
100
80
3000
6000
9000
12000
15000
18000
21000

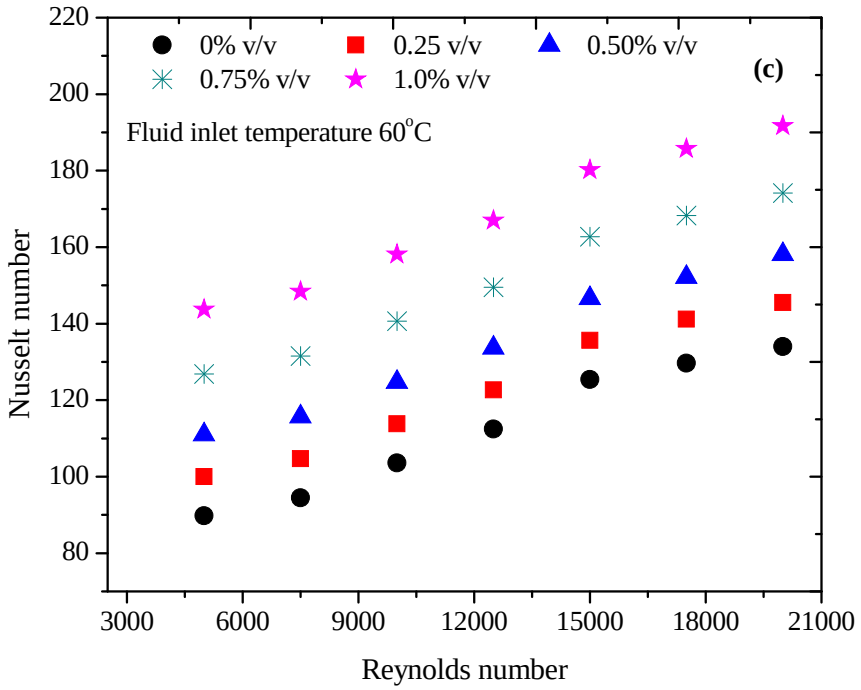
0% v/v
0.25 v/v
0.50% v/v
0.75% v/v
1.0% v/v
(c)
Fluid inlet temperature 60°C
Nusselt number
Reynolds number
220
200
180
160
140
120
100
80
3000
6000
9000
12000
15000
18000
21000

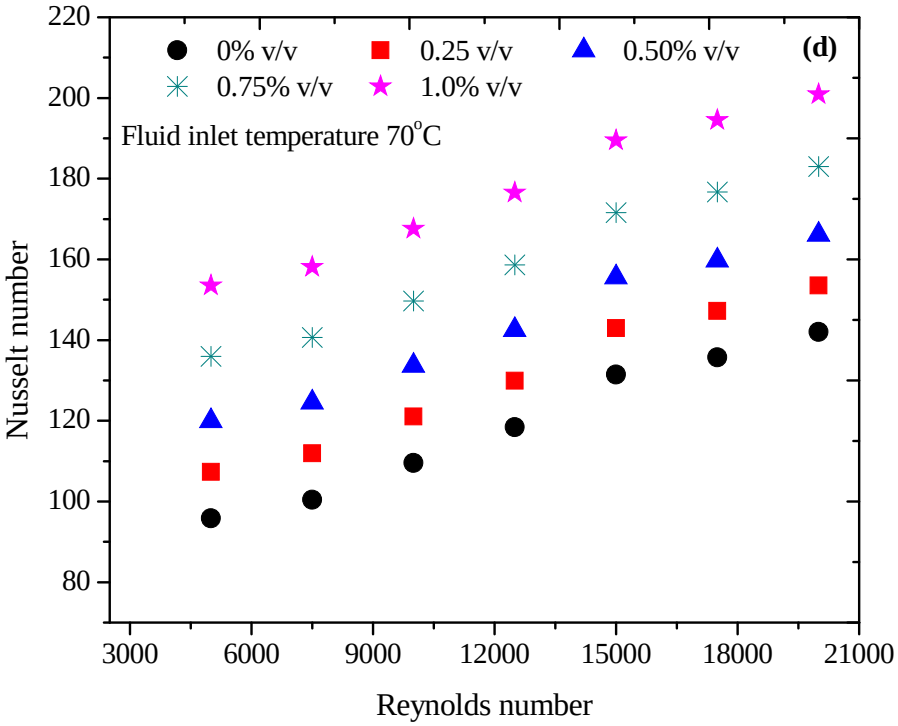
0% v/v
0.25 v/v
0.50% v/v
0.75% v/v
1.0% v/v
(d)
Fluid inlet temperature 70°C
Nusselt number
Reynolds number
220
200
180
160
140
120
100
80
3000
6000
9000
12000
15000
18000
21000

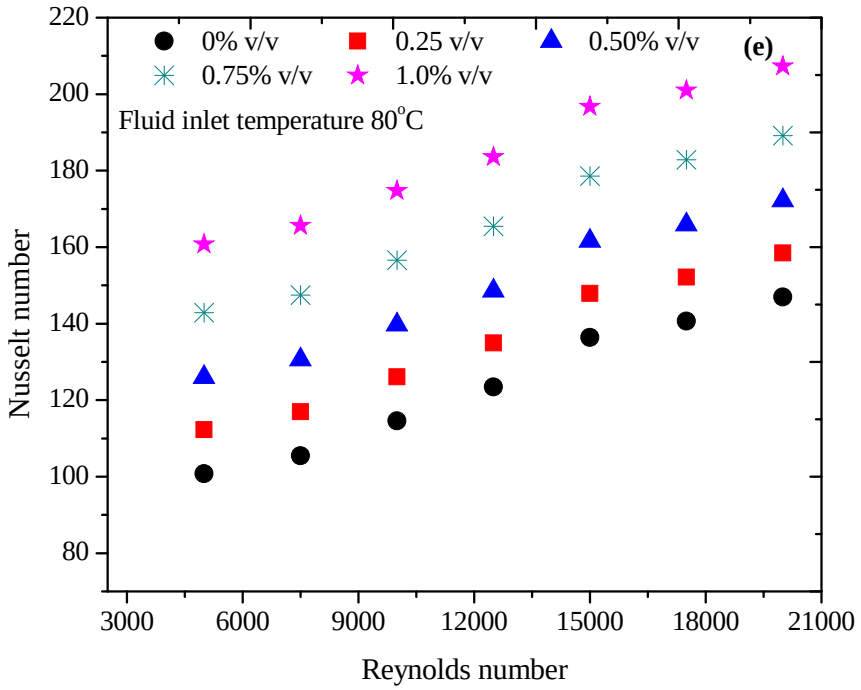

Figure 5.2: Variation of Nusselt number with Reynolds number and particle concentration at different fluid inlet temperature (a) 40 ºC, (b) 50 ºC, (c) 60 ºC, (d) 70 ºC and 80 ºC

5.2.1. Effect of aluminum oxide nanoparticles

The variation of Nusselt number for base fluid and nanofluids in the vertical tube for different Reynolds number is shown in figure. 5.1. It can be inferred from this figure that concentration of nanoparticles plays a vital role in enhancing the Nusselt number and suspending the nanoparticles in base fluid leads to an increase in heat transfer coefficient for flat vertical tubes of radiator. As discussed, the addition of alumina nanoparticles improved the thermal conductivity of base fluid and this in turn enhanced the heat transfer performance. Besides the thermal conductivity, the flow pattern of base fluid also changes with the addition of nanoparticles. Hence, the wall temperature of tube increases because of increase in heat transfer rate due to the Brownian motion of nanoparticles near the tube wall at high Reynolds numbers. As the thermal conductivity is not sole responsible factor for heat transfer enhancement, apart from this chaotic movement contributes to heat transfer performance. Due to small size of nanoparticles might be important mechanism for heat transfer augmentation. Chaotic movement of small and fine particles accelerates the energy exchange process in fluid. As the rotational motions of nanoparticles are high-speed and in random directions, the motion behaviors of rotating fluid elements are chaotic. And momentum exchange will be strengthened due to the chaotic movements of rotating fluid elements. The development of

thermal boundary layer near the flat tube wall surface was delayed due to chaotic motion of nanoparticles, which resulted in increased heat transfer at the entrance region of the flat tube. The Brownian motion of nanoparticles enhances the heat transfer through the thermal conductance in nanoparticles of direct contribution due to the motion of nanoparticles that transport the heat and indirect contribution due to the nano convection of the fluid surrounding individual nanoparticle.

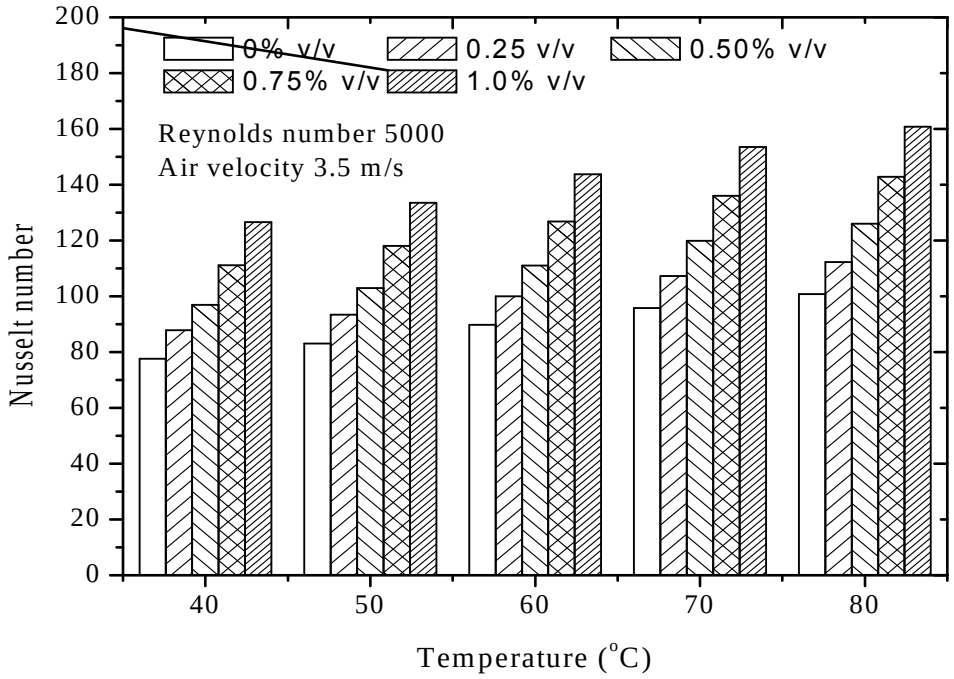

Figure 5.3: Comparison of Nusselt number at fixed Reynolds number, air velocity and different fluid inlet temperatures

The Nusselt number enhancement with 0.25% v/v nanoparticle concentration was 8% for the Reynolds number 20000 and it enhanced further to 40% when the particle concentration was increased to 1.0% v/v for the same Reynolds number. This enhancement is consistent with the numerical studies on flat tube by Zhao et al. (2016), Vajjha et al. (2015) and Elsebay et al. (2015).

In addition, the heat transfer was significantly affected by fluid inlet temperature as shown in figure 5.2 (a-e). With the rise in fluid inlet temperature, the heat transfer performance increased because of the increase in thermal conductivity and decrease in density and viscosity of fluids. As the inlet temperature of nanofluid was increased from 40°C to 60°C, the heat transfer performance improved by 13% and this enhancement further increased to 28% as the inlet temperature was raised to 80°C for a particular fluid velocity and particle concentration (1.0% v/v). The comparison of Nusselt number at different temperatures is shown in figure 5.3. Similar numerical findings on variation of

heat transfer coefficient for a flat tube with fluid inlet temperatures have been reported by Zhao et al. (2016). In addition, the heat transfer performance also increased with increasing the air flow rate over the tube and resulted in a decrease in the nanofluid temperature at the outlet of the flat tube. It was noticed that increasing the air flow rate from 2 to 4 m/s causes 12% enhancement in heat transfer for 1.0% v/v nanofluid. Similar results were observed with other particle concentrations, Reynolds numbers and inlet temperatures of nanofluid. By suspension of nanoparticles in the base fluid enhances the heat performance and the reason of this enhancement is suspended nanoparticles increase the specific surface area and heat capacity of nanofluids. The dispersion of nanoparticles flattens the transverse the temperature gradient of the fluid. The interaction and collision among nanoparticles, fluid and flow passage intensified. The mixing fluctuation and turbulence of fluid intensified.

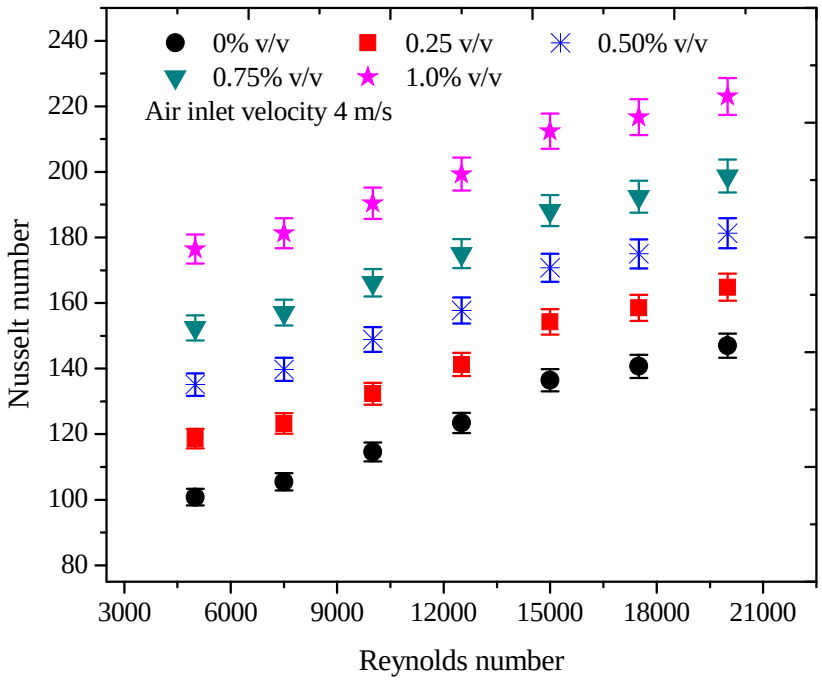

Figure 5.4: Variation of Nusselt number with Reynolds number and particle concentration

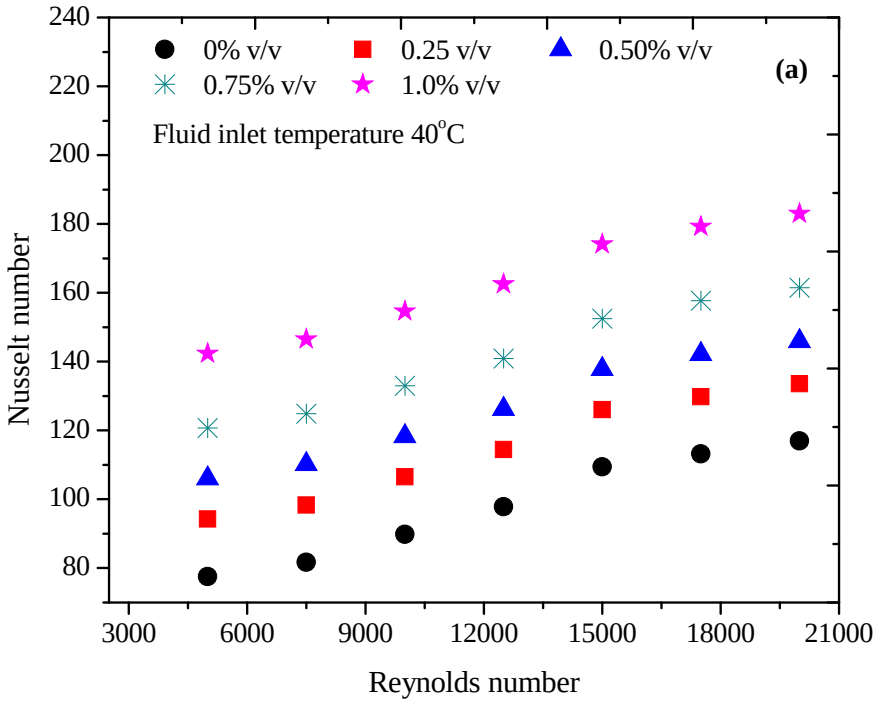
0% v/v
0.25 v/v
0.50% v/v
0.75% v/v
1.0% v/v
(a)
Fluid inlet temperature 40°C
Nusselt number
Reynolds number
240
220
200
180
160
140
120
100
80
3000
6000
9000
12000
15000
18000
21000

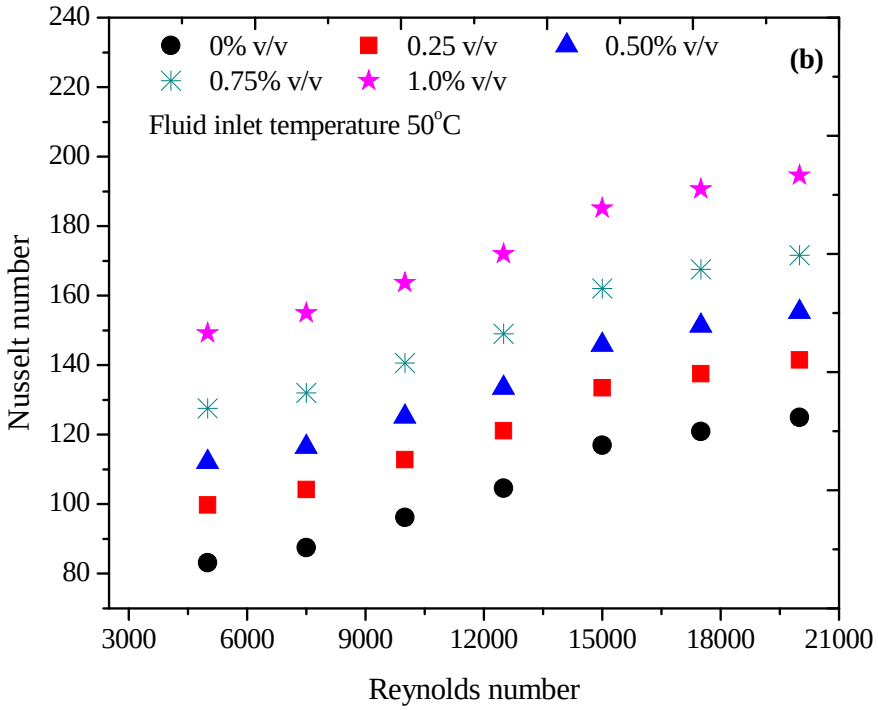
0% v/v
0.25 v/v
0.50% v/v
0.75% v/v
1.0% v/v
(b)
Fluid inlet temperature 50°C
Nusselt number
Reynolds number
240
220
200
180
160
140
120
100
80
3000
6000
9000
12000
15000
18000
21000

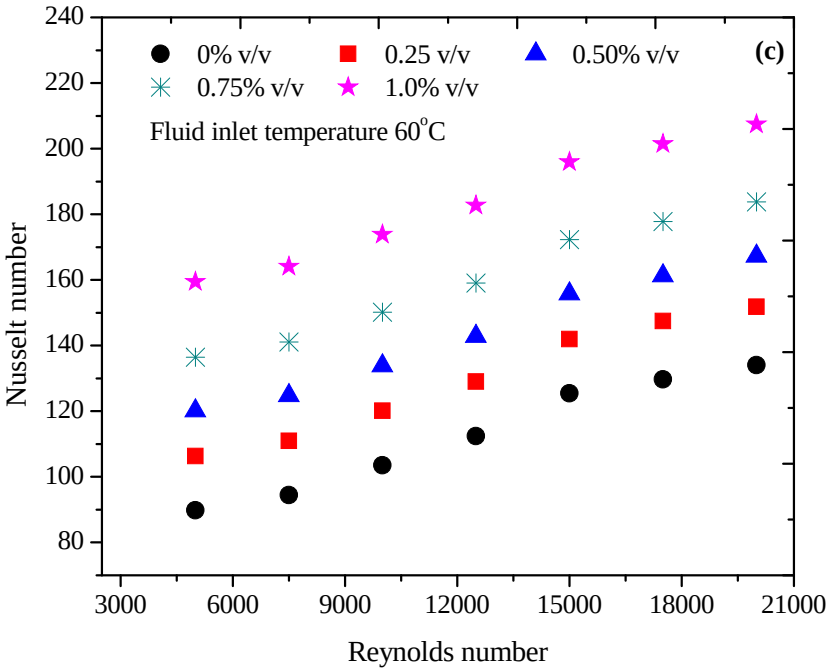
0% v/v
0.25 v/v
0.50% v/v
0.75% v/v
1.0% v/v
(c)
Fluid inlet temperature 60°C
Nusselt number
Reynolds number
240
220
200
180
160
140
120
100
80
3000
6000
9000
12000
15000
18000
21000

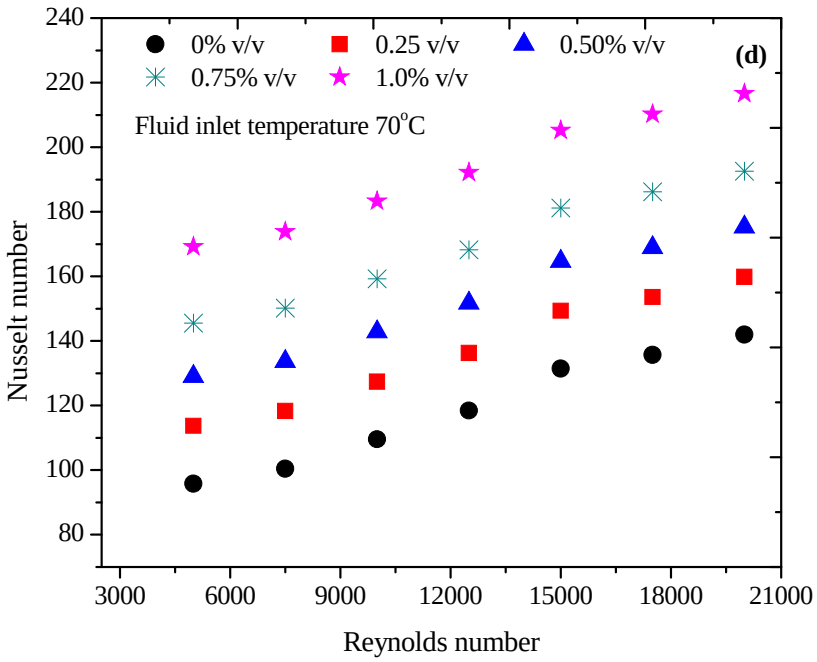
0% v/v
0.25 v/v
0.50% v/v
0.75% v/v
1.0% v/v
(d)
Fluid inlet temperature 70°C
Nusselt number
Reynolds number
240
220
200
180
160
140
120
100
80
3000
6000
9000
12000
15000
18000
21000

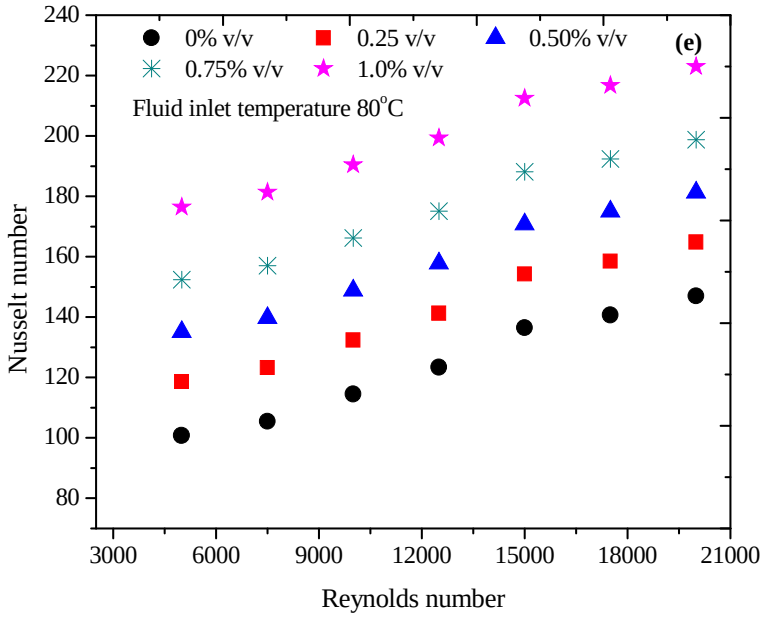

Figure 5.5: Variation of Nusselt number with Reynolds number and copper oxide nanoparticle concentration at different fluid inlet temperature (a) 40 ºC, (b) 50 ºC, (c) 60 ºC, (d) 70 ºC and (e) 80 ºC

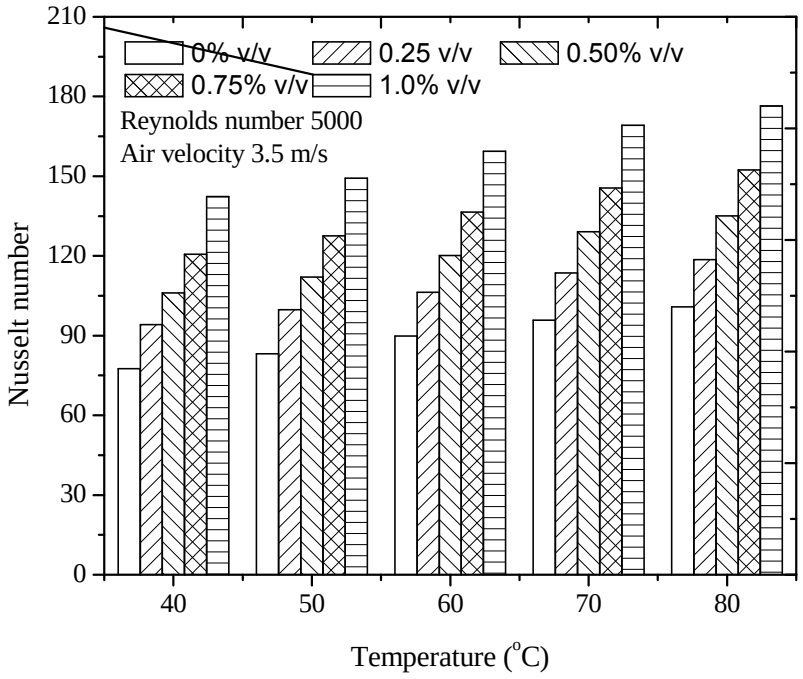

Figure 5.6: Effect of fluid inlet temperature on Nusselt number at fixed Reynolds number and air velocity at different copper oxide nanoparticle concentrations

5.2.2. Effect of copper oxide nanoparticles

The copper oxide/water nanofluids with nanoparticles loading of 0.25% v/v – 1.0% v/v concentration is also used in this study. The variation of Nusselt number with Reynolds number and particle concentration is shown in figure 5.4. The Nusselt number for nanofluids at different concentrations of copper oxide nanoparticles was higher than that of base fluid and it increased with increase in nanoparticles concentration as well as Reynolds number of nanofluids. The enhancement of Nusselt number as compared to the base fluid was 18% for 0.25% v/v concentration of nanoparticles for Reynolds number 5000 and this enhancement was up to 12% as the Reynolds number of nanofluids increased up to 20000. Furthermore, heat transfer enhancement increased up to 51% for the 1.0 % v/v concentration of copper oxide/water nanofluids for Reynolds number 20000. The Nusselt number for nanofluids and base fluid also increased with increase in fluid inlet temperature as shown in figure 5.5 (a-e). As the inlet temperature increased from 30°C to 40°C, 6% enhancement in heat transfer was observed and this enhancement increased to 21% as inlet temperature was increased to 80°C for fixed Reynolds number and particle concentration. The maximum enhancement was approximately 60% for 1.0% concentration of nanofluids for Reynolds number 5000 and fluid inlet temperature 80°C. The heat transfer rate for nanofluids was more than base fluids because, thermal conductivity of copper oxide nanofluids is higher than that of base fluid; but, thermal conductivity is not the sole reason for heat transfer enhancement and there could be other reasons for the heat transfer enhancement. At higher temperatures, the nanoparticles are uniformly distributed due to the Brownian motion of nanoparticles, which leads to heat transfer enhancement. The chaotic motion of nanoparticles delays the development of thermal boundary layer on the tube wall surface, due to which, the heat transfer rate at entrance region of tube increases. Other reasons for the heat transfer enhancement could be energy transfer between the nanoparticles due to dispersion in base fluid and viscosity gradient due to particle migration. The similar results of heat transfer enhancement of flat tube with nanofluids have been reported by previous researchers in their numerical and experimental studies.

Heat transfer performance of copper based nanofluids was higher than that of aluminum oxide nanofluids as the thermal conductivity of copper oxide nanoparticles is higher than aluminum oxide nanoparticle. With the use aluminum oxide nanoparticles about 40% enhancement in heat transfer performance was observed as compared to the base fluid while with copper oxide nanoparticles, 51% enhancement was higher than base fluid under the same operating condition in the experimentations. The presence of nanoparticles and their random motion within the base fluid cause the thickness of thermal boundary layer to reduce and it has important contribution to such heat transfer improvement.

A correlation has been developed of heat transfer characteristics for single flat vertical tube to evaluate the performance of nanofluids. The correlation has been developed considering the the various parameters i.e. nanoparticle concentration, fluid inlet temperature, Reynolds number, thermophysical properties (thermal conductivity, viscosity, density, specific heat capcity) and particle type . Like wise the experimental results, in correlation results Nusselt number increased with increase in nanoparticles concentration, fluid inlet temperature, flow rate etc. The Nusselt number estimated based upon the considering the effect of addition of the nanoparticles in the base fluid at different concentration. This is observed from fact that Nusselt number, Reynolds number and Prandtl number are the functions of various thermophysical properties which are significantly changed with nanoparticles concentration. So the developed correlation is the function of particle volume concentration, Reynolds number and Prandtl number. The experimental Nusselt number of aluminum oxide and copper oxide nanofluids were compared with the developed mathematical correlation as given equation 5.2. The experimental and predicted model Nusselt number for aluminum oxide and copper nanofluids is shown in figure 5.7 and figure 5.8 respectively. The R-square value for alumina oxide nanofluids 0.97 and copper oxide nanofluids 0.98 is observed.

$$Nu = 0.023\mathrm{Re}^{0.77}\mathrm{Pr}^{0.39} + (73\varphi - 1.11)\mathrm{Re}^{3.40}(\varphi - 0.36)\mathrm{Pr}^{0.416}(\varphi - 0.2) \qquad (5.1)$$

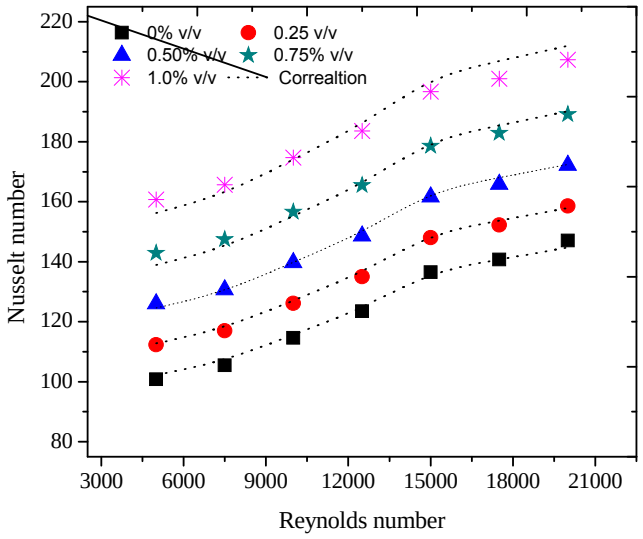

Figure 5.7: Experimental and correlation Nusselt number of Al_2O_3 nanofluids

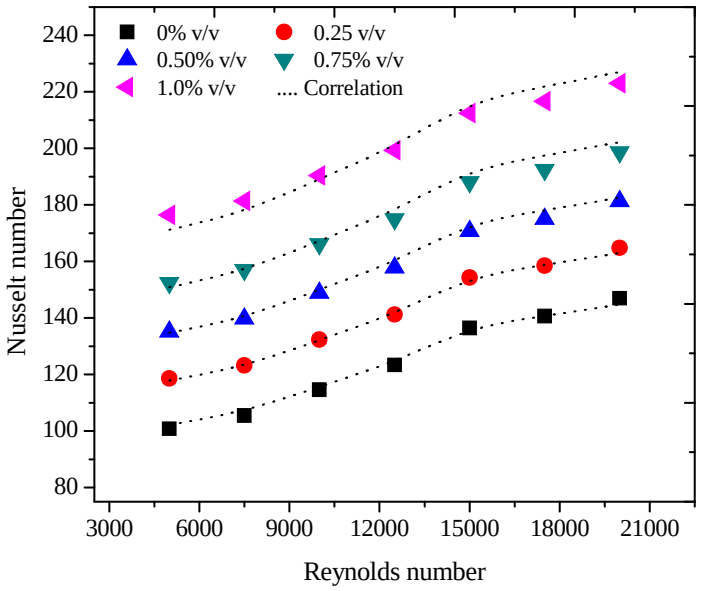

Figure 5.8: Experimental and correlation Nusselt number of copper oxide nanofluids

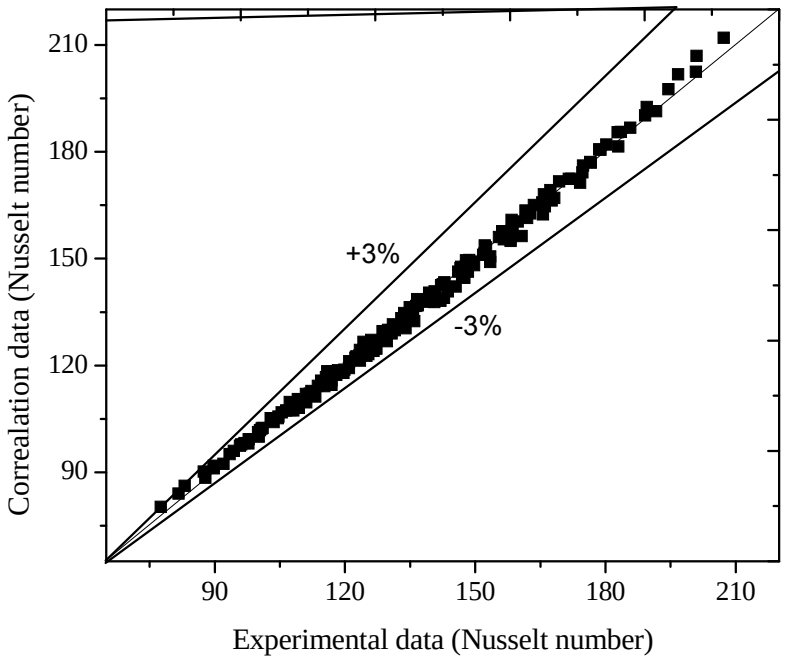

Figure 5.9: Comparison of experimental Nusselt number and correlation Nusselt number nanofluids

5.3. Fluid flow performance

5.3.1. Pressure drop

Besides the heat transfer coefficient, pressure drop calculations are also important in determining the feasibility for practical application of nanofluids. The pressure drop inside the tube depends on Reynolds number, density and viscosity of nanofluids. Figure 5.10 shows the pressure drop of base fluid and nanofluids in the flat tube for different Reynolds numbers and particle concentrations. Pressure drop increased with increasing alumina nanoparticle concentration as well as Reynolds number. The pressure drop observed for 0.25% v/v nanofluids was 1.5% and 1.6% higher that of the base fluid for Reynolds numbers 5000 and 20000, respectively. Further, these values increased to 5% and 6% times, respectively, when the nanoparticle concentration was increased to 1.0% v/v. This increase in pressure drop might be attributed to the fact that viscosity of the base fluid increases with increase in particle concentration.

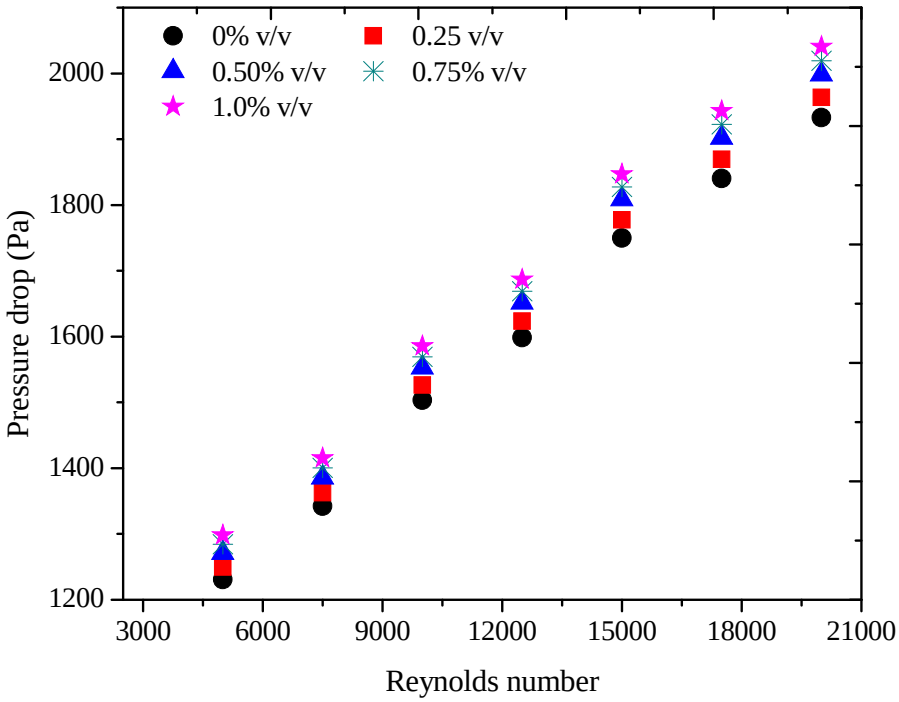

Figure 5.10: Variation of pressure drop in flat tube with Reynolds number and aluminum oxide particle concentration.

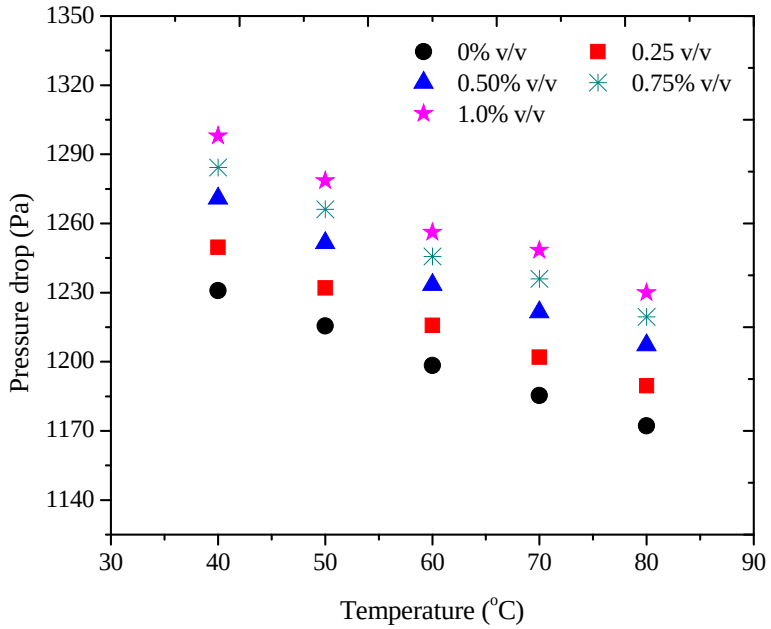

Figure 5.11: Effect of fluid inlet temperature on pressure drop in flat tube with aluminum oxide particle concentration

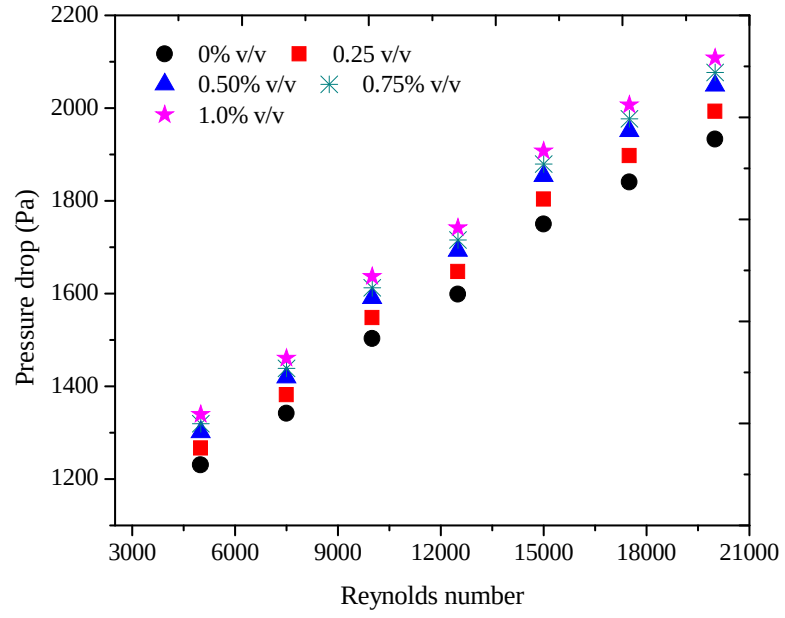

Figure 5.12: Variation of pressure drop in flat tube with Reynolds number and copper oxide particle concentration

On the other hand, a rise in the inlet temperature of nanofluid resulted in a decrease in the pressure drop as shown in figure 5.11, because of the decreased density and viscosity of nanofluids.

The variation of pressure drop in flat tube with different Reynolds numbers and copper oxide nanoparticle concentrations as shown in figure 5.12. The pressure drop increased with increase in Reynolds number and particles concentration. For 0.25% v/v of nanoparticles, pressure drop for Reynolds number 5000 was 3% and 3.2% for Reynolds number 20000 in comparison with the base fluid and this increased to 8.5% and 9% when the concentration was changed to 1.0% v/v for same Reynolds numbers. The reason for increase in pressure drop might be attributed to the fact that viscosity of base fluid increases with increase in particle concentration. Another reason for change in pressure drop could be the chaotic motion of nanoparticles in base fluid. As the inlet temperature of fluid increases, there was a small change in pressure drop as shown in figure 5.13.

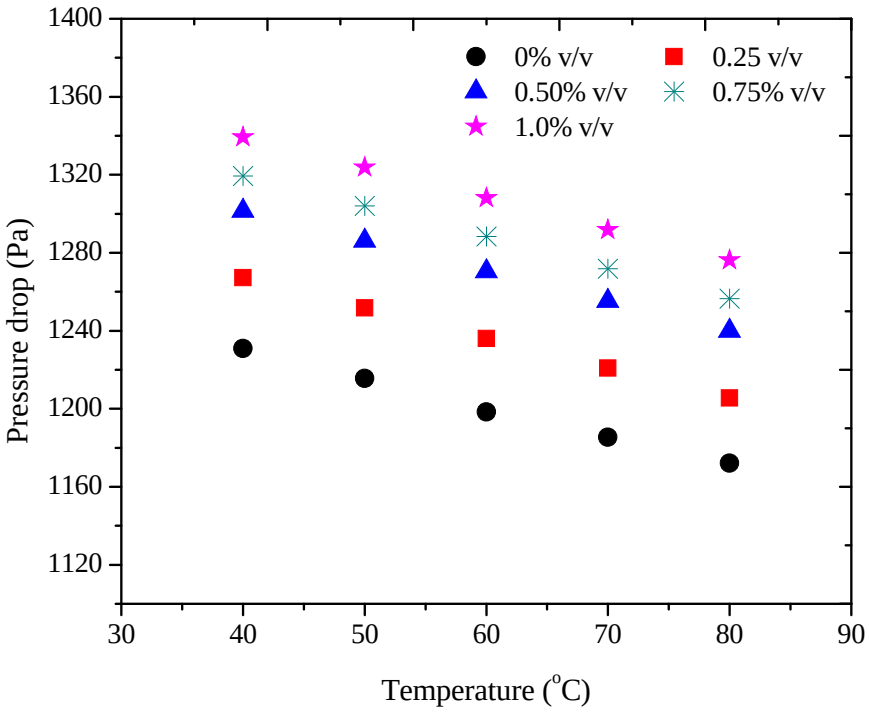

Figure 5.13: Effect of fluid inlet temperature on pressure drop in flat tube with copper oxide particle concentration

With rise in fluid temperature, the viscosity and density of nanofluids decreased causing a similar decrease in pressure drop.

5.3.2. Friction factor

The friction factor (*f*) of nanofluid in the flat tube increased with increase in Al_2O_3 nanoparticle concentration as shown in figure 5.14. However, it decreased with increase in Reynolds number and the lowest friction factor value was obtained for the base fluid (water) at the Reynolds number ~ 20000. The deviation of friction factor of alumina nanofluids from the base fluid decreased as the Reynolds number was increased. The friction factor for alumina oxide nanofluids was 0.5% higher than the base fluid for the Reynolds number 5000 and increased up 0.9% as the Reynolds number increased up to 20000 for 0.25% v/v of nanoparticles. As the nanoparticles concentration increased to 1.0% v/v, the friction factor also increased approximately 2.5%. For the copper oxide nanoparticles, the friction factor was 1.6%, 2.85%, 3.41% and 4.3% higher than of base fluid for 0.25%, 0.50%, 0.75% and 1.0% v/v nanoparticle loadings respectively as shown in figure 5.15.

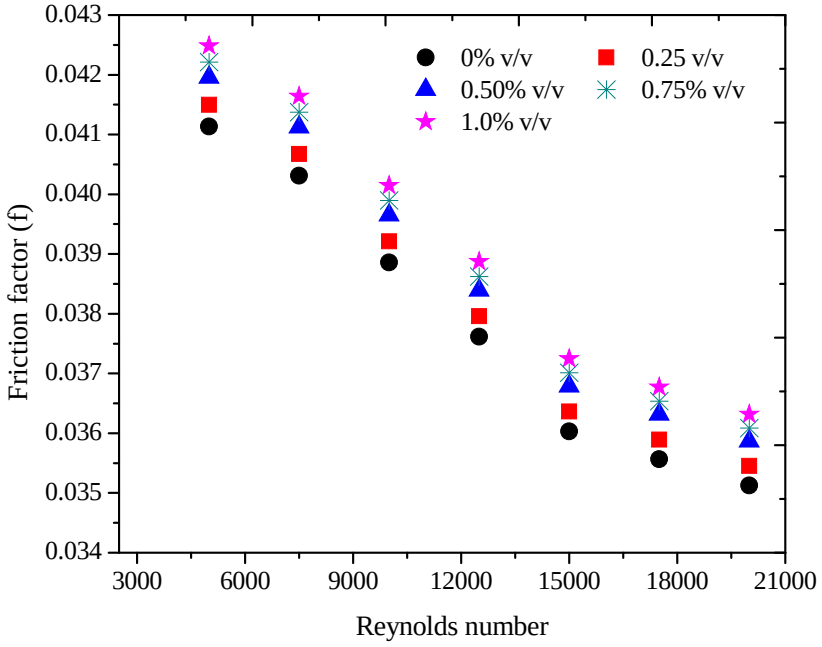

Figure 5.14: Variation of friction factor in flat tube with Reynolds number and aluminum oxide particle concentration

5.3.3. Pumping power

The pumping power needed by aluminum oxide and copper oxide nanofluids was considerably higher than that needed for the base fluid as shown in figure 5.16 and figure 5.17. The pumping

power increased exponentially with increase in particle concentration as well as Reynolds number. The pumping power required for aluminum oxide 0.25% v/v nanofluid for Reynolds numbers 5000 and 20000, respectively, was 1.51% and 1.61% higher than the base fluid and it increased to 5.4% and 5.57%, respectively, when the particle concentration was increased to 1.0% v/v. The pumping power required for copper oxide 0.25% v/v nanofluid for Reynolds numbers 5000 and 20000, respectively, was 2.9% and 3.1% higher than the base fluid and it increased to 8.81% and 9.1%, respectively, when the particle concentration was increased to 1.0% v/v. The increase in density and viscosity of nanofluids with increasing the particle concentration significantly increased the pumping power. Vajjha et al. (2010) also concluded the same through their numerical studies on a flat tube.

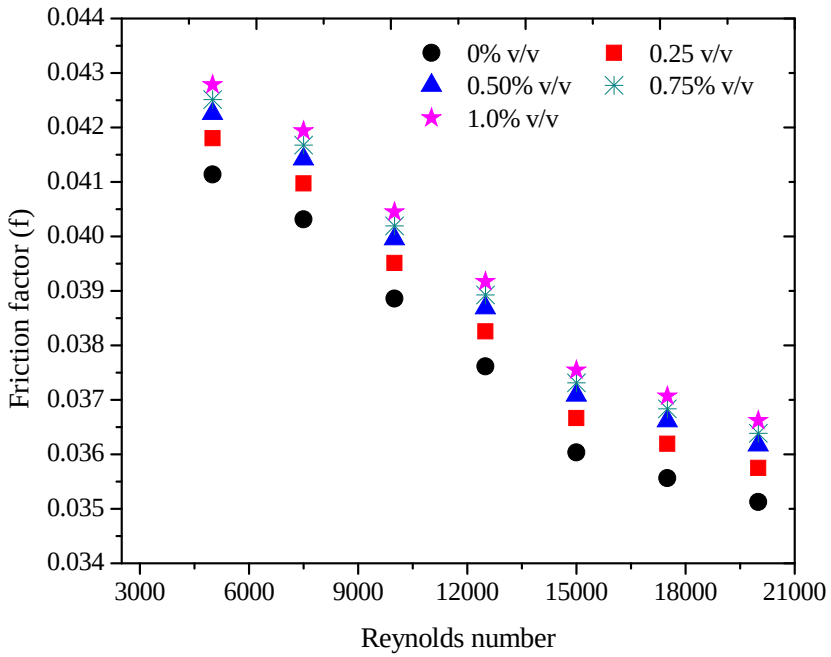

Figure 5.15: Variation of friction factor in flat tube with Reynolds number and copper oxide particle concentration

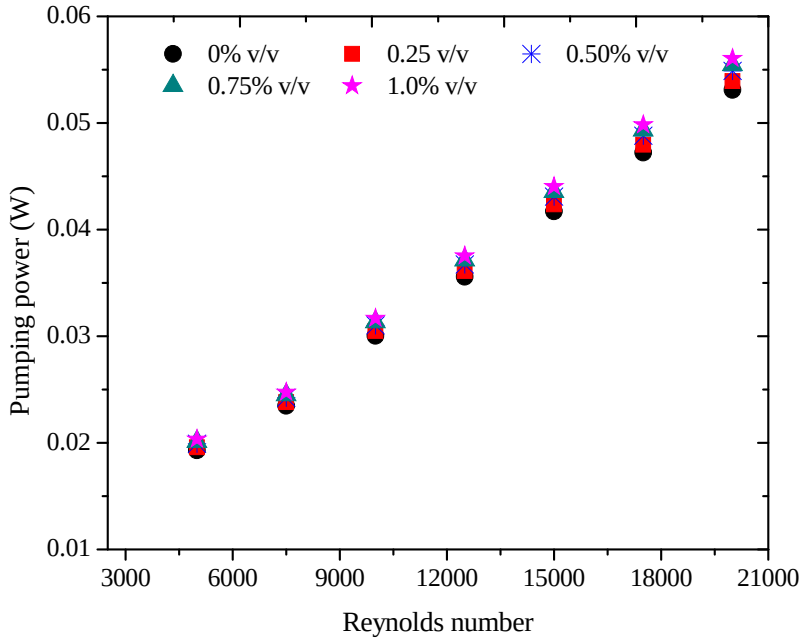

Figure 5.16: Variation of pumping power in flat tube with Reynolds number and aluminum oxide particle concentration

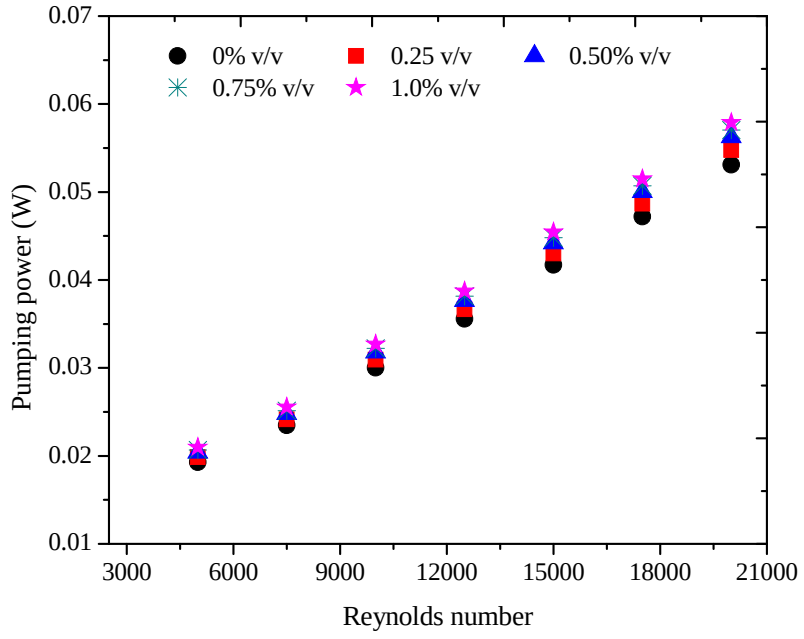

Figure 5.17: Variation of pumping power in flat tube with Reynolds number and copper oxide particle concentration

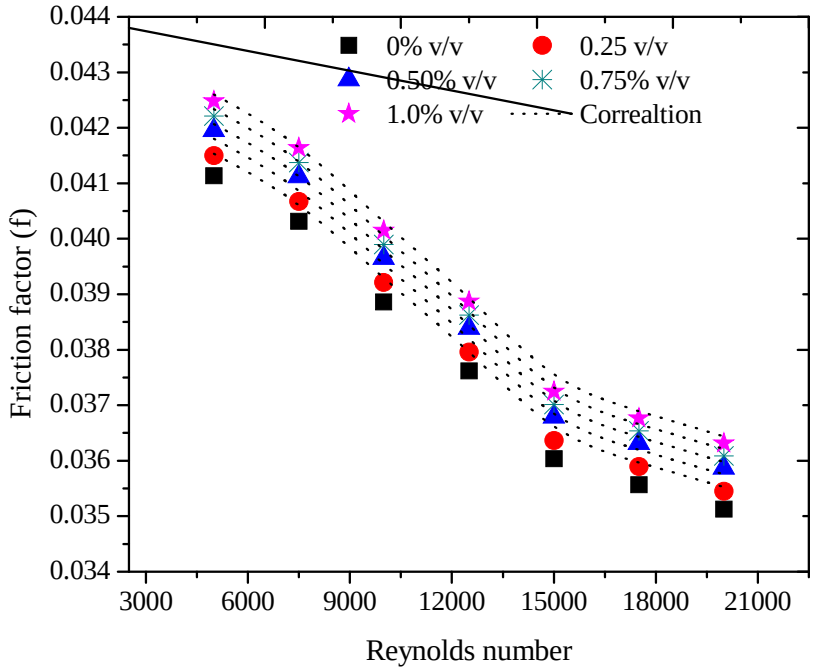

Figure 5.18: Experimental and correlation friction factor of aluminum oxide nanofluids

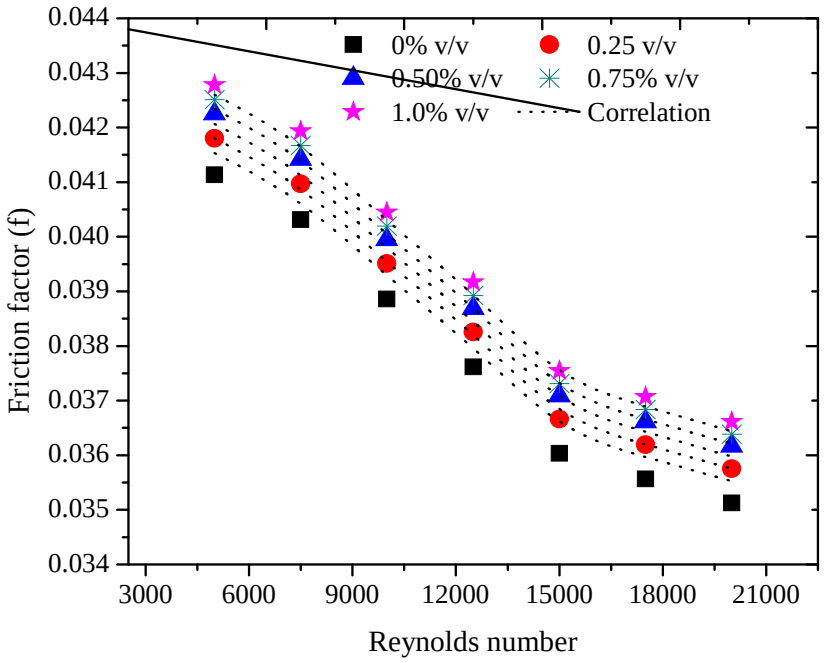

Figure 5.19: Experimental and correlation friction factor of copper oxide nanofluids

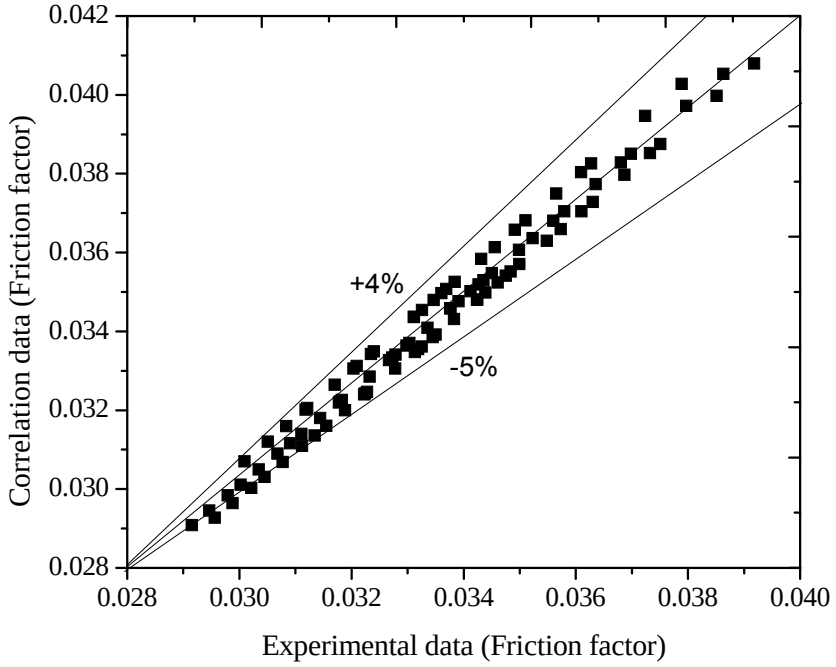

Figure 5.20: Comparison of experimental friction factor and predicted friction factor nanofluids

A general mathematical correlation (equation 5.2) for friction factor was developed to predict the friction factor of flat tube for aluminum oxide and copper oxide nanoparticles for different particle concentrations and Reynolds number. The experimental friction factor of copper oxide nanofluids were compared with the developed mathematical correlation as given equation 5.2. The **e**xperimental and predicted model friction factor for aluminum oxide and copper nanofluids is shown in figure 5.18 and figure 5.19 respectively. The R-square value for alumina oxide nanofluids 0.97 and copper oxide nanofluids 0.98 is observed.

$$f = 0.3164\,\mathrm{Re}^{-0.29}(1.24 + ¤)^{3.16} \qquad (5.2)$$

5.4. Heat transfer performance of nanofluids in compact heat exchanger

In first stage, the performance of aluminum oxide and copper oxide nanofluids was evaluated for single flat vertical tube and second stage, the heat transfer and fluid flow performance of nanofluids was evaluated in compact heat exchanger which consisted the multiple flat vertical tube. The base fluid and prepared nanofluids employed as the working fluid to evaluate the performance of

nanofluids in compact. The heat transfer performance evaluated at various fluid inlet temperature such as 40 ºC, 50 ºC, 60 ºC, 70 ºC and 80 ºC and at Reynolds number range from 5000 to 15000 and water based nanofluids in the range of 0.25% v/v to 1% v/v concentration of alumina oxide and copper oxide nanoparticles.

5.4.1. Nusselt number

The variation of Nusselt number with different Reynolds number and particle concentration at different fluid inlet temperature (a) 40 ºC, (b) 50 ºC, (c) 60 ºC, (d) 70 ºC and 80 ºC for aluminum oxide and copper nanofluids is shown in figure 5.21 and 5.22 respectively. The addition of nanoparticles plays a vital role in enhancing the Nusselt number and suspending the nanoparticles in base fluid leads to an increase in heat transfer performance of radiator. The enhancement in Nusselt number with copper oxide nanofluids is higher than of aluminum oxide nanofluids for the same operating conditions. The Nusselt number enhancement with 0.25% v/v of aluminum oxide and copper oxide nanoparticle concentration was 8% and 12% respectively as compared to the base fluid for the Reynolds number 14000, and it enhanced further to 28% and 31% as the particle concentration was increased to 1.0% v/v for the same Reynolds number. With the rise in fluid inlet temperature, the Nusselt number increased because of the increase in thermal conductivity and decrease in density and viscosity of fluids. As the inlet temperature of nanofluids was increased from 40°C to 60°C, the heat transfer performance improved by 9% and 8% and this enhancement further increased to 24% and 15% as the inlet temperature was raised to 80°C for a particular fluid velocity and aluminum oxide and copper oxide particle concentration respectively. In addition, the heat transfer performance also increased with increasing the air flow rate over the tubes and resulted in a decrease in the nanofluid temperature at the outlet of the flat tubes. It was noticed that increasing the air flow rate from 2 to 4 m/s causes maximum 17% enhancement in heat transfer for 1.0% v/v nanofluid. Similar results were observed with other particle concentrations, Reynolds numbers and inlet temperatures of nanofluid. Heat transfer performance of copper based nanofluids was higher than that of aluminum oxide nanofluids as the thermal conductivity of copper oxide nanoparticles is higher than aluminum oxide nanoparticle. With the use aluminum oxide nanoparticles about 28% enhancement in heat transfer performance was observed as compared to the base fluid while with copper oxide nanoparticles, 31% enhancement was higher than base fluid under the same operating condition in the experimentations. The higher thermal conductivity of nanofluids as compared to base fluid, the flow pattern of base fluid also changes with the addition of nanoparticles are the responsible factors for Nusslet number enhancement.

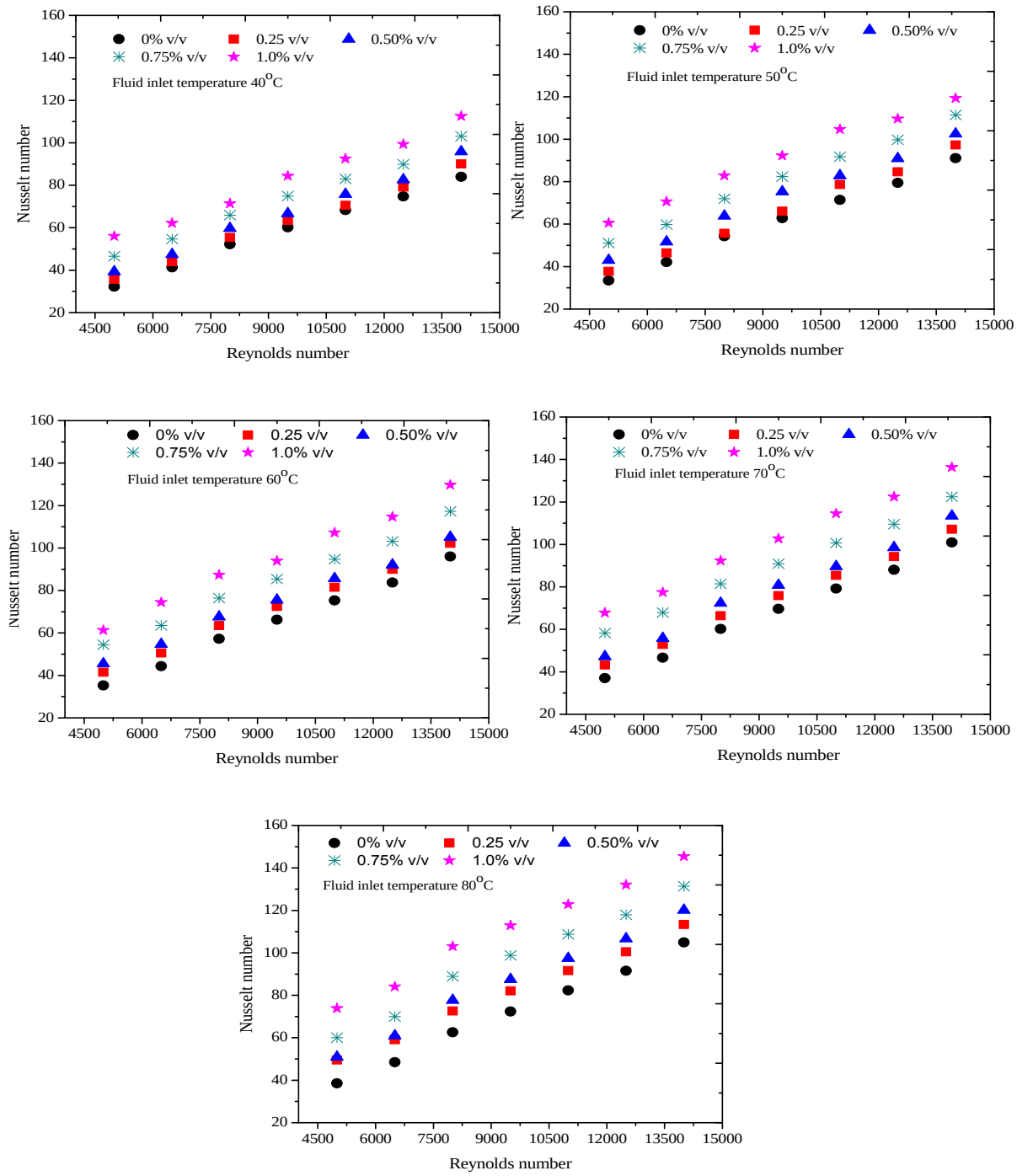

Figure 5.21: Variation of Nusselt number with Reynolds number and aluminum oxide nanoparticle concentration at different fluid inlet temperature (a) 40 ºC, (b) 50 ºC, (c) 60 ºC, (d) 70 ºC, (e) 80 ºC

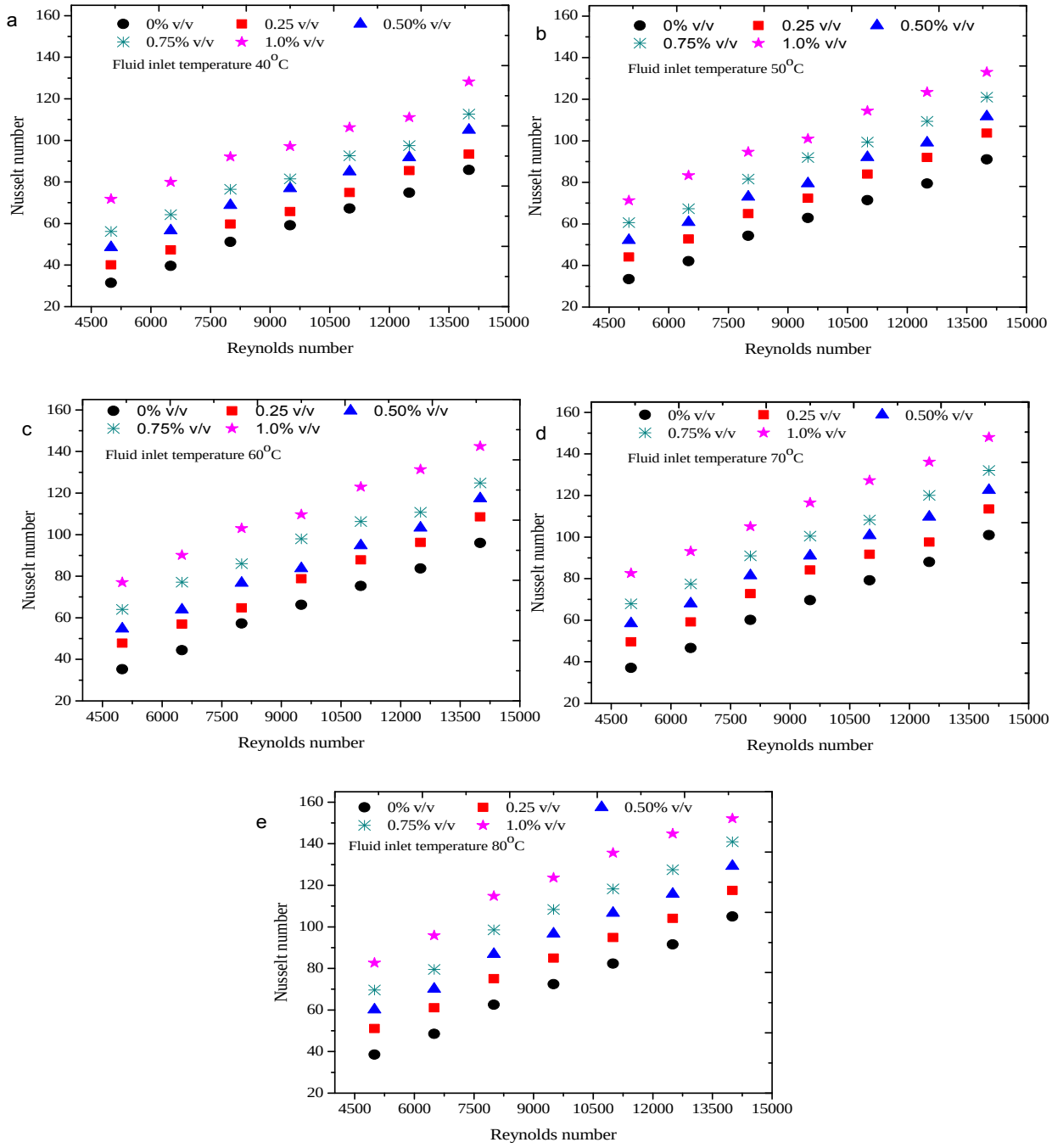

Figure 5.22: Variation of Nusselt number with Reynolds number and copper oxide nanoparticle concentration at different fluid inlet temperature (a) 40 ºC, (b) 50 ºC, (c) 60 ºC, (d) 70 ºC (e) 80 ºC

The wall temperature increment due to the Brownian motion of nanoparticles near the tube wall at high Reynolds numbers and development of thermal boundary layer near the flat tube wall surface was delayed due to chaotic motion of nanoparticles, which resulted in increased heat transfer.

5.4.2. Heat transfer coefficient

The thermal performance directly depends upon the heat transfer coefficient. The heat transfer coefficient is calculated by taking the difference between the average of inlet and outlet temperature (bulk mean temperature) and wall temperature. The variation of heat transfer coefficient for base fluid and nanofluids in the compact heat exchanger with Reynolds number, fluid inlet temperature and nanoparticle concentration (aluminum oxide and copper oxide) is shown in figure 5.23. The heat transfer coefficient for nanofluids of copper oxide nanoparticles was higher than that of different concentrations of aluminum oxide nanoparticles and followed by base fluid and it increased with increase in nanoparticles concentration as well as Reynolds number of nanofluids. The enhancement of heat transfer coefficient as compared to the base fluid was 25% for alumina oxide and 29% for copper oxide nanofluids at 0.25% v/v concentration of nanoparticles for Reynolds number 5000 and this enhancement increased up to 30% and 34% as the Reynolds number of nanofluids increased up to 14000. Furthermore, heat transfer coefficient enhancement increased up to 38% and 45% for the 1.0% v/v concentration of aluminum oxide and copper oxide/water nanofluids respectively for Reynolds number 14000. The heat transfer coefficient for nanofluids and base fluid also increased with increase in fluid inlet temperature. As the inlet temperature increased from 40°C to 50°C, 10% and 13% for aluminum oxide and copper oxide respectively, enhancement in heat transfer was observed and this enhancement increased to 31% and 34% respectively, as inlet temperature was increased to 80°C for fixed Reynolds number and particle concentration. The maximum enhancement was approximately 45% for 1.0% v/v copper oxide concentration of nanofluids for Reynolds number 14000 and fluid inlet temperature 80°C. The heat transfer coefficient for nanofluids was more than base fluids because, thermal conductivity of nanofluids is higher than that of base fluid but, thermal conductivity is not the sole reason for heat transfer enhancement and there could be other reasons for the heat transfer enhancement. At higher temperatures, the nanoparticles are uniformly distributed due to the Brownian motion of nanoparticles, which leads to heat transfer enhancement.

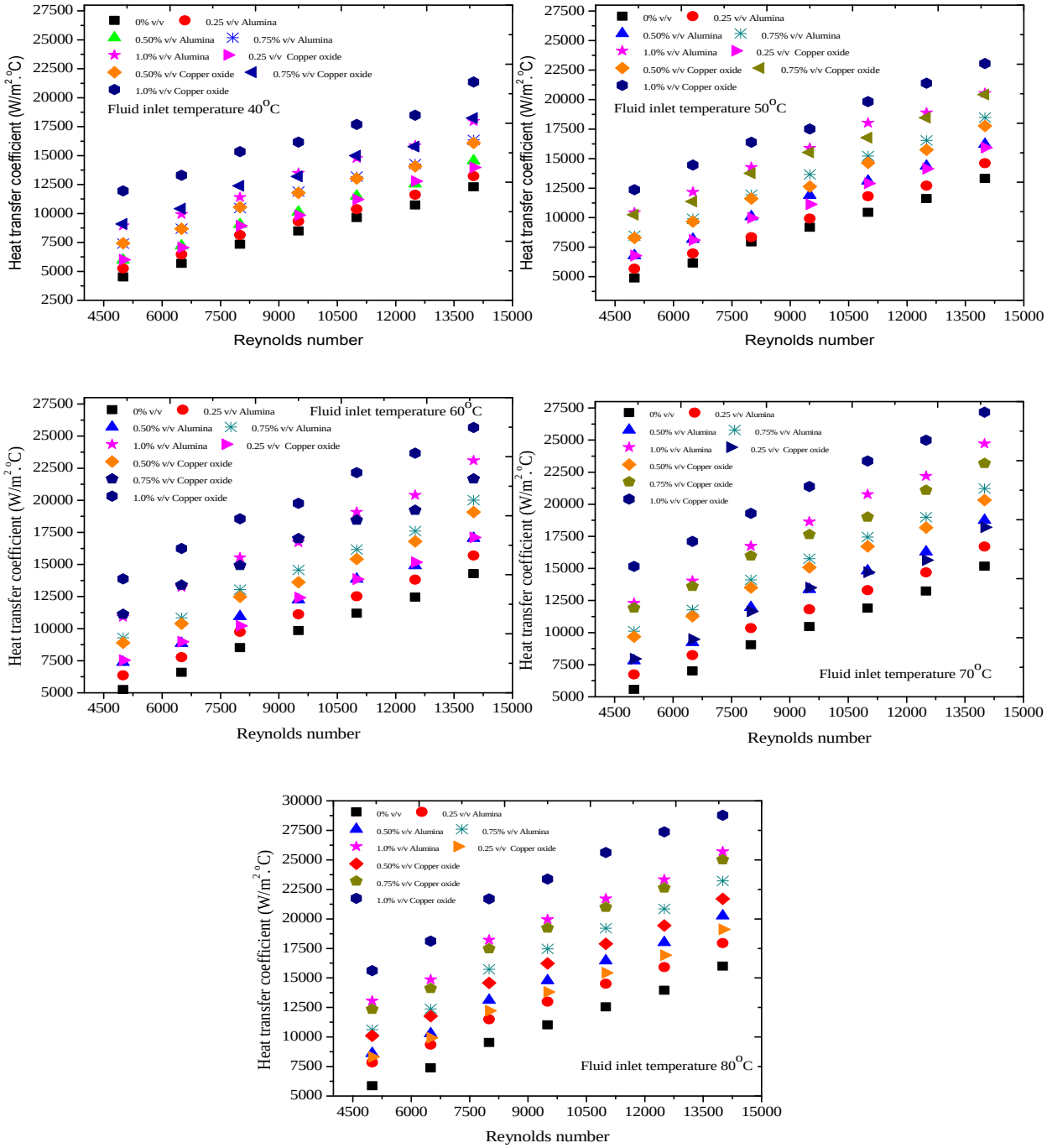

Figure 5.23: Variation of heat transfer coefficient with Reynolds number and copper oxide particle concentration at different fluid inlet temperature (a) 40 ºC, (b) 50 ºC, (c) 60 ºC, (d) 70 ºC (e) 80 ºC

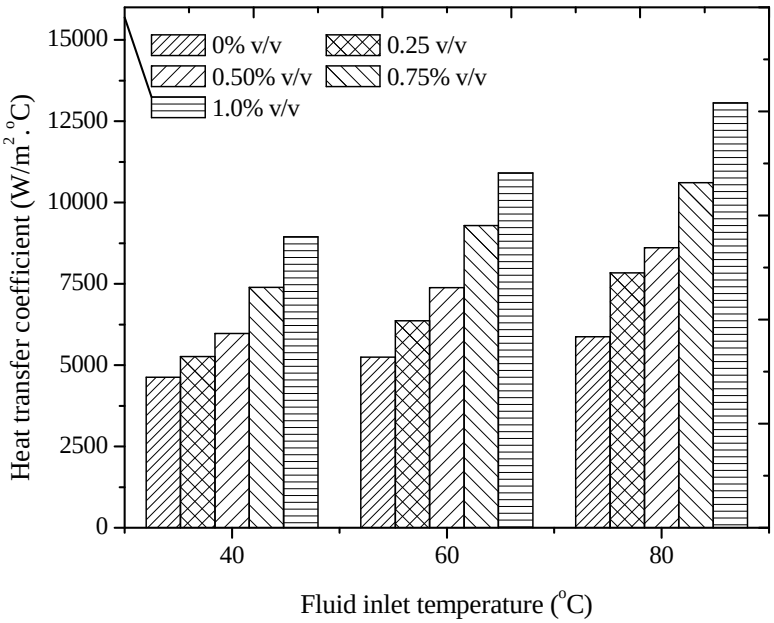

Figure 5.24: Comparison of heat transfer coefficient for different aluminum oxide particle concentration at different fluid inlet temperature

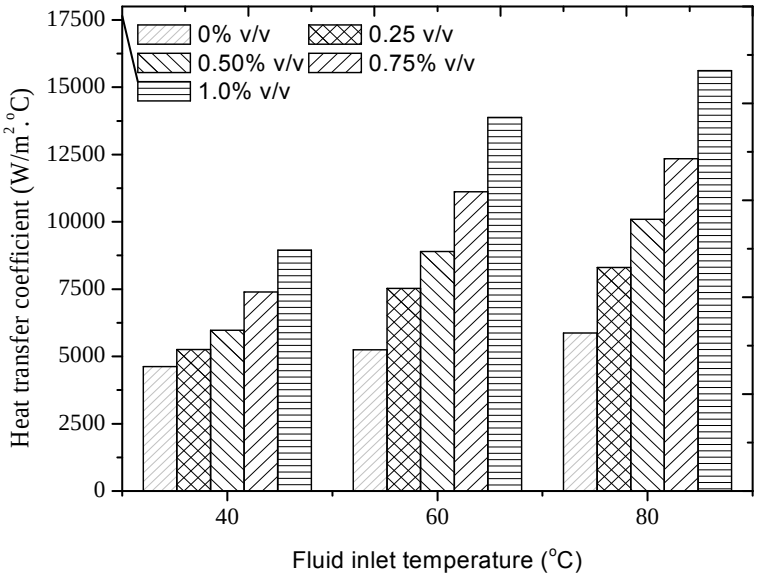

Figure 5.25: Comparison of heat transfer coefficient for different copper oxide particle concentration at different fluid inlet temperature

Other reasons for the heat transfer enhancement could be energy transfer due to particle migration. The particle migration is due to the spatial gradient in shear rate. Particle migration due to these effects could result in significant non uniformity in particle concentration over tube section in high particle concentration. The non uniformity resulting from the particle migration leads to higher Nusselt number which dends upon Peclet number and particles concentration. The similar results of heat transfer enhancement with nanofluids have been reported by previous researchers in their numerical and experimental studies [15,18,20]. The comparison of heat transfer coefficient for aluminum oxide nanofluids and copper oxide nanofluids at different temperature is shown in figure 5.24 and figure 5.25, respectively.

5.4.3. Heat transfer rate

The heat transfer rate of air side increased with increase in nanoparticle concentration and flow rate of air side as shown in the figure 5.26. As seen there is good agreement between the air side and liquid (base fluid and nanofluids) for each experiment. As the air mass flow rate increased from 0.101 kg/s to 0.223 kg/s the air side heat transfer rate increased from 252 W to 413 W for the 0% v/v loading of nanoparticles while it increased from 316 W to 526 W for aluminum oxide nanoparticles and 406 W to 809 W/ for copper oxide nanoparticles at 0.25% v/v concentration at fluid inlet temperature 40 ^{o}C. This enhancement is approximately 20% to 22% for aluminum oxide nanofluids and 37% to 48% for copper oxide nanofluids higher as comparison to base fluid. As the nanoparticle concentration increased up to 1.0% v/v, heat transfer increased up to 23% for aluminum oxide nanofluids and 32% for copper oxide nanofluids for the fixed mass flow rate of air and fluid inlet temperature. In case of air side heat transfer rate the maximum enhancement 62% was observed for the copper oxide nanofluids for the fixed the flow rate and heat transfer rate for copper oxide nanofluids was higher than the aluminum oxide nanofluids for all concentration of nanoparticles. The heat transfer rate of liquid side was also increased with increase in nanoparticle concentration and flow rate of liquid side as shown in the figure 5.27. The liquid side heat transfer rate enhanced up to 9% with aluminum oxide nanoparticles and 23% with copper oxide nanofluids for 0.25% v/v concentration of nanoparticles loading in the base fluid for fixed flow rate liquid at inlet temperature 40 ^{o}C. This enhancement is increased up to 54% for aluminum oxide nanofluids and 58% for copper oxide nanofluids for the fixed mass flow rate and at fixed fluid inlet temperature nanofluids. The heat transfer rate is also increased with increase in fluid inlet temperature i.e. as the fluid inlet temperature increased from 40 ^{o}C to 80 ^{o}C the heat transfer increased by 45% and 50% for aluminum oxide and copper oxide nanoparticle loading in the fluid. Moreover heat transfer rate enhancement for the air side is more than liquid side with the addition of nanoparticles as shown in

figure5.28.

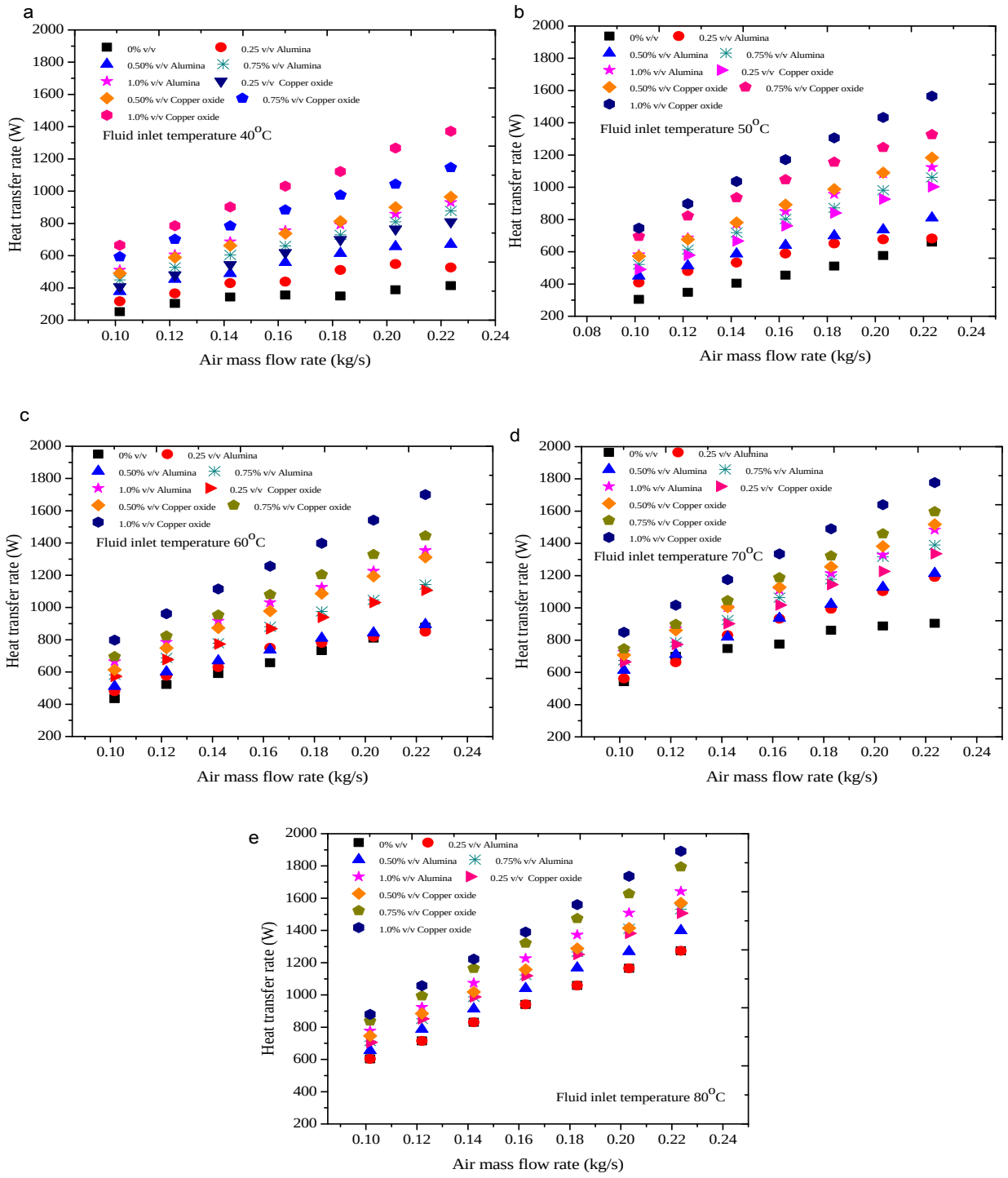

Figure 5.26: Effect of Reynolds number, particle concentration and fluid inlet temperature on air side heat transfer rate

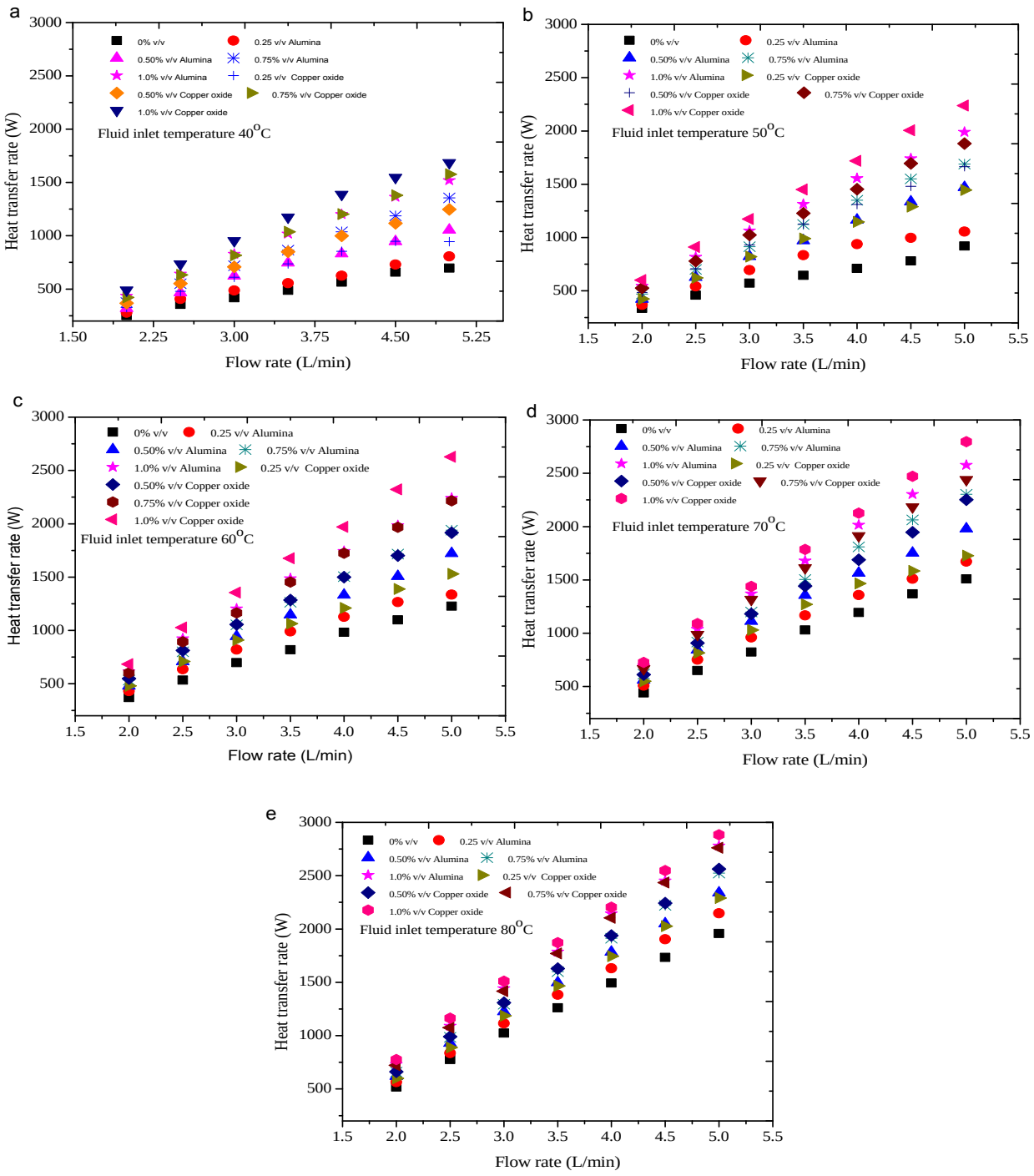

Figure 5.27: Effect of Reynolds number, particle concentration and fluid inlet temperature on liquid side heat transfer rate

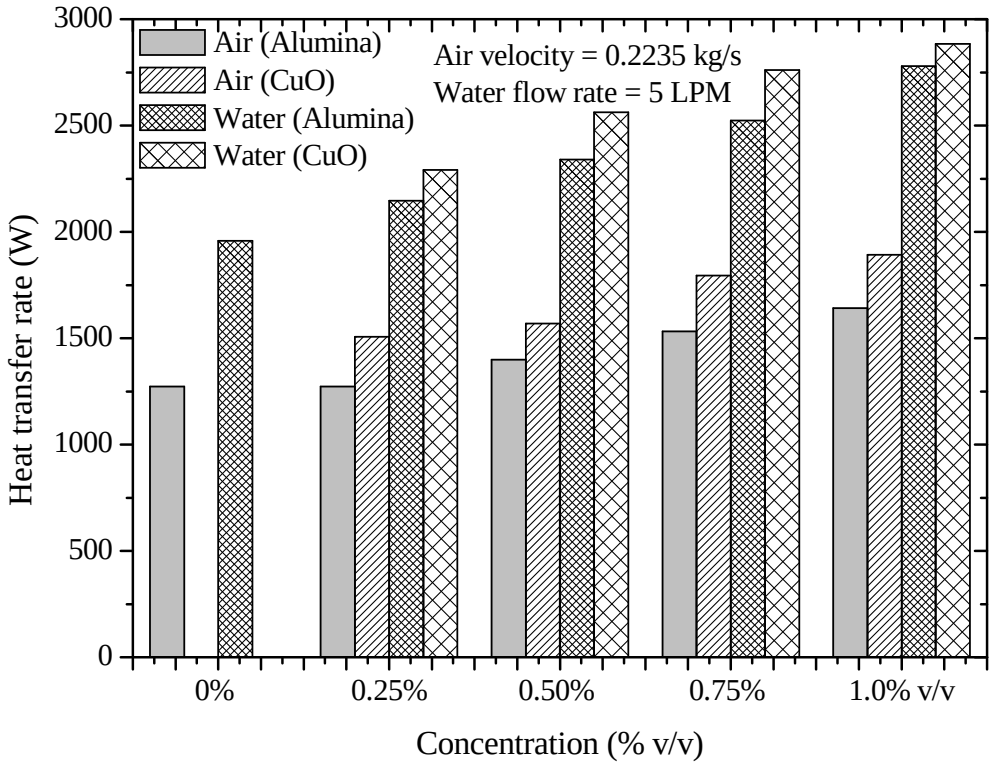

Figure 5.28: Comparison of heat transfer rate for air side and liquid side of compact heat exchanger with aluminum oxide and copper oxide nanofluids

5.4.4 Overall heat transfer coefficient

The results of overall heat transfer coefficient were compared in figure 5.29 for different nanoparticle (aluminum oxide and copper oxide) at different Reynolds number and fluid inlet temperatures. It was observed that overall heat transfer coefficient increased with increasing the nanoparticle concentration, Reynolds number of nanofluids and air as well as the fluid inlet temperature. As the Reynolds number increased from 5000 to 14000 the overall heat transfer coefficient for the compact heat exchanger (radiator) increased from 93 $W/m^2.^oC$ to 173 $W/m^2.^oC$ for the 0% v/v loading of nanoparticles while it increased from 96 $W/m^2.^oC$ to 187 $W/m^2.^oC$ for aluminum oxide nanoparticles and 100 $W/m^2.^oC$ to 191 $W/m^2.^oC$ for copper oxide nanoparticles at 0.25% v/v concentration at fluid inlet temperature 40 ^oC. This enhancement is approximately 3% to 7% for aluminum oxide nanofluids and 7% to 10% for copper oxide nanofluids higher as comparison to base fluid for same operating conditions.

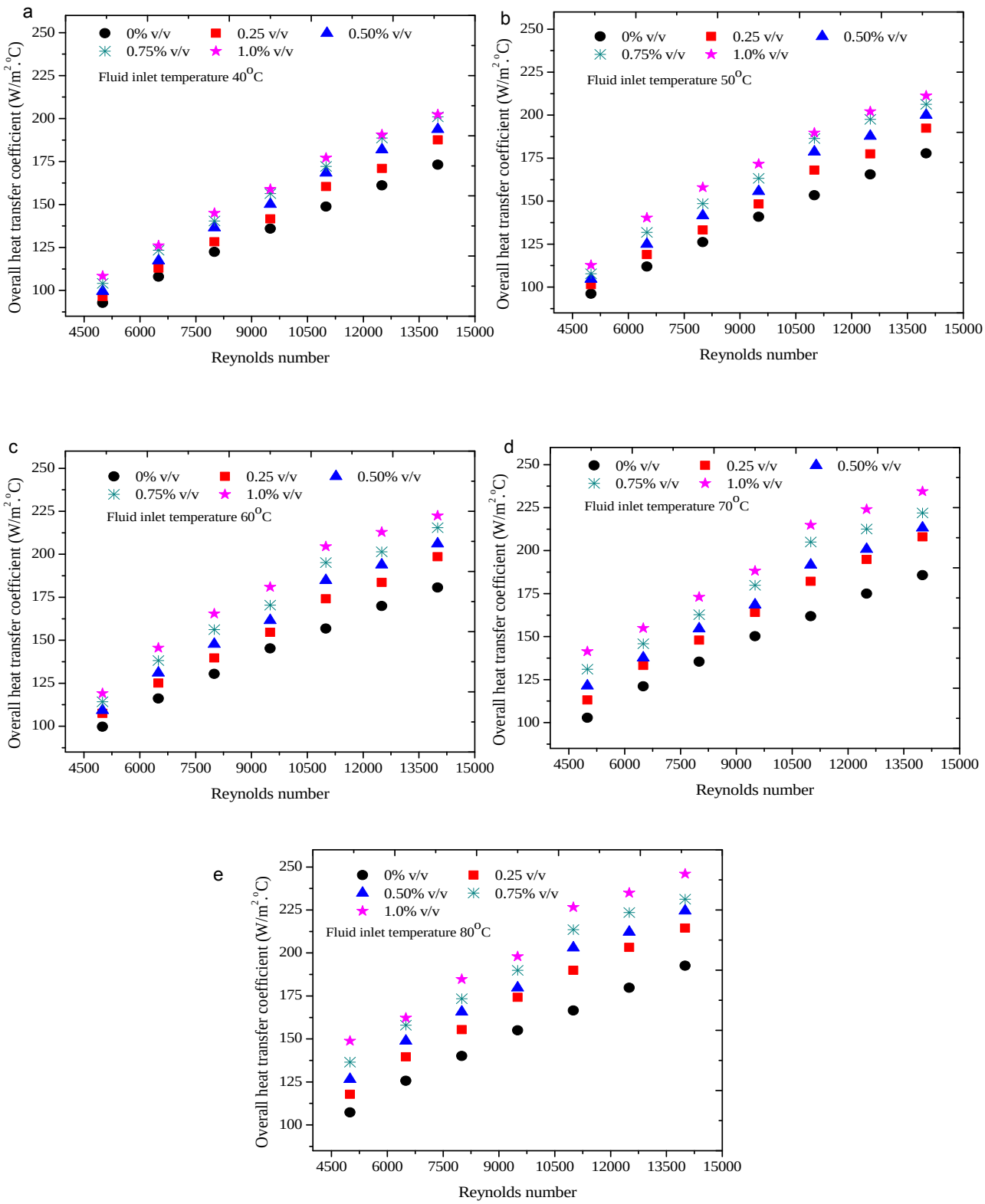

Figure 5.29: Variation of overall heat transfer coefficient with Reynolds number and particle concentration, temperature, (a) 40 ºC, (b) 50 ºC, (c) 60 ºC, (d) 70 ºC (e) 80 ºC

As the nanoparticles concentration was increased from 0.25% v/v to 1.0% v/v the overall heat transfer coefficient for the radiator increased from 192 W/m^2.^{o}C to 211 W/m^2.^{o}C for the aluminum oxide nanofluids while it increased from 198 W/m^2.^{o}C to 220 W/m^2.^{o}C for copper oxide nanoparticles for fixed Reynolds and fluid inlet temperature 50 ^{o}C. This enhancement is approximately 8% to 16% for aluminum oxide nanofluids and 10% to20% for copper oxide nanofluids higher as comparison to base fluid for same operating conditions. The overall heat transfer coefficient was also increased with increase in fluid inlet temperature. As the fluid inlet temperature number increased from 40 ^{o}C to 80 the overall heat transfer coefficient for the radiator increased from W/m^2.^{o}C to 192 W/m^2.^{o}C for the 0% v/v loading of nanoparticles while it increased from 202 W/m^2.^{o}C to 245 W/m^2.^{o}C for aluminum oxide nanoparticles and 207 W/m^2.^{o}C to 254 W/m^2.^{o}C for copper oxide nanoparticles at 1.0% v/v concentration at Reynolds number 14000. This enhancement is approximately 14% to 21% for aluminum oxide nanofluids and 16% to 25% for copper oxide nanofluids higher as comparison to base fluid for same operating conditions. The enhancement in overall heat transfer coefficient with Reynolds number and air velocities is due to addition of nanoparticles in base fluid which enhance the thermal conductivity of water side fluid. With increase in air velocity the convective heat transfer coefficient and external heat flux of air side increases which is also contribute to overall heat transfer coefficient enhancement. The comparison of overall heat transfer coefficient with aluminum oxide nanofluids and copper oxide nanofluids is shown in figure 5.30 and figure 5.31 respectively.

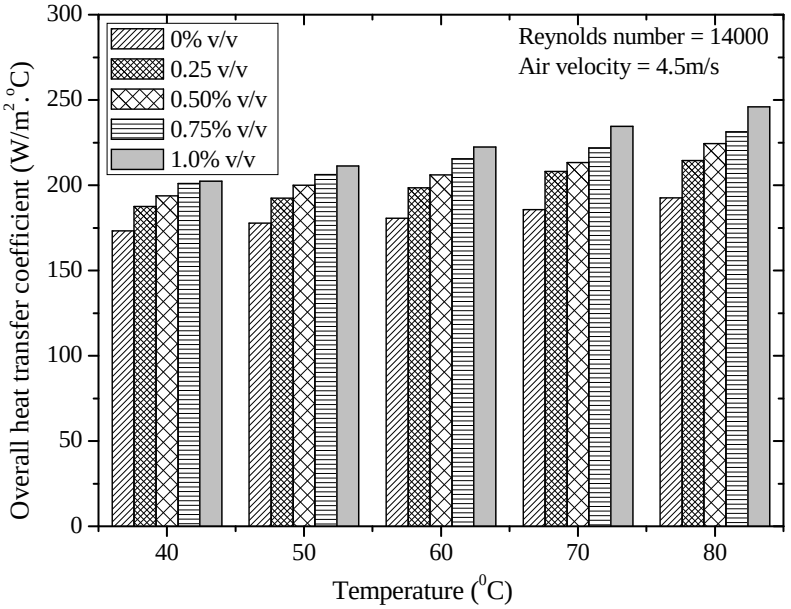

Figure 5.30: Comparison of overall heat transfer coefficient with aluminum oxide nanofluids

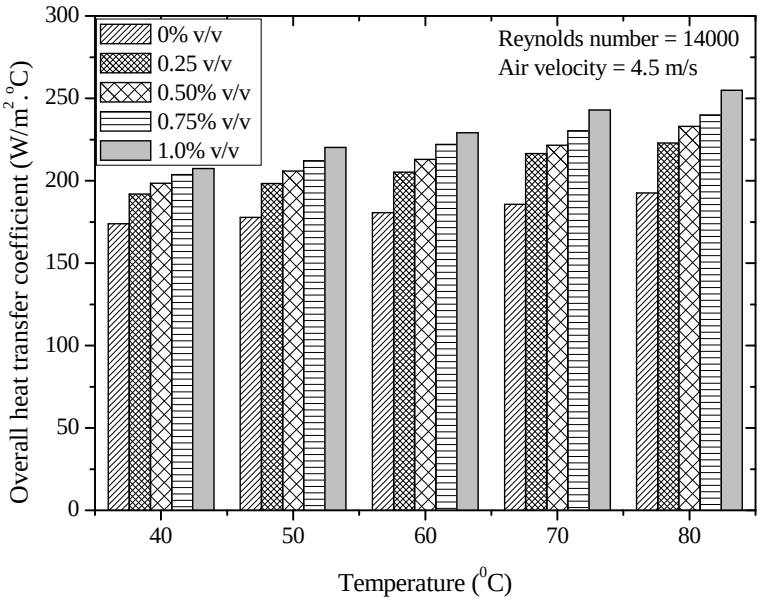

Figure 5.31: Comparison of overall heat transfer coefficient with copper oxide nanofluids

5.5. Fluid flow performance

Besides the heat transfer coefficient, pressure drop calculations are also important in determining the feasibility for practical application of nanofluids. The experiments were performed at high Reynolds number (turbulent flow region) and fluid flow performance evaluated different operating conditions.

5.5.1 Pressure drop

The pressure drop inside the compact heat exchanger depends on Reynolds number, density and viscosity of nanofluids. The pressure drop of base fluid and nanofluids in the compact heat exchanger for different Reynolds numbers and particle concentrations is shown in figure 5.32 and figure 5.33. The pressure drop increased with increasing nanoparticle concentration as well as Reynolds number. Pressure drop for copper oxide nanofluids is considerably higher than aluminum oxide nanofluids for all concentrations of nanoparticles and also higher than of base at same operating conditions. The reason for increase in pressure drop might be attributed to the fact that viscosity of base fluid increases with increase in particle concentration. For 0.25% v/v of nanoparticles, pressure drop for Reynolds number 5000 was 2.73% and 5% higher than the base fluid with addition of aluminum oxide and copper oxide nanoparticle respectively and this

enhancement in pressure drop increased by 10.12% and 11% in comparison to base fluid when the concentration was changed to 1.0% v/v for same Reynolds numbers. For the fixed concentration of nanoparticles (1.0% v/v), as compared to base the fluid pressure drop for nanofluids increased from 10% to 15% for alumina nanofluids and 11% to 17% for the copper oxide nanofluids as the Reynolds number increased from 5000 to 14000. Another reason for change in pressure drop could be the chaotic motion of nanoparticles in base fluid. As the inlet temperature of fluid increases, there was a small change in pressure drop. The pressure drop was influenced a little by decreasing with increasing the fluid inlet temperature because viscosity of base fluid and nanofluids decreases with increasing the fluid inlet temperature (which reduces the pressure drop at higher temperature).

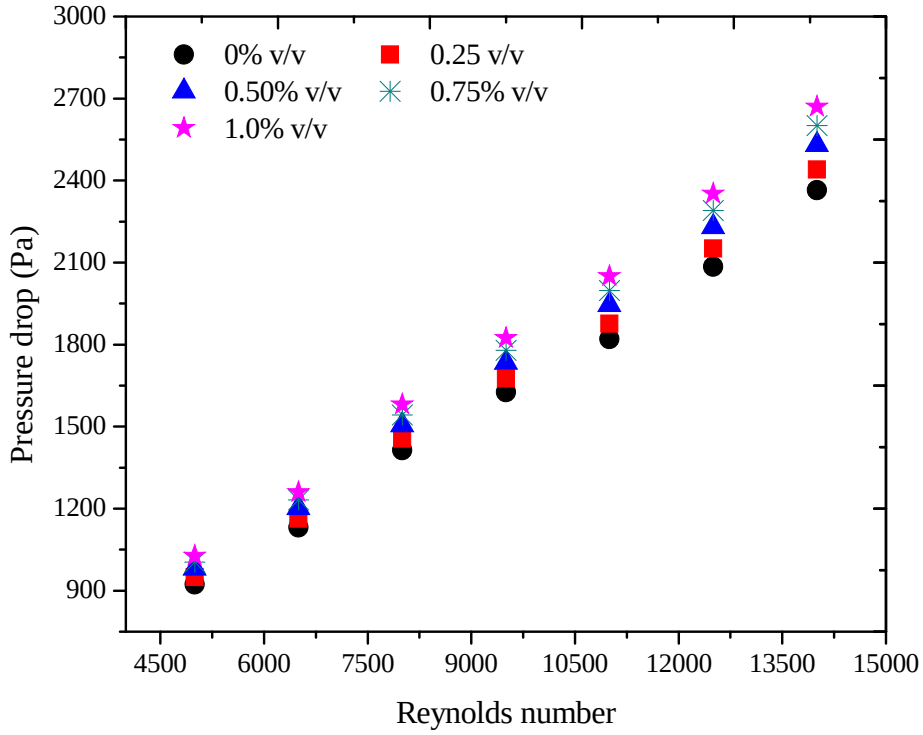

Figure 5.32: Variation of pressure drop in compact heat exchanger with Reynolds number and aluminum oxide particle concentration

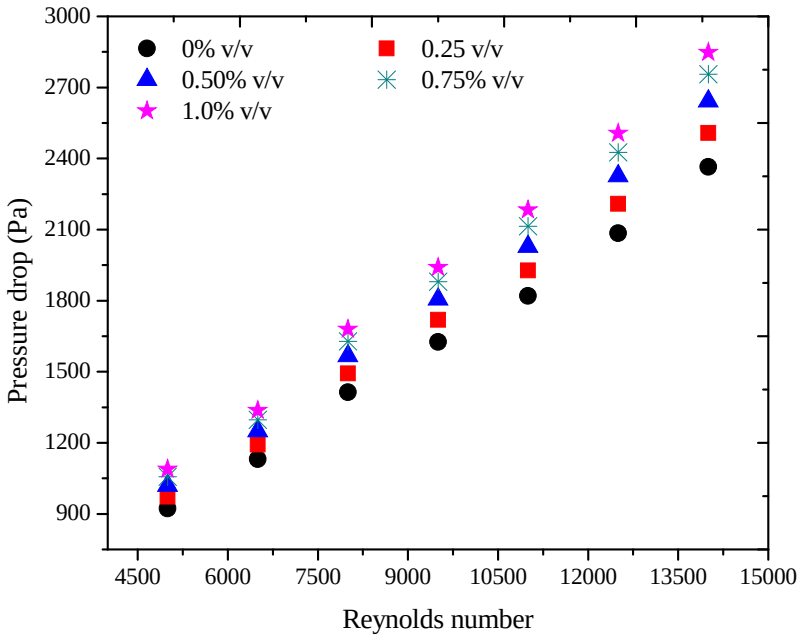

Figure 5.33: Variation of pressure drop in compact heat exchanger with Reynolds number and copper oxide particle concentration

5.5.2 Friction factor

As shown in figure 5.34 and figure 5.35, the friction factor (*f*) of nanofluid in the compact heat exchanger increased with increase in Al_2O_3 and Cuo nanoparticle concentration. For all concentration, friction factor increased with increase in nanoparticle loading in base fluid. However, it decreased with increase in Reynolds number and the lowest friction factor value was obtained for the base fluid (water) at the Reynolds number ~ 14000. For the low concentration of nanoparticle (0.25% v/v) and low Reynolds number, the increase in friction factor of nanofluids was very low which was approximately 2% while this enhancement is increased up to 8% for high concentration of nanoparticles (1.0% v/v) of aluminum oxide. For fixed concentration of nanoparticle at high Reynolds number, the friction factor increased approximately same. As the Reynolds number increased from 5000 to 14000, the value of friction factor was decreased by approximately 19%. The friction factor for copper oxide nanofluids was higher than base fluid as well as aluminum oxide nanofluids for all concentration of nanoparticles. The friction factor with copper oxide nanoparticles at low nanoparticles concentration (0.25% v/v) and Reynolds number (5000) was 4% higher and at high nanoparticles concentration (1.0% v/v) and Reynolds number (14000) was 13% higher than that of base fluid (water). For copper oxide nanofluids the value of friction factor is also decreased with increase in Reynolds number.

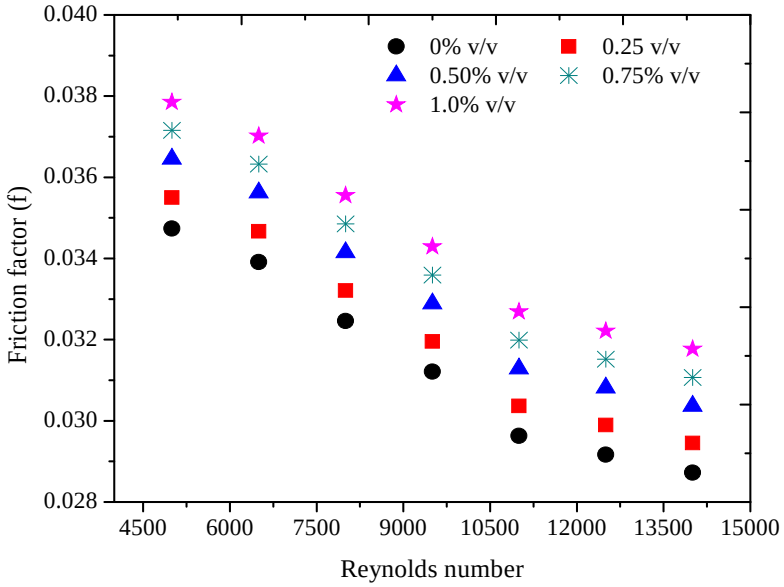

Figure 5.34: Variation of friction factor in compact heat exchanger with Reynolds number and aluminum oxide particle concentration

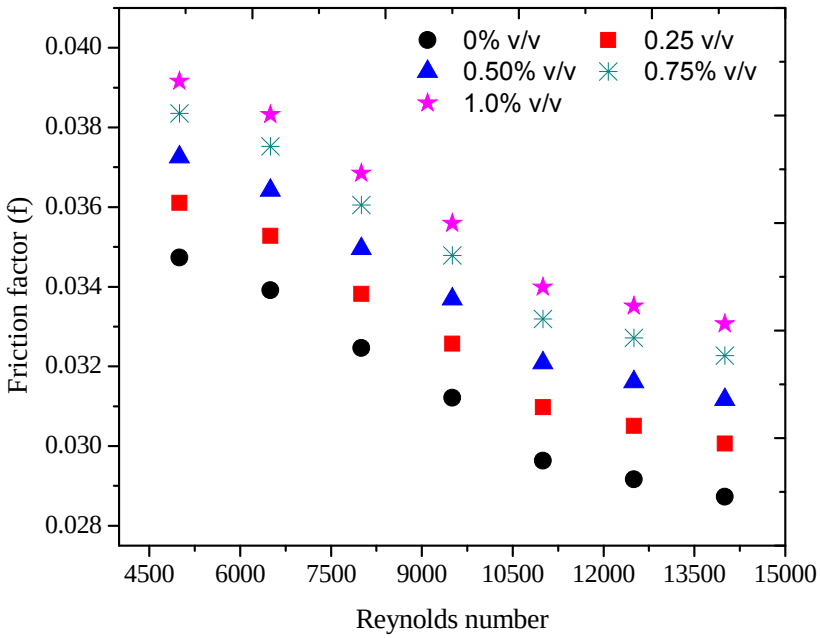

Figure 5.35: Variation of friction factor for compact heat exchanger with Reynolds number and copper oxide particle concentration

5.5.3. Pumping power

The pumping power needed by aluminum oxide nanofluids and copper oxide was higher than that needed for the base fluid. The pumping power increased exponentially with increase in particle concentration as well as Reynolds number as shown in figure 5.36 and figure 5.37. The pumping power required for 0.25% v/v aluminum oxide nanofluids for Reynolds numbers 5000 to 14000 was maximum 3% higher than the base fluid and it increased up to maximum 10%, when the particle concentration was increased to 1.0% v/v while the pumping power required for 0.25% v/v copper oxide nanofluids for Reynolds numbers 5000 to 14000 was maximum 5% higher than the base fluid and it increased up to maximum 16%, when the particle concentration was increased to 1.0% v/v. The increase in density and viscosity of nanofluids with increasing the particle concentration significantly increased the pumping power.

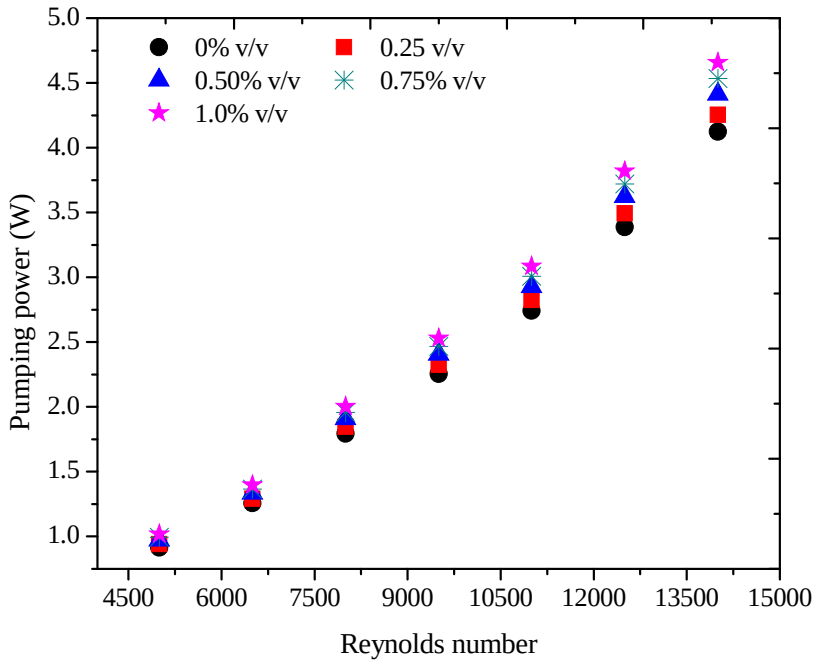

Figure 5.36: Effect of Reynolds number and aluminum oxide particle concentration on pumping power of compact heat exchanger

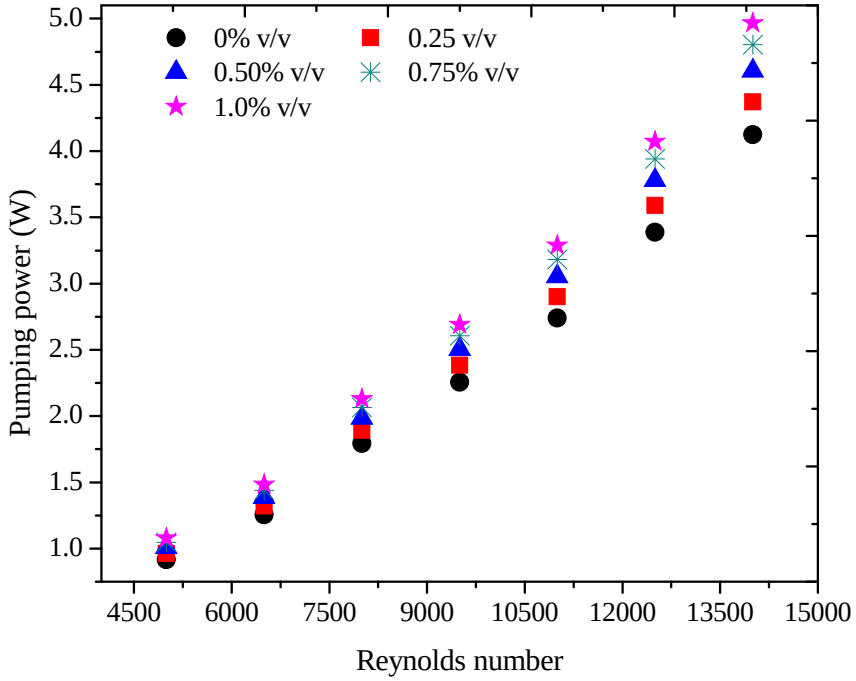

Figure 5.37: Effect of Reynolds number and copper oxide particle concentration on pumping power of compact heat exchanger

5.6. Closure

This chapter investigates the performance of aluminium oxide and copper oxide nanofluids in single flat vertical tube and compact heat exchanger (consisted multiple flat tube). The convective heat transfer performance and fluid flow performance enhanced with using of nanofluids. The maximum heat transfer enhancement was observed with copper oxide nanofluids at 1.0% v/v concentration of nanoparticles. By suspension of nanoparticles in the base fluid enhances the heat performance and the reason of this enhancement is suspended nanoparticles increase the specific surface area and heat capacity of nanofluids. The dispersion of nanoparticles flattens the transverse the temperature gradient of the fluid. The interaction and collision among nanoparticles, fluid and flow passage intensified. The mixing fluctuation and turbulence of fluid intensified. The percentage of pumping power increase as compared to base is less than the percentage of heat transfer enhancement so use of nanofluids instead of conventional fluids has more advantages**.**

CHAPTER 6

CONCLUSIONS AND FUTURE SCOPE

The present work investigated the detailed study of nanofluids preparation, stability of nanofluids and estimation of thermophysical properties i.e. thermal conductivity, density, viscosity and specific heat capacity. The fabrication of experimental setup for single flat vertical tube and compact heat exchanger has been done and analytical model for the evaluation of performance of compact heat exchanger has discussed. The performance of aluminum oxide and copper oxide nanofluids in single flat tube and compact heat exchanger (which consisted the multiple flat tubes) was estimated and model for heat transfer and pressure drop characteristics developed. This chapter presents the concluding remarks of the research work and future scope of the work.

1. In present thesis work, nanofluids were prepared from 0 – 1.0% v/v concentration of nanoparticles. The aluminium oxide nanofluids were prepared without use of any surfactant while copper oxide nanofluids with use of surfactant. For the copper oxide nanoparticles, 0.2 wt% of SDS was added to prepare the stable copper oxide nanofluids.
2. The stability of nanofluids is checked by Zeta potential, measuring the absorbance using UV-vis spectrophotometer and thermal conductivity. The aluminum oxide nanofluids remain stable more than 15 days and the stability of copper oxide nanofluids with reference to Zeta potential values was observed up to 10^{th} day of nanofluids preparation.
3. The thermal conductivity enhanced significantly with increase in particle concentration and temperature. The density and viscosity increased with increasing the particle concentration, while they both decreased with increase in temperature.
4. The thermal conductivity of nanofluids was more sensitive to temperature than that of the base fluid. The thermal conductivity of alumina nanofluid with 1.0% v/v concentration at 30°C was 8% higher than that of the base fluid whereas at 80°C it was 21% higher than that of the base fluid. With 0.1% of CuO nanoparticles at 30^oC, the enhancement of thermal conductivity was only 2% and at 90^oC this enhancement increased up to approximately 4%. For a higher particle concentration of 1.0%, the enhancement in thermal conductivity increased from 12% to 25% as the temperature was raised from 30^oC to 80^oC. The enhancement of thermal conductivity declines as the temperature of fluid rise from 80°C to 90°C.
5. With an increase in alumina particle concentration from 0.1 to 1.0% v/v, the viscosity of nanofluid at 30°C is 2.3% and 19.82% respectively higher than that of the base fluid. The

viscosity of copper oxide nanofluids increased from 2.8% to 20.46% as the nanoparticles concentration was increased from 0.1% to 1.0% v/v.

6. In comparison with the base fluid, the density was 0.3% higher for 0.1% v/v aluminum oxide nanofluid and 2.8% higher for 1.0 vol% nanofluids at 30°C. The increase in density of copper oxide nanofluids as compared to the base fluid was 0.3% for 0.1% v/v particle concentration and 4.41% for particle concentration of 1.0% v/v.
7. The heat capacity of nanofluids increases with temperature but diminishes with increase in particle volume concentration. The heat capacity decreased by 1% for 0.1% v/v concentration of copper oxide nanoparticles and heat capacity decreased up to 0.8% as the nanoparticles concentration increases up to 1.0% v/v.
8. The nanoparticles plays a vital role in enhancing the Nusselt number and suspending the nanoparticles in base fluid leads to an increase in heat transfer coefficient for flat vertical tubes of radiator. The heat transfer rate increased with increase in fluid inlet temperature, particle concentration, Reynolds number as well as air inlet velocity.
9. The Nusselt number enhancement with 0.25% v/v aluminum oxide nanoparticle concentration was 8% for the Reynolds number 20000, respectively, and it enhanced further to 40% when the particle concentration was increased to 1.0% v/v for the same Reynolds number. The enhancement of Nusselt number as compared to the base fluid was 18% for 0.25% v/v concentration of nanoparticles for Reynolds number 5000 and this enhancement was up to 12% as the Reynolds number of nanofluids increased up to 20000. Furthermore, heat transfer enhancement increased up to 51% for the 1.0 % v/v concentration of copper oxide/water nanofluids for Reynolds number 20000.
10. As the inlet temperature of nanofluid was increased from 40°C to 60°C, the heat transfer performance improved by 13% and this enhancement further increased to 28% as the inlet temperature was raised to 80°C for a particular fluid velocity and particle concentration (1.0% v/v). It was noticed that increasing the air flow rate from 2 to 4 m/s causes 12% enhancement in heat transfer for 1.0% v/v nanofluids.
11. By suspension of nanoparticles in the base fluid enhances the heat performance and the reason of this enhancement is suspended nanoparticles increase the specific surface area and heat capacity of nanofluids. The dispersion of nanoparticles flattens the transverse the temperature gradient of the fluid. The interaction and collision among nanoparticles, fluid and flow passage intensified. The mixing fluctuation and turbulence of fluid intensified.

12. The pressure drop increased with increasing the Reynolds number and particle volume concentration, while it slightly decreased with increase in fluid inlet temperature because density and viscosity decrease with increase in temperature. The pressure drop observed for 0.25% v/v nanofluid was 1.5% and 1.6% higher that of the base fluid for Reynolds numbers 5000 and 20000, respectively.
13. For 0.25% v/v of copper oxide nanoparticles, pressure drop for Reynolds number 5000 was 3% and 3.2% for Reynolds number 20000 in comparison with the base fluid and this increased to 8.5% and 9% when the concentration was changed to 1.0% v/v for same Reynolds numbers.
14. The friction factor (*f*) of nanofluid in the flat tube increased with increase in Al_2O_3 and CuO nanoparticle concentration. However, it decreased with increase in Reynolds number and the lowest friction factor value was obtained for the base fluid (water) at the Reynolds number ~ 20000.The friction factor for aluminum oxide nanofluids was 0.5% higher than the base fluid for the Reynolds number 5000 and increased up 0.9% as the Reynolds number increased up to 20000 for 0.25% vol. of nanoparticles. As the nanoparticles concentration increased to 1.0 vol.%, the friction factor also increased approximately 2.5%. For the copper oxide nanoparticles, the friction factor was 1.6%, 2.85%, 3.41% and 4.3% higher than of base fluid for 0.25%, 0.50%, 0.75% and 1.0% vol. nanoparticle loadings.
15. The pumping power needed by nanofluids was considerably higher than that needed for the base fluid. The pumping power required for 0.25% v/v nanofluid for Reynolds numbers 5000 and 20000, respectively, was 1.5% and 1.7% higher than the base fluid and it increased to 5.3% and 5.7%, respectively, when the particle concentration was increased to 1.0% v/v. The pumping with use copper oxide nanofluids was 9% higher in flat tube than of base fluid at higher Reynolds number.
16. The heat transfer performance of compact heat exchanger evaluated at various fluid inlet temperature such as 40 ^{o}C, 50 ^{o}C, 60 ^{o}C, 70 ^{o}C and 80 ^{o}C and at Reynolds number range from 5000 to 14000 and water based nanofluids in the range of 0.25% v/v to 1% v/v concentration of alumina oxide and copper oxide nanoparticles.
17. The Nusselt number enhancement with 0.25% v/v of aluminum oxide and copper oxide nanoparticle concentration was 8% and 12% respectively as compared to the base fluid for the Reynolds number 14000, and it enhanced further to 28% and 31% as the particle concentration was increased to 1.0% v/v for the same Reynolds number.
18. With the rise in fluid inlet temperature, the Nusselt number increased because of the increase in thermal conductivity of fluids. As the inlet temperature of nanofluids was increased from

40°C to 60°C, the heat transfer performance improved by 9% and this enhancement further increased to 24% and 15% as the inlet temperature was raised to 80°C

19. The heat transfer rate increased with increase in fluid inlet temperature, particle concentration, Reynolds number as well as air inlet velocity. The maximum enhancement in heat transfer coefficient was about 31% at 1.0% v/v concentration as compared to the base fluid.
20. Heat transfer enhancement was more than the enhancement in the thermal conductivity of nanofluid at same temperature and concentration. This indicates that besides thermal conductivity, other factors such as fluid inlet temperature, Reynolds number and air velocity also affect heat transfer coefficient.
21. The overall heat transfer coefficient for the compact heat exchanger (radiator) increased with increase addition of nanoparticles (aluminum oxide nanoparticles and copper oxide nanoparticles). The enhancement is approximately 3% to 7% for aluminum oxide nanofluids and 7% to 10% for copper oxide nanofluids higher as comparison to base fluid for same operating conditions. As the nanoparticles concentration was increased from 0.25% v/v to 1.0% v/v the overall heat transfer coefficient enhanced approximately 8% to 16% for aluminum oxide nanofluids and 10% to 20% for copper oxide nanofluids higher as comparison to base fluid for same operating conditions.
22. The pressure drop along the compact heat exchanger also increased by 16% with Reynolds number as well as nanoparticles loading, while slightly decreased up to 2% with increase in fluid temperature. The maximum increase in pressure drop was 16% than base fluid for 0.5% v/v nanoparticles at Reynolds number 15000.
23. The friction factor also increased by 10% with increase in nanoparticle concentration, while it decreased with increase in Reynolds number. The friction factor for copper oxide nanofluids was higher than base fluid as well as aluminum oxide nanofluids for all concentration of nanoparticles. The friction factor with copper oxide nanoparticles at low nanoparticles concentration (0.25% v/v) and Reynolds number (5000) was 4% higher and at high nanoparticles concentration (1.0% v/v) and Reynolds number (14000) was 13% higher than that of base fluid (water).
24. The pumping power required for aluminum oxide and copper oxide nanofluids higher than the base fluid and it increased up to maximum 10%, as the particle concentration was increased to 1.0% v/v.

This study proves that the size of automotive cooling system can decreased with the use of nanofluids in place of conventional cooling fluids because the heat transfer is the primary concern for cooling systems.

Future Scope

1. In the present work, thermophysical properties i.e. thermal conductivity, viscosity, density and specific heat capacity of oxide nanofluids measured. The thermophysical properties of hybrid nanofluids (combinations of two or more nanoparticles) which can improve the thermal conductivity of nanofluids.
2. In the present work, performance of nanofluids in single plain flat tube is estimated. The work can be extended by modification of tube i.e. with the use inserts and dimples on the surface of flat tube.
3. The performance of compact heat exchanger is estimated with water as the base fluid. In the cold areas, ethylene glycol is mixed in the base fluid as the coolant. So research can be carried out with mixture of ethylene glycol and water with different concentration of nanoparticles.
4. The copper, aluminum nanoparticles, carbon nanotubes, silver, gold, diamond nanoparticles and graphene nano platelets and water – ethylene glycol mixture can be used as the coolant fluid to evaluate the performance of flat tube.
5. Experimental study on the behaviour of water ethylene glycol mixture with mutliwalled carbon nanotube can be carried out as the thermal conductivity of multiwalled carbon nanotube is higher than aluminum oxide and copper oxide nanofluids.

REFERENCES

1. A.A. Abbasian Arani, J. Amani, Experimental investigation of diameter effect on heat transfer performance and pressure drop of TiO_2-water nanofluid, Exp. Therm. Fluid Sci. 44, (2013), 520–533.
2. H. Heidary, A. Abbassi, M.J. Kermani, Enhanced heat transfer with corrugated flow channel in anode side of direct methanol fuel cells, Energy Convers. Manag. 75, (2013), 748–760.
3. M. Khoshvaght-Aliabadi, F. Hormozi, A. Zamzamian, Role of channel shape on performance of plate-fin heat exchangers: Experimental assessment, Int. J. Therm. Sci. 79, (2014), 183–193.
4. L.D. Tijing, B.C. Pak, B.J. Baek, D.H. Lee, A study on heat transfer enhancement using straight and twisted internal fin inserts, Int. Commun. Heat Mass Transf. 33, (2006), 719–726.
5. S.K. Das, S.U.S. Choi, W. Yu, T. Pradeep, Nanofluids: Science and Technology, 2007.
6. R. Saidur, K.Y. Leong, H.A. Mohammad, A review on applications and challenges of nanofluids, Renew. Sustain. Energy Rev. 15, (2011), 1646–1668.
7. C. Sitprasert, P. Dechaumphai, V. Juntasaro, A thermal conductivity model for nanofluids including effect of the temperature-dependent interfacial layer, J. Nanoparticle Res. 11, (2009), 1465-1476.
8. M.P. Beck, Y. Yuan, P. Warrier, A.S. Teja, The thermal conductivity of alumina nanofluids in water, ethylene glycol, and ethylene glycol + water mixtures, J. Nanoparticle Res. 12, (2010), 1469–1477.
9. L. Godson, B. Raja, D.M. Lal, S. Wongwises, Experimental Investigation on the thermal conductivity and viscosity of silver-deionized water nanofluid, Exp. Heat Transf. 23, (2010), 317–332.
10. M.M. Elias, I.M. Mahbubul, R. Saidur, M.R. Sohel, I.M. Shahrul, S.S. Khaleduzzaman, S. Sadeghipour, Experimental investigation on the thermo-physical properties of Al_2O_3 nanoparticles suspended in car radiator coolant, Int. Commun. Heat Mass Transf. 54, (2014), 48–53.
11. R.S. Vajjha, D.K. Das, P.K. Namburu, Numerical study of fluid dynamic and heat transfer performance of Al_2O_3 and CuO nanofluids in the flat tubes of a radiator, Int. J. Heat Fluid Flow. 31, (2010), 613–621.
12. V. Delavari, S.H. Hashemabadi, CFD simulation of heat transfer enhancement of Al_2O_3/ water and Al_2O_3/ ethylene glycol nano fl uids in a car radiator, Appl. Therm. Eng. 73, (2014), 378–388.
13. D.P. Kulkarni, R.S. Vajjha, D.K. Das, D. Oliva, Application of aluminum oxide nanofluids in diesel electric generator as jacket water coolant, Appl. Therm. Engg. 28, (2008), 1774–1781.
14. S.M. Peyghambarzadeh, S.H. Hashemabadi, M. Naraki, Y. Vermahmoudi, Experimental study of overall heat transfer coefficient in the application of dilute nanofluids in the car radiator, Appl. Therm. Eng. 52, (2013), 8–16.

15. J. Buongiorno, D.C. Venerus, N. Prabhat, T. McKrell, J. Townsend, R. Christianson, Y. V. Tolmachev, P. Keblinski, L.W. Hu, J.L. Alvarado, I.C. Bang, S.W. Bishnoi, M. Bonetti, F. Botz, A. Cecere, Y. Chang, G. Chen, H. Chen, S.J. Chung, M.K. Chyu, S.K. Das, R. Di Paola, Y. Ding, F. Dubois, G. Dzido, J. Eapen, W. Escher, D. Funfschilling, Q. Galand, J. Gao, P.E. Gharagozloo, K.E. Goodson, J.G. Gutierrez, H. Hong, M. Horton, K.S. Hwang, C.S. Iorio, S.P. Jang, A.B. Jarzebski, Y. Jiang, L. Jin, S. Kabelac, A. Kamath, M.A. Kedzierski, L.G. Kieng, C. Kim, J.H. Kim, S. Kim, S.H. Lee, K.C. Leong, I. Manna, B. Michel, R. Ni, H.E. Patel, J. Philip, D. Poulikakos, C. Reynaud, R. Savino, P.K. Singh, P. Song, T. Sundararajan, E. Timofeeva, T. Tritcak, A.N. Turanov, S. Van Vaerenbergh, D. Wen, S. Witharana, C. Yang, W.H. Yeh, X.Z. Zhao, S.Q. Zhou, A benchmark study on the thermal conductivity of nanofluids, J. Appl. Phys. 106, (2009).

16. N.A.C. Sidik, H.A. Mohammed, O.A. Alawi, S. Samion, A review on preparation methods and challenges of nanofluids, Int. Commun. Heat Mass Transf. 54, (2014), 115–125.

17. Y. Li, J. Zhou, S. Tung, E. Schneider, S. Xi, A review on development of nanofluid preparation and characterization, Powder Technol. 196, (2009), 89–101.

18. H. Akoh, Y. Tsukasaki, S. Yatsuya, A. Tasaki, Magnetic properties of ferromagnetic ultrafine particles prepared by vacuum evaporation on running oil substrate, J. Crys. Growth. 45, (1978), 495-500.

19. R. Saxena, D. Gangacharyulu, V.K. Bulasara, Heat transfer and pressure drop characteristics of dilute alumina–water nanofluids in a pipe at different power inputs, Heat Transf. Eng. 18, (2016), 1554-1565.

20. M. Naraki, S.M. Peyghambarzadeh, S.H. Hashemabadi, Y. Vermahmoudi, Parametric study of overall heat transfer coefficient of CuO/water nanofluids in a car radiator, Int. J. Therm. Sci. 66, (2013), 82–90.

21. N. Putra, W. Roetzel, S.K. Das, Natural convection of nano-fluids, Heat Mass Transf. 39, (2003), 775–784.

22. Y. Vermahmoudi, S.M. Peyghambarzadeh, S.H. Hashemabadi, M. Naraki, Experimental investigation on heat transfer performance of Fe_2O_3/water nanofluid in an air-finned heat exchanger, Eur. J. Mech. B/Fluids. 44, (2014), 32–41.

23. M. Wagener, B.S. Murty, B. Gunther, Preparation of metal suspension by high pressure DC-sputtering on magnetro rotating drum, 457, (1997), 149–154.

24. J.A. Eastman, U.S. Choi, S. Li, L.J. Thompson, S. Lee, Enhanced thermal conductivity through the development of nanofluids, 457, (1997), 3–11.

25. B. Bajaj, H.I. Joh, S.M. Jo, G. Kaur, A. Sharma, M. Tomar, V. Gupta, S. Lee, Controllable one step copper coating on carbon nanofibers for flexible cholesterol biosensor substrates, J. Mater. Chem. B. 4, (2015), 229–236.

26. M. Elsebay, I. Elbadawy, M.H. Shedid, M. Fatouh, Numerical resizing study of Al_2O_3 and CuO nanofluids in the flat tubes of a radiator, Appl. Math. Model. 40, (2015), 6437–6450.

27. R.A. Buhrman, C.G. Granqvist, Lognormal size distributions from magnetization measurements on small superconducting Al particles log-normal size distributions from

magnetization measurements on small superconducting AI particles, J. Applied Phy. 2220, (2002), 1–4.

28. H. Chen, W. Yang, Y. He, Y. Ding, L. Zhang, C. Tan, A.A. Lapkin, D. V. Bavykin, Heat transfer and flow behaviour of aqueous suspensions of titanate nanotubes (nanofluids), Powder Technol. 183, (2008), 63–72.

29. V. Kumaresan, R. Velraj, Thermochimica Acta Experimental investigation of the thermo-physical properties of water – ethylene glycol mixture based CNT nanofluids, Thermochem. Acta. 545, (2012), 180–186.

30. M. Liu, M.C. Lin, C.Y. Tsai, C. Wang, Enhancement of thermal conductivity with Cu for nanofluids using chemical reduction method, Int. J. Heat Mass Transf. 49, (2006), 3028–3033.

31. Z. Haddad, C. Abid, H.F. Oztop, A. Mataoui, A review on how the researchers prepare their nanofluids, Int. J. Therm. Sci. 76, (2014), 168–189.

32. N. Ali, J.A. Teixeira, A. Addali, A review on nanofluids : fabrication , stability , and thermophysical properties, J. of Nano. (2018), 1-33.

33. K.A. Wepasnick, B.A. Smith, J.L. Bitter, D.H. Fairbrother, Chemical and structural characterization of carbon nanotube surfaces, Anal Bio. Chem. 396, (2011), 1003–1014.

34. Q. Yu, Y.J. Kim, H. Ma, Q. Yu, J. Kim, H. Ma, Nanofluids with plasma treated diamond nanoparticles nanofluids with plasma treated diamond nanoparticles, App. Phy. Lett. 92, (2014), 103111-3.

35. H.E. Ahmed, M.I. Ahmed, M.Z. Yusoff, Numerical and experimental comparative study on nanofluids flow and heat transfer in a ribbed triangular duct, Exp. Heat Transf. 6152, (2015), 1–24.

36. K.B. Anoop, T. Sundararajan, S.K. Das, Effect of particle size on the convective heat transfer in nanofluid in the developing region, Int. J. Heat Mass Transf. 52, (2009), 2189–2195.

37. M. Chandrasekar, S. Suresh, A. Chandra Bose, Experimental studies on heat transfer and friction factor characteristics of Al_2O_3/water nanofluid in a circular pipe under laminar flow with wire coil inserts, Exp. Therm. Fluid Sci. 34, (2010), 122–130.

38. M. Chandrasekar, S. Suresh, A. Chandra Bose, Experimental investigations and theoretical determination of thermal conductivity and viscosity of Al_2O_3/water nanofluid, Exp. Therm. Fluid Sci. 34, (2010), 210–216.

39. H.A. Mintsa, G. Roy, C.T. Nguyen, D. Doucet, New temperature dependent thermal conductivity data for water-based nanofluids, Int. J. Therm. Sci. 48, (2009), 363–371.

40. S.M.S. Murshed, K.C. Leong, C. Yang, Investigations of thermal conductivity and viscosity of nanofluids, Int. J. Therm. Sci. 47, (2008), 560–568.

41. S.M.S. Murshed, K.C. Leong, C. Yang, A combined model for the effective thermal conductivity of nanofluids, Appl. Therm. Eng. 29, (2009), 2477–2483.

42. S. Jana, A. Salehi-khojin, W. Zhong, Enhancement of fluid thermal conductivity by the addition of single and hybrid nano-additives, Thermo. Chem. 462, (2007), 45–55.

43. C.A.N. De Castro, S.M.S. Murshed, M.J. V Lourenço, F.J. V Santos, M.L.M. Lopes, J.M.P. França, Enhanced thermal conductivity and specific heat capacity of carbon nanotubes ionano fluids, 62, (2012), 34–39.

44. S.M.S. Murshed, C. A. N. de Castro, Predicting the thermal conductivity of nanofluids—effect of Brownian motion of nanoparticles, J. Nanofluids. 1, (2012), 180–185.

45. L.S. Sundar, M.H. Farooky, S.N. Sarada, M.K. Singh, Experimental thermal conductivity of ethylene glycol and water mixture based low volume concentration of Al_2O_3 and CuO nanofluids, Int. Commun. Heat Mass Transf. 41, (2013), 41–46.

46. T.P. Teng, Y.H. Hung, T.C. Teng, H.E. Mo, H.G. Hsu, The effect of alumina/water nanofluid particle size on thermal conductivity, Appl. Therm. Eng. 30, (2010), 2213–2218.

47. S. Kakaç, A. Pramuanjaroenkij, Review of convective heat transfer enhancement with nanofluids, Int. J. Heat Mass Transf. 52 (2009) 3187–3196.

48. Y. Xuan, Q. Li, Heat transfer enhancement of nanofluids, Int. J. Heat and Fluid Flow. 21, (2000), 58–64.

49. S.M.S. Murshed, K.C. Leong, C. Yang, Enhanced thermal conductivity of TiO_2 — water based nanofluids, 44 (2005) 367–373.

50. C.H. Li, G.P. Peterson, Experimental investigation of temperature and volume fraction variations on the effective thermal conductivity of nanoparticle suspensions (nanofluids), J. of App. Phy. 99, (2006), 084314-8.

51. H. Xie, J. Wang, T. Xi, Y. Liu, F. Ai, H. Xie, J. Wang, T. Xi, Y. Liu, F. Ai, Thermal conductivity enhancement of suspensions containing nanosized alumina particles, J. of App. Phy. 91, (2012), 4568-4572.

52. R.S. Vajjha, D.K. Das, International Journal of Heat and Mass Transfer Experimental determination of thermal conductivity of three nanofluids and development of new correlations, Int. J. Heat Mass Transf. 52, (2009), 4675–4682.

53. B. Wang, X. Wang, W. Lou, J. Hao, Thermal conductivity and rheological properties of graphite/oil nanofluids, Colloids Surfaces A Physicochem. Eng. Asp. 414, (2012), 125–131.

54. H.E. Patel, S.K. Das, T.S.S. Nair, B. George, T. Pradeep, H.E. Patel, S.K. Das, T. Sundararajan, Thermal conductivities of naked and monolayer protected metal nanoparticle based nanofluids, J. of App. Phy. 83, (2005), 1–4.

55. M.C.S. Reddy, V.V. Rao, Experimental studies on thermal conductivity of blends of ethylene glycol-water-based TiO_2 nano fluids , Int. Commun. Heat Mass Transf. 46, (2013), 31–36.

56. R.S. Khedkar, S.S. Sonawane, K.L. Wasewar, Influence of CuO nanoparticles in enhancing the thermal conductivity of water and monoethylene glycol based nanofluids, Int. Commun. Heat Mass Transf. 39, (2012), 665–669.

57. Y.J. Hwang, Y.C. Ahn, H.S. Shin, C.G. Lee, G.T. Kim, H.S. Park, J.K. Lee, Investigation on characteristics of thermal conductivity enhancement of nanofluids, Current App. Phy. 6, (2006), 1068–1071.

58. J. Koo, C. Kleinstreuer, A new thermal conductivity model for nanofluids, J. Nanoparticle Res. 6, (2004), 577–588.

59. R.L. Hamilton, O.K. Crosser, Thermal Conductivity of Heterogeneous Two-Com Ponent Systems, I EC Fundumentals. 1, (1959), 187–191.

60. W. Yu, S.U.S. Choi, The role of interfacial layers in the enhanced thermal conductivity of nanofluids: A renovated Maxwell model, J. Nanoparticle Res. 5, (2003,) 167–171..

61. S. Lee, Measuring thermal conductivity of fluids containing oxide nanoparticles, Trans. Of ASME, 121, (2013),280-289.

62. J. Hong, D. Kim, Thermochimica Acta Effects of aggregation on the thermal conductivity of alumina/water nanofluids, Thermochim. Acta. 542, (2012), 28–32.

63. X. Wang, X. Xu, Thermal Conductivity of Nanoparticle – Fluid Mixture, J. of Ther. and Heat Tran. 13, (1999), 474-480.

64. J.A. Eastman, S.U.S. Choi, S. Li, W. Yu, L.J. Thompson, Anomalously increased effective thermal conductivities of ethylene glycol- based nanofluids containing copper nanoparticles Anomalously increased effective thermal conductivities of ethylene glycol-based nanofluids containing copper nanoparticles, J. of App. Phy. 78, (2012), 718-720.

65. P. Thiesen, Temperature dependance of thermal conductivity enhancement for nanofluids, J. of Heat Trans. 125, (2013), 567–574.

66. D. Wen, Y. Ding, Experimental investigation into convective heat transfer of nanofluids at the entrance region under laminar flow conditions, Int. J. Heat Mass Transf. 47, (2004), 5181–5188.

67. I.M. Mahbubul, R. Saidur, M.A. Amalina, In fl uence of particle concentration and temperature on thermal conductivity and viscosity of Al_2O_3 / R141b nanorefrigerant, Int. Commun. Heat Mass Transf. 43, (2013), 100–104.

68. K.R. Priya, K.S. Suganthi, K.S. Rajan, Transport properties of ultra-low concentration CuO – water nanofluids containing non-spherical nanoparticles, Int. J. Heat Mass Transf. 55, (2012), 4734–4743.

69. H.T. Zhu, C.Y. Zhang, Y.M. Tang, J.X. Wang, Novel Synthesis and Thermal Conductivity of CuO Nanofluid, J. Phy. Chem. 111, (2007), 1646–1650.

70. X. Wei, H. Zhu, T. Kong, L. Wang, Synthesis and thermal conductivity of Cu_2O nanofluids, Int. J. of Heat and Mass Trans. 52, (2009), 4371–4374.

71. M. Kole, T.K. Dey, Role of interfacial layer and clustering on the effective thermal conductivity of CuO – gear oil nanofluids, Exp. Therm. Fluid Sci. 35, (2011), 1490–1495.

72. H. Zhu, D. Han, Z. Meng, D. Wu, C. Zhang, Preparation and thermal conductivity of CuO nanofluid via a wet chemical method, Nano. Res. Lett. 6, (2011), 2–7.

73. M. Saterlie, H. Sahin, B. Kavlicoglu, Y. Liu, O. Graeve, Particle size effects in the thermal conductivity enhancement of copper-based nanofluids, Nano. Res. Lett. 6, (2011), 1–7.

74. R. Pa, B. Barbe, E. Blanco, C. Casanova, Thermal conductivity and specific heat capacity measurements of CuO nanofluids,J. of Ther. Cal. 115, (2014), 1883–1891.

75. C.T. Nguyen, F. Desgranges, N. Galanis, G. Roy, T. Mare, S. Boucher, H. Angue Mintsa, Viscosity data for Al_2O_3-water nanofluid-hysteresis: is heat transfer enhancement using nanofluids reliable?, Int. J. Therm. Sci. 47, (2008), 103–111.

76. C.T. Nguyen, F. Desgranges, G. Roy, N. Galanis, T. Mare, S. Boucher, H. Angue Mintsa, Temperature and particle-size dependent viscosity data for water-based nanofluids - Hysteresis phenomenon, Int. J. Heat Fluid Flow. 28, (2007), 1492–1506.

77. K. Bashirnezhad, S. Bazri, M.R. Safei, M. Goodarzi, M. Dahari, O. Mahian, A.S. Dalkilic, S. Wongwises, Viscosity of nanofluids: A review of recent experimental studies, Int. Comm. in Heat and Mass Trans, (2016), 1-10.

78. J. Jeong, C. Li, Y. Kwon, J. Lee, S. Hyung, R. Yun, Particle shape effect on the viscosity and thermal conductivity of ZnO nanofluids, Int. J. Refrig. 36, (2013), 2233–2241.

79. X. Wang, X. Xu, S.U. S. Choi, Thermal conductivity of nanoparticle - fluid mixture, J. Thermophys. Heat Transf. 13, (1999), 474–480.

80. R. Prasher, D. Song, J. Wang, P. Phelan, Measurements of nanofluid viscosity and its implications for thermal applications, Appl. Phys. Lett. 89, (2006), 2–5.

81. M.J. Pastoriza-Gallego, C. Casanova, J.L. Legido, M.M. Piñeiro, CuO in water nanofluid: Influence of particle size and polydispersity on volumetric behaviour and viscosity, Fluid Phase Equilib. 300, (2011), 188–196.

82. M. Kole, T.K. Dey, Effect of aggregation on the viscosity of copper oxide e gear oil nano fluids, Int. J. Therm. Sci. 50, (2011), 1741–1747.

83. W. Duangthongsuk, S. Wongwises, Measurement of temperature-dependent thermal conductivity and viscosity of TiO_2-water nanofluids, Exp. Therm. Fluid Sci. 33, (2009), 706–714.

84. L.S. Sundar, E.V. Ramana, M.K. Singh, A.C.M. Sousa, Thermal conductivity and viscosity of stabilized ethylene glycol and water mixture Al_2O_3 nano fluids for heat transfer applications : An experimental study, Int. Commun. Heat Mass Transf. 56, (2014), 86–95.

85. B. Aladag, H. Salma, N. Doner, T. Maré, D. Steven, B. Aladag, H. Salma, N. Doner, T. Maré, D. Steven, Experimental investigations of the viscosity of nanofluids at low temperatures, App. Energy. 97, (2012), 876-880.

86. J. Grzywa, A. Witek, M. Cholewa, Influence of anisotropic pressure on viscosity and electrorheology of diethylene glycol-based $MgAl_2O_4$ nanofluids, Nano Exp. 9, (2014), 2-13.

87. S.M.S. Murshed, P. Estellé, A state of the art review on viscosity of nano fluids, Rew. And Sus. Energy Rew. 76, (2017), 1134–1152.

88. S. Halelfadl, N. Doner, Viscosity of carbon nanotubes water based nanofluids : Influence of concentration and temperature, Int. J. of Ther. Sci. 12, (2013), 1-15.

89. S. Zeroual, H. Loulijat, E. Achehal, P. Estellé, A. Hasnaoui, S. Ouaskit, Viscosity of Ar-Cu nano fl uids by molecular dynamics simulations : Effects of nanoparticle content , temperature and potential interaction, J. Mol. Liq. 268, (2018), 490–496.

90. T. Yiamsawas, O. Mahian, A. Selim, S. Kaewnai, Experimental studies on the viscosity of TiO_2 and Al_2O_3 nanoparticles suspended in a mixture of ethylene glycol and water for high temperature applications, Appl. Energy. 111, (2013), 40–45.

91. B.G.K. Batchelor, The effect of Brownian motion on the bulk stress in a suspension of spherical particles, J. of Fluid Mech. 83, (1977), 97-117.

92. S.E.B. Maaga, C.T. Nguyen, N. Galanis, G. Roy, Heat transfer behaviours of nanofluids in a uniformly heated tube, Superlattices Microstruct. 35, (2004), 543–557.

93. M. Harkirat, K. Sandhu, D. Gangacharyulu, An experimental study on stability and some thermophysical properties of multiwalled carbon nanotubes with water-ethylene glycol mixtures, Parti. Sci. Tech. 6351 (2016).

94. G.S. Sokhal, D. Gangacharyulu, V.K. Bulasara, Heat transfer and pressure drop performance of alumina – water nanofluid in a flat vertical tube of a radiator, Chem. Eng. Commun. 205, (2018), 257–268.

95. G. Singh, D. Gangacharyulu, V.K. Bulasara, Experimental investigation of the effect of heat transfer and pressure drop on performance of a flat tube by using water-based Al_2O_3/nanofluids, Int. J. Energy a Clean Environ. 19, (2018), 1–17.

96. S.N. Shoghl, J. Jamali, M.K. Moraveji, Electrical Conductivity , Viscosity , and Density of Different Nanofluids : An experimental study In this study , the thermophysical properties of water based nanofluids were investigated, Exp. Therm. Fluid Sci. 19, (2016), 17-23.

97. R.S. Vajjha, D.K. Das, R.S. Vajjha, D.K. Das, Measurements of specific heat and density of Al_2O_3 nanofluid, 1063, (2008) 361-370.

98. P. Taylor, R.S. Vajjha, D.K. Das, B.M. Mahagaonkar, Density measurement of different nanofluids and their comparison with theory density measurement of different nanofluids, Petroleum Sci. and Tech. (2009) 37–41.

99. F. Yousefi, Z. Amoozandeh, A new model to predict the densities of nanofluids using statistical mechanics and artificial intelligent plus principal component analysis, Chi. J. of Che.Engg. (2016), 17-24.

100. E. Montazer, E. Salami, H. Yarmand, Z. Zaman, C. Mahidzal, Development of a new density correlation for carbon-based nanofluids using response surface methodology, J. Therm. Anal. Calorim. 4, (2018), 1-9.

101. G. Żyła, J.P. Vallejo, L. Lugo, Isobaric heat capacity and density of ethylene glycol based nanofluids containing various nitride nanoparticle types: an experimental study, J. Mol. Liq. 261, (2018), 530-539.

102. I.M. Mahbubul, R. Saidur, M.A. Amalina, Thermal conductivity , viscosity and density of R141b refrigerant based nanofluid, Procedia Eng. 56, (2013), 310–315.

103. A. Mariano, M.J. Pastoriza-gallego, L. Lugo, A. Camacho, S. Canzonieri, M.M. Pi, Fluid phase equilibria thermal conductivity, rheological behaviour and density of non-Newtonian ethylene glycol-based SnO_2 nanofluids, 337, (2013), 119–124.

104. I.M. Shahrul, I.M. Mahbubul, S.S. Khaleduzzaman, R. Saidur, M.F.M. Sabri, A comparative review on the specific heat of nano fluids for energy perspective, Renweable and Sus. Energy Reviews. 38, (2014), 88–98.

105. H. Riazi, T. Murphy, G.B. Webber, R. Atkin, S.S. Mostafavi, R.A. Taylor, International Journal of Thermal Sciences Specific heat control of nano fl uids : A critical review, Int. J. Therm. Sci. 107, (2016), 25–38.

106. E. De Robertis, E.H.H. Cosme, R.S. Neves, A.Y. Kuznetsov, A.P.C. Campos, S.M. Landi, C.A. Achete, Application of the modulated temperature differential scanning calorimetry technique for the determination of the speci fi c heat of copper nano fluids, Appl. Therm. Eng. 41, (2012), 10–17.

107. J. Choi, Y. Zhang, Numerical simulation of laminar forced convection heat transfer of Al_2O_3 water nanofluid in a pipe with return bend, Int. J. Therm. Sci. 55, (2012), 90–102.

108. S. Sonawane, K. Patankar, A. Fogla, B. Puranik, U. Bhandarkar, S.S. Kumar, An experimental investigation of thermo-physical properties and heat transfer performance of Al_2O_3 -aviation turbine fuel nano fluids, Appl. Therm. Eng. 31, (2011), 2841–2849.

109. Xuan, W. Roetzel, Conceptions for heat transfer correlation of nano fuids, Int. J. of Heat and Mass Trans. 43, (2000), 3701–3707.

110. J. Liu, F. Wang, L. Zhang, X. Fang, Z. Zhang, Thermodynamic properties and thermal stability of ionic liquid-based nano fluids containing graphene as advanced heat transfer fluids for medium-to-high-temperature applications, Renew. Energy. 63, (2014), 519–523.

111. A. Mohebbi, Prediction of speci fi c heat and thermal conductivity of nano fluids by a combined equilibrium and non-equilibrium molecular dynamics simulation, J. Mol. Liq. 175, (2012), 51–58.

112. H. Nieh, T. Teng, C. Yu, Enhanced heat dissipation of a radiator using oxide nano-coolant, Int. J. Therm. Sci. 77, (2014), 252–261.

113. M.N. Pantzali, A.G. Kanaris, K.D. Antoniadis, A.A. Mouza, S. V Paras, Effect of nanofluids on the performance of a miniature plate heat exchanger with modulated surface, Int. J. Heat Fluid Flow. 30, (2009), 691–699.

114. D. Shin, D. Banerjee, Specific heat of nanofluids synthesized by dispersing alumina nanoparticles in alkali salt eutectic, Int. J. Heat Mass Transf. 74, (2014), 210–214.

115. M. Xi, C. Pan, Optimal concentration of alumina nanoparticles in molten Hitec salt to maximize its specific heat capacity, Int. J. Heat Mass Transf. 70, (2014), 174–184.

116. N. Reddy, K. Murugesan, Numerical investigations on the advantage of nanofluids under DDMC in a lid-driven cavity, Heat Trans. Asian Res. 46, (2017), 1065-1086.

117. V. Bhalla, H. Tyagi, Parameters in fluencing the performance of nanoparticles-laden fl uid-based solar thermal collectors : A review on optical properties, Renew. Sus. Energy Res. 84, (2018), 12–42.

118. V. Khullar, Potential heat transfer fluids (nanofluids) for direct volumetric absorption-based solar thermal systems, J. Ther. Sci..10, (2018), 1–13.

119. V. Khullar, V. Bhalla, H. Tyagi, Potential heat transfer fluids (nanofluids) for direct volumetric absorption-based solar thermal systems, J. Ther. Sci.. (2018).

120. T. Sivasakthivel, M. Philippe, K. Murugesan, V. Verma, P. Hu, Experimental thermal performance analysis of ground heat exchangers for space heating and cooling applications, Renew. Energy. 113, (2017), 1168–1181.

121. T. Sivasakthivel, K. Murugesan, P.K. Sahoo, Optimization of ground heat exchanger parameters of ground source heat pump system for space heating applications, Energy. 78, (2014), 573-586.

122. S.Z. Heris, M.N. Esfahany, S.G. Etemad, Experimental investigation of convective heat transfer of Al_2O_3/water nanofluid in circular tube, Int. J. Heat and Fluid Flow. 28, (2007), 203–210.

123. X. Wang, A.S. Mujumdar, Heat transfer characteristics of nanofluids : a review, Int. J. of Thermal Sci. 46, (2007), 1–19.

124. J. Yang, F. Li, Y. He, Y. Huang, B. Jiang, Experimental study on the characteristics of heat transfer and flow resistance in turbulent pipe flows of viscoelastic-fluid-based Cu nanofluid, Int. J. Heat Mass Transf. 62, (2013), 303–313.

125. S. Suresh, K.P. Venkitaraj, P. Selvakumar, M. Chandrasekar, Effect of Al_2O_3 – Cu / water hybrid nanofluid in heat transfer, Exp. Therm. Fluid Sci. 38, (2012), 54–60.

126. M. Zarringhalam, A. Karimipour, D. Toghraie, Experimental study of the effect of solid volume fraction and Reynolds number on heat transfer coefficient and pressure drop of CuO-Water nanofluid, Exp. Therm. Fluid Sci. 76, (2016), 342–351.

127. M.M. Heyhat, F. Kowsary, A.M. Rashidi, S. Alem Varzane Esfehani, A. Amrollahi, Experimental investigation of turbulent flow and convective heat transfer characteristics of alumina water nanofluids in fully developed flow regime, Int. Commun. Heat Mass Transf. 39, (2012), 1272–1278.

128. A.A.A. Arani, J. Amani, Experimental study on the effect of TiO_2 – water nanofluid on heat transfer and pressure drop, Exp. Therm. Fluid Sci. 42, (2012), 107–115.

129. W. Duangthongsuk, S. Wongwises, Heat transfer enhancement and pressure drop characteristics of TiO_2 – water nanofluid in a double-tube counter flow heat exchanger, Int. J. Heat Mass Transf. 52, (2009), 2059–2067.

130. S.K. Das, N. Putra, W. Roetzel, Pool boiling characteristics of nano-fluids, Int. J. Heat Mass Transf. 46, (2003), 851–862.

131. B. Farajollahi, S.G. Etemad, M. Hojjat, International Journal of Heat and Mass Transfer Heat transfer of nanofluids in a shell and tube heat exchanger, Int. J. Heat Mass Transf. 53, (2010), 12–17.

132. G. Roy, C.T. Nguyen, Numerical investigation of laminar flow and heat transfer in a radial flow cooling system with the use of nanofluids, Superl. and Micro. 35, (2004), 497–511.

133. K. Khanafer, K. Vafai, M. Lightstone, Buoyancy-driven heat transfer enhancement in a two-dimensional enclosure utilizing nanofluids, Int. J. Heat Mass Transf. 46, (2003), 3639–3653.

134. Y. Xuan, Z. Yao, Lattice Boltzmann model for nanofluids, Heat Mass Tansf. 41, (2005), 199–205.

135. Y. Xuan, K. Yu, Q. Li, Investigation on flow and heat transfer of nanofluids by the thermal Lattice Boltzmann model, Progress in Comp. Fluid Dynam. 5, (2005), 13–19.

136. A. Ghozatloo, A. Rashidi, M. Shariaty-niassar, Convective heat transfer enhancement of graphene nanofluids in shell and tube heat exchanger, Exp. Therm. Fluid Sci. 53, (2014), 136–141.

137. S. Halelfadl, P. Estellé, T. Maré, Heat transfer properties of aqueous carbon nanotubes nanofluids in coaxial heat exchanger under laminar regime, Exp. Therm. Fluid Sci. 55, (2014), 174–180.

138. S. Won, S. Young, C. Hwa, I. Cheol, Effect of nanofluids on reflood heat transfer in a long vertical tube, Int. J. Heat Mass Transf. 55, (2012), 4766–4771.

139. Y. He, Y. Jin, H. Chen, Y. Ding, D. Cang, H. Lu, Heat transfer and flow behaviour of aqueous suspensions of TiO_2 nanoparticles (nanofluids) flowing upward through a vertical pipe, Int. J. Heat Mass Transf. 50, (2007), 2272–2281.

140. S.M. Peyghambarzadeh, S.H. Hashemabadi, S.M. Hoseini, M. Seifi Jamnani, Experimental study of heat transfer enhancement using water/ethylene glycol based nanofluids as a new coolant for car radiators, Int. Commun. Heat Mass Transf. 38, (2011), 1283–1290.

141. K.Y. Leong, R. Saidur, S.N. Kazi, A.H. Mamun, Performance investigation of an automotive car radiator operated with nano fluid-based coolants (nano fluid as a coolant in a radiator), Appl. Therm. Eng. 30,, (2010) 2685–2692.

142. S.M. Peyghambarzadeh, S.H. Hashemabadi, M.S. Jamnani, S.M. Hoseini, Improving the cooling performance of automobile radiator with Al_2O_3/water nanofluid, Appl. Therm. Eng. 31, (2011), 1833–1838.

143. S. El, B. Maïga, C.T. Nguyen, N. Galanis, G. Roy, T. Maré, M. Coqueux, Heat transfer enhancement in turbulent tube flow using Al_2O_3 nanoparticle suspension, Int. J. of Numerical Methods Heat and Fluid Flow. 16, (2006), 275-292.

144. Y. Yang, Z.G. Zhang, E.A. Grulke, W.B. Anderson, G. Wu, Heat transfer properties of nanoparticle-in-fluid dispersions (nanofluids) in laminar flow, Int. J. Heat Mass Transf. 48, (2005), 1107–1116.

145. Y. Xuan, Q. Li, Investigation on convective heat transfer and flow features of nanofluids, J. Heat Transf. 125, (2013), 151–155.

146. W. Duangthongsuk, S. Wongwises, An experimental study on the heat transfer performance and pressure drop of TiO_2 -water nanofluids flowing under a turbulent flow regime, Int. J. Heat Mass Transf. 53, (2010), 334–344.

147. S. El, B. Maïga , S. Joseph, C.T. Nguyen, G. Roy, N. Galanis, Heat transfer enhancement by using nanofluids in forced convection flows, Int. J. Heat and Fluid Flow. 26, (2005), 530–546.

148. A.R. Sajadi, M.H. Kazemi, Investigation of turbulent convective heat transfer and pressure drop of TiO_2 / water nano fluid in circular tube, Int. Commun. Heat Mass Transf. 38, (2011) 1474–1478.

149. L.S. Sundar, M.T. Naik, K. V Sharma, M.K. Singh, T.C. Siva, Experimental investigation of forced convection heat transfer and friction factor in a tube with Fe_3O_4 magnetic nanofluid, Exp. Thermal Fluid Sci. 37, (2012) 65–71.

150. L. Godson, B. Raja, D. Mohan, S. Wongwises, Convective heat transfer of nanofluids with correlations, Particuology. 9, (2011), 626–631.

151. R.S. Vajjha, D.K. Das, D.P. Kulkarni, Development of new correlations for convective heat transfer and friction factor in turbulent regime for nanofluids, Int. J. of Heat and Mass Transf. 53, (2010), 4607–4618.

152. K. V Sharma, L.S. Sundar, P.K. Sarma, Estimation of heat transfer coef fi cient and friction factor in the transition fl ow with low volume concentration of Al_2O_3 nano fluid flowing in a circular tube and with twisted tape insert, Int. Commun. Heat Mass Transf. 36, (2009), 503–507.

153. S. Suresh, K.P. Venkitaraj, P. Selvakumar, Comparative study on thermal performance of helical screw tape inserts in laminar flow using Al_2O_3/ water and CuO/ water nanofluids, Superlattices Microstruct. 49, (2011), 608–622.

154. S. Suresh, K.P. Venkitaraj, P. Selvakumar, M. Chandrasekar, Effect of Al_2O_3 – Cu/ water hybrid nanofluid in heat transfer, Exp. Thermal Fluid Sci. 38, (2012), 54–60.

155. S. Suresh, M. Chandrasekar, S.C. Sekhar, Experimental studies on heat transfer and friction factor characteristics of CuO / water nanofluid under turbulent flow in a helically dimpled tube, Exp. Thermal Fluid Sci. 35, (2011), 542–549.

156. A. Ghadimi, R. Saidur, H.S.C. Metselaar, A review of nanofluid stability properties and characterization in stationary conditions, Int. J. Heat Mass Transf. 54, (2011), 4051–4068.

157. S.K. Das, N. Putra, P. Thiesen, W. Roetzel, Temperature dependence of thermal conductivity enhancement for nanofluids, J. Heat Transfer. 125, (2003), 567–574.

158. S.P. Jang, S.U.S. Choi, Role of Brownian motion in the enhanced thermal conductivity of nanofluids, Appl. Phys. Lett. 84, (2004), 4316–4318.

159. R. Prasher, P. Bhattacharya, P.E. Phelan, Brownian-motion-based convective-conductive model for the effective thermal conductivity of nanofluids, J. Heat Transfer. 128, (2006), 588-595.

160. M. Hojjat, S.G. Etemad, R. Bagheri, J. Thibault, Rheological characteristics of non-Newtonian nanofluids: Experimental investigation, Int. Commun. Heat Mass Transf. 38, (2011), 144–148.

161. P.K. Namburu, D.P. Kulkarni, D. Misra, D.K. Das, Viscosity of copper oxide nanoparticles dispersed in ethylene glycol and water mixture, Exp. Therm. Fluid Sci. 32, (2007), 397–402.

162. R.S. Vajjha, D.K. Das, B.M. Mahagaonkar, Density measurement of different nanofluids and their comparison with theory, Pet. Sci. Technol. 27, (2009), 612–624.

163. I.M. Mahbubul, R. Saidur, M. A. Amalina, Thermal conductivity, viscosity and density of R141b refrigerant based nanofluid, Procedia Eng. 56, (2013), 310–315.

164. D.K. Das, Specific heat measurement of three nanofluids and development of new correlations, J. Heat Transf. 131 (2016) 1–7.

165. N. Zhao, J. Yang, H. Li, Z. Zhang, S. Li, Numerical investigations of laminar heat transfer and flow performance of Al_2O_3-water nanofluids in a flat tube, Int. J. Heat Mass Transf. 92, (2016), 268–282.

APPENDIX

Calculation procedure for performance of compact heat exchanger.

1) **Frontal Area**
   Air side
   $A_{fr,a} = L_r H_r$ = 0.197806 m^2
   Coolant side
   $A_{fr,h} = D_r H_r$ = 0.006368 m^2
2) **Total Transfer Area**
   Coolant side
   $A_{t,h} = NL_r[2(L_{it} - H_{it}) + ®(H_{it})]$ = 0.64270 m^2
   Volume of radiator
   $V_r = L_r D_r H_r$ = 0.0031649 m^3
3) **Total transfer area/Total exchanger area**
   Air side
   $\sim_a = \frac{\times b_c}{(b_c + b_a + (2 \times a))}$ = 500.552 m^2/m^3

   Coolant side
   $\sim_h = \frac{A_{t,c}}{V_r}$ = 203.073 m^2/m^3
4) **Total flow area/Frontal area**
   $\pm_a = \sim_a r_{h,a}$ = 0.1780m^2
5) **Free flow area**
   Air side
   $A_{c,a} = A_{fr,a} \pm_a$ = 0.0352 m^2
   Coolant side
   $A_{c,h} = N\left[(L_{it} - H_{it})H_{it} + \frac{®}{4}H_{it}^2\right]$ = 0.00141 m^2
6) **Hydraulic diameter**
   Coolant side
   $D_{h.h} = \frac{4\left[(L_{it} - H_{it})H_{it} + \frac{®}{4}H_{it}\right]}{2(L_{it} - H_{it}) + ®H_{it}}$ = 0.00439 m

7) **Air side calculations**
   Air side calculations and its thermophysical properties are given below
   V_a = 5.5 m/sec. $°_a$ = 1.154 Kg/m^3 k_a=0.02364 W/(m.K)
   $C_{p,a}$ = 1006 J/(Kg.K) $«_a$ = 0.0000173 Kg/(m.s) D_{ha} = 0.001423 m
8) **Mass flow rate**
   $m_a = °_a \times A_{c,a} \times V_a$ = 0.223564 Kg/sec.
9) **Heat capacity rate**
   $C_a = m_a \times C_{p,a}$ = 224.905
10) **Reynolds number**

$$\mathrm{Re}_a = \frac{\rho_a \times V_a \times D_{h,a}}{\mu_a} = 522.068$$

11) **Colburn factor**

$$j_a = \frac{0.1459}{\mathrm{Re}^{0.3588}} = 0.0154502$$

12) **Prandtl number**

$$\mathrm{Pr}_a = \frac{\mu \times C_p}{k_a} = 0.73620$$

13) **Convective heat transfer coefficient**

$$h_a = \frac{j_a \times \rho_a \times V_a \times C_{p,a}}{\mathrm{Pr}_a^{2/3}} = 120.995 \text{ W/(m}^2\text{.K)}$$

14) **Fin parameter**

$$m = \sqrt{\frac{2 \times h_a}{k_f \times \delta}} = 94.409 \text{ m}$$

15) **Fin efficiency**

$$\eta = \frac{\tanh(m.L_f)}{m.L_f} = 0.9710$$

16) **Surface effectiveness**

$$\eta_0 = 1 - (1 - \eta) \times A_{ft} = 0.9744$$

17) **Hot Fluid side calculations**

Air side calculations and its thermophysical properties are given below

ρ_h = 992.3 Kg/m^3 k_h = 0.6305 W/(m.K)

$C_{p,h}$ = 4179 J/(Kg.K) μ_h = 0.000653 Kg/(m.s) $D_{h,h}$ = 0.004392 m

$T_{h,\ inlet}$ = 41.42°C $T_{h,\ outlet}$ = 31°C

$T_{a,\ inlet}$ = 22.63°C $T_{a,\ outlet}$ = 24.6°C $T_{surface}$ = 23.95

$$T_{bulk.mean} = \frac{T_{h,inlet} + T_{h,outlet}}{2} = 36.21°C$$

Flow rate = 1LPM

18) **Fluid mass flow rate**

$$W = \frac{Flow.Rate}{60} = 0.01667$$

19) **Heat capacity rate**

$$C_h = W \times C_{p,h} = 69.371$$

20) **Volume Flow Rate**

$G_w = W/A_{c,h}$= 11.737

21) **Reynolds Number**

$$\mathrm{Re}_h = \frac{G_h \times D_{h,h}}{\mu_h} = 2661.69$$

22) **Prandtl Number**

$$\mathrm{Pr}_h = \frac{\mu_h \times C_{p,h}}{k_h} = 4.32$$

23) **Nusselt number**

$$Nu_h = 0.3164 \mathrm{Re}_h^{-0.25} \left(\frac{\circ_h}{\circ_c} \right)^{0.797} \left(\frac{\ll_h}{\ll_c} \right)^{0.108} = 18.84$$

24) **Convective heat transfer coefficient**

$$h_h = \frac{Nu_h \times k_h}{D_{h,h}} = 2703.05 \text{ W/(m}^2\text{.K)}$$

25) **Overall heat transfer coefficient**

$$\frac{1}{U_a} = \frac{1}{\text{¦}_0 \cdot h_a} + \frac{1}{\left(\frac{\sim_h}{\sim_a} \right) \cdot h_h} = 0.00932$$

$$U_a = 107.27 \text{ W/(m}^2\text{.K)}$$

26) **Number of transfer units**

$$NTU = \frac{U_a \cdot \sim_a \cdot V_r}{C_{\min}} = 0.755$$

27) **Capacity ratio**

$$C^* = \frac{C_{\min}}{C_{\max}} = 0.30844$$

28) **Effectiveness**

$$£ = 1 - \exp\left\{ -\frac{1}{C^*} \left[1 - \exp\left(-C^* \cdot NTU \right) \right] \right\} = 0.4903$$

29) **Heat absorbed**

$$Q = W \times C_{p,h} \left(T_{h,inlet} - T_{h,outlet} \right) = 722.84 \text{ W}$$

30) **Friction factor**

$$f = 0.316 \, \mathrm{Re}_{nf}^{-0.25} \left(\frac{\circ_{nf}}{\circ_{bf}} \right)^{0.797} \left(\frac{\ll_{nf}}{\ll_{bf}} \right)^{0.108} = 0.044$$

Table A 1: Variation of Nusselt number with different conditions with aluminum oxide nanofluids

Temperature (ºC)	Flow rate (LPM)	Nusselt number			
		0% v/v	0.25 v/v	0.50% v/v	0.75% v/v
40	1.0	77.56	87.88	96.88	111.12
	1.25	81.71	92.03	101.03	115.27
	1.5	89.84	100.16	109.16	123.40
	1.75	97.78	108.10	117.10	131.34
	2.0	109.38	119.70	128.70	142.94
	2.25	113.18	123.50	133.00	148.10
	2.5	116.95	127.27	136.77	151.87
60	1.0	89.80	100.02	111.00	126.87
	1.25	94.44	104.66	115.64	131.51
	1.5	103.55	113.77	124.75	140.62
	1.75	112.44	122.66	133.64	149.51
	2.0	125.43	135.65	146.63	162.71
	2.25	129.69	141.19	152.17	168.25
	2.5	134.00	145.50	158.10	174.18
80	1.0	100.80	112.30	125.97	142.85
	1.25	105.44	116.94	130.61	147.49
	1.5	114.55	126.05	139.72	156.60
	1.75	123.44	134.94	148.61	165.49
	2.0	136.43	147.93	161.60	178.60
	2.25	140.69	152.19	165.86	182.86
	2.5	147.00	158.50	172.17	189.17

Table A2 : Comparison of experimental data and correlation data of Nusselt number at different aluminum oxide nanoparticles concentration

Flow rate (LPM)	Nusselt number							
	0.25% v/v		0.50% v/v		0.75% v/v		1.0% v/v	
	Exp. data	Corr. data	Exp. data	Corr. data	Exp. data	Corr. data	Exp. data	Corr. data
1.00	112.30	112.80	125.97	124.63	142.85	138.94	160.74	156.27
1.25	116.94	117.69	130.61	129.84	147.49	144.55	165.61	162.40
1.50	126.05	127.17	139.72	139.91	156.60	155.39	174.72	174.22
1.75	134.94	136.31	148.61	149.59	165.49	165.78	183.61	185.53
2.00	147.93	149.46	161.60	163.50	178.60	180.67	196.72	201.70
2.25	152.19	153.72	165.86	167.99	182.86	185.47	200.98	206.90
2.50	158.50	157.92	172.17	172.42	189.17	190.20	207.29	212.03

Table A 3: Variation of Nusselt number with different conditions with copper oxide nanofluids

Temperature (ºC)	**Flow rate (LPM)**	**Nusselt number**			
		0% v/v	**0.25 v/v**	**0.50% v/v**	**0.75% v/v**
40	1.0	77.56	94.20	106.02	120.69
	1.25	81.71	98.35	110.17	124.84
	1.5	89.84	106.48	118.30	132.97
	1.75	97.78	114.42	126.24	140.91
	2.0	109.38	126.02	137.85	152.51
	2.25	113.18	129.82	142.15	157.67
	2.5	116.95	133.59	145.91	161.44
60	1.0	89.80	106.34	120.15	136.44
	1.25	94.44	110.98	124.79	141.08
	1.5	103.55	120.09	133.89	150.19
	1.75	112.44	128.98	142.78	159.08
	2.0	125.43	141.97	155.78	172.28
	2.25	129.69	147.51	161.31	177.82
	2.5	134.00	151.82	167.25	183.75
80	1.0	100.80	118.62	135.12	152.42
	1.25	105.44	123.26	139.76	157.06
	1.5	114.55	132.37	148.86	166.17
	1.75	123.44	141.26	157.75	175.06
	2.0	136.43	154.25	170.75	188.17
	2.25	140.69	158.51	175.00	192.43
	2.5	147.00	164.82	181.32	198.74

Table A 4 : Comparison of experimental data and correlation data of Nusselt number at different copper oxide nanoparticles concentration

	Nusselt number							
	0.25% v/v		0.50% v/v		0.75% v/v		1.0% v/v	
Flow rate (LPM)	Exp. data	Corr. data	Exp. data	Corr. data	Exp. data	Corr. data	Exp. data	Corr. data
1.00	118.62	117.90	135.12	134.77	152.42	150.94	176.46	171.25
1.25	123.26	122.79	139.76	139.98	157.06	156.55	181.33	177.38
1.50	132.37	132.27	148.86	150.05	166.17	167.39	190.44	189.20
1.75	141.26	141.41	157.75	159.73	175.06	177.78	199.33	200.51
2.00	154.25	154.56	170.75	173.64	188.17	192.67	212.44	216.68
2.25	158.51	158.82	175.00	178.13	192.43	197.47	216.70	221.88
2.50	164.82	163.02	181.32	182.56	198.74	202.20	223.01	227.01

Table A 5: Variation of pressure drop with different conditions with aluminum oxide nanofluids

Flow rate (LPM)	Pressure Drop (Pa)				
	0% v/v	**0.25 v/v**	**0.50% v/v**	**0.75% v/v**	**1.0 % v/v**
1.25	1230.83	1249.68	1270.85	1284.33	1297.97
1.5	1342.02	1362.64	1385.86	1400.55	1415.42
1.75	1503.18	1526.42	1552.69	1569.14	1585.81
2.0	1598.60	1623.45	1651.66	1669.14	1686.87
2.25	1749.85	1777.27	1808.55	1827.67	1847.09
2.5	1840.42	1869.33	1902.35	1922.46	1942.89

Table A 6: Variation of pressure drop with different conditions with copper oxide nanofluids

Flow rate (LPM)	Pressure Drop (Pa)				
	0% v/v	**0.25 v/v**	**0.50% v/v**	**0.75% v/v**	**1.0 % v/v**
1.25	1230.83	1267.15	1301.50	1319.41	1339.25
1.5	1342.02	1381.89	1419.48	1439.01	1460.64
1.75	1503.18	1548.41	1590.79	1612.67	1636.91
2.0	1598.60	1647.25	1692.60	1715.86	1741.65
2.25	1749.85	1803.94	1854.01	1879.46	1907.71
2.5	1840.42	1897.58	1950.38	1977.15	2006.86

Table A 7: Comparison of experimental data and correlation data of friction factor at different aluminum oxide nanoparticles concentration

Flow rate (LPM)	Friction factor							
	0.25% v/v		0.50% v/v		0.75% v/v		1.0% v/v	
	Exp. data	Corr. data	Exp. data	Corr. data	Exp. data	Corr. data	Exp. data	Corr. data
1.00	0.04150	0.04180	0.04196	0.04207	0.04221	0.04233	0.04248	0.04260
1.25	0.04067	0.04097	0.04112	0.04123	0.04137	0.04149	0.04164	0.04176
1.50	0.03921	0.03951	0.03965	0.03976	0.03990	0.04002	0.04015	0.04027
1.75	0.03796	0.03826	0.03839	0.03850	0.03863	0.03875	0.03887	0.03899
2.00	0.03636	0.03666	0.03679	0.03690	0.03701	0.03713	0.03725	0.03737
2.25	0.03589	0.03619	0.03632	0.03643	0.03654	0.03666	0.03677	0.03689
2.50	0.03545	0.03575	0.03587	0.03598	0.03609	0.03621	0.03632	0.03644

Table A 8: Comparison of experimental data and correlation data of friction factor at different copper oxide nanoparticles concentration

Flow rate (LPM)	Friction factor							
	0.25% v/v		0.50% v/v		0.75% v/v		1.0% v/v	
	Exp. data	Corr. data	Exp. data	Corr. data	Exp. data	Corr. data	Exp. data	Corr. data
1.00	0.04113	0.04153	0.04180	0.04180	0.04226	0.04207	0.04251	0.04233
1.25	0.04031	0.04071	0.04097	0.04097	0.04142	0.04123	0.04167	0.04149
1.50	0.03886	0.03926	0.03951	0.03951	0.03995	0.03976	0.04020	0.04002
1.75	0.03761	0.03801	0.03826	0.03826	0.03869	0.03850	0.03893	0.03875
2.00	0.03603	0.03643	0.03666	0.03666	0.03709	0.03690	0.03731	0.03713
2.25	0.03556	0.03596	0.03619	0.03619	0.03662	0.03643	0.03684	0.03666
2.50	0.03512	0.03552	0.03575	0.03575	0.03617	0.03598	0.03639	0.03621

Publications based on research work

SCI Indexed

1. Gurpreet Singh Sokhal, D. Gangacharyulu, Vijaya Kumar Bulasara, "Heat transfer and pressure drop performance of water based Al_2O_3 in vertical flat tube of radiator". *Chemical Engineering Communications, Vol. 205, Issue 2, pp. 257-268, 2018. (Taylor and Francis I.F. = 1.282*). doi.org/10.1080/00986445.2017.1387853
2. Gurpreet Singh Sokhal, D. Gangacharyulu, Vijaya Kumar Bulasara, "Influence of copper oxide nanoparticles on the thermophysical properties and performance of flat tube of vehicle cooling system" *Vacuum, Vol. 157, pp. 268-276, 2018. (Elsevier, I.F. 2.10).* doi.org/10.1016/j.vacuum.2018.08.048

SCOPUS indexed

1. Gurpreet Singh Sokhal, D. Gangacharyulu, Vijaya Kumar Bulasara, "Experimental investigation of effect on heat transfer and pressure drop performance of flat tube with using water based Al_2O_3 nanofluids". *International Journal of Energy for Clean Environment, Vol. 19, pp. 1-17, 2018. (Begell House – I.F. 1.2)*
2. Gurpreet Singh Sokhal, D. Gangacharyulu, Vijaya Kumar Bulasara, "Numerical study on performance of flat tube with water based copper oxide nanofluids" Materials Today-Proceedings, 2018, In press (Elsevier)

International conferences

1. Gurpreet Singh Sokhal, D. Gangacharyulu, Vijaya Kumar Bulasara, "Experimental investigation on heat transfer and pressure drop performance of flat tube with using water based Al_2O_3 nanofluids". *2nd Thermal and Fluids Engineering Conference and 4th International Workshop on Heat Transfer. Las Vegas, USA.*
2. Gurpreet Singh, Sokhal, D. Gangacharyulu, Vijaya Kumar Bulasara, Enhancement of heat transfer performance of flat vertical tube using copper oxide/water nanofluids, *24th National and 2nd International ISHMT-ASTFE Heat and Mass Transfer Conference (IHMTC-2017) December 27-30, 2017, BITS Pilani, Hyderabad, India.*